The Hong Kong Polytechnic University

Department of Applied Biology and Chemical Technology

Protein Engineering of Class A and C *β*-lactamases for *β*-lactam Antibiotic Dtection

Tsang Man Wah

A thesis submitted in the partial fulfillment of the requirements for

the Degree of Doctor of Philosophy

August 2006

Certificate of Originality

I hereby declare that this thesis is my own work and that, to the best of my knowledge and belief, it reproduces no material previously published or written nor material which has been accepted for the award of any other degree or diploma, except where due acknowledgement has been made in the text.

Tsang Man Wah

August 2006

Abstract

With respect to the increasing demands for efficient screening systems for *β*-lactam compounds, a fluorescent *β*-lactamase E166Cf has been previously exploited for the purpose of generic detection of *β*-lactam antibiotics and *β*-lactamase inhibitors. Fabrication of this novel E166Cf sensor has been regarded as an innovative technology as it started a great milestone in the biosensor development by opening up the possibility of turning a non-allosteric *β*-lactam hydrolytic enzyme into a turn-on sensor for its substrates and inhibitors. E166Cf showed excellent properties as a sensing tool, including high sensitivity and amenability for high-throughput screening. However, owing to the differential substrate preference of the various classes of *β*-lactamases, E166Cf, based on a class A *β*-lactamase, demonstrated better responses to its preferred penicillin-type substrates than the cephalosporins. In order to have a biosensor specific for sensing cephalosporins, in this project, we aimed at constructing a class C *β*-lactamase, which shows a substrate preference on cephalosporins, into a fluorescent biosensor. In addition, it was postulated that this class C *β*-lactamase-based sensor would also be important for identifying potent class C *β*-lactamase inhibitors.

In our study, a class C β-lactamase from *Enterobacter cloacae* P99 was engineered by rational design into a fluorescent protein designated as V211Cf for sensing β-lactam antibiotics and β-lactamase inhibitors. This novel V211Cf was a fluorescein-labeled β-lactamase prepared by labeling the V211C mutant of P99 β-lactamase with a thiol-reactive fluorescein-5-maleimide. The fluorescein molecule was tethered to this unique cysteine-containing mutant at the 211 position that is in close proximity to the active site via a maleimide linker. Kinetic analysis of V211Cf indicated that there was no loss of binding efficiency and hydrolytic capability of V211Cf with a fluorophore attached in vicinity to the active site. We had successfully tethered a fluorescent probe at the proximity of the active site with restoring enzyme activity.

The fluorescein molecule located in close proximity of the active site in V211Cf could report the local environment changes at the enzyme active site. As revealed by fluorometric studies, addition of the two main classes of β-lactam antibiotics, including penicillins and cephalosporins, triggered fluorescence enhancements of V211Cf. Such increased signals then disappeared according to the rate of the hydrolysis of the substrates by V211Cf. In addition, V211Cf displayed distinct signal patterns for the β-lactamase inhibitors, including

clavulanic acid, sulbactam, tazobactam, and transition-state analogs. These results indicated that V211Cf can probe for the presence of the *β*-lactam antibiotics and *β*-lactamase inhibitors. In addition, time-resolved fluorescence measurement of V211Cf allows real-time studies on the enzyme-substrate/-inhibitor interactions.

With the aim of optimizing the performance of V211Cf in the detection for *β*-lactam antibiotics, Y150S/V211Cf, a derivative of V211Cf, was also constructed. As a catalytically-impaired derivative, Y150S/V211Cf did not hydrolyse the substrates, thus improving the signal stability. Furthermore, Y150S/V211Cf only showed fluorescence signals in the presence of cephalosporins but not penicillins, thus it was specific in sensing cephalosporin-type antibiotics.

Comparison of performance was made among the class C labeled-*β*-lactamases, V211Cf and Y150S/V211Cf, as well as the previously reported class A *β*-lactamase-based E166Cf in the detection of *β*-lactam antibiotics. While E166Cf was superior to the fluorescent class C *β*-lactamases in sensitivity, the fluorescein-modified class C *β*-lactamases demonstrated a more rapid response time for sensing cephalosporins than E166Cf.

To conclude, our results demonstrated for the first time the feasibility of the application of fluorescein-labeled class C β-lactamases for sensing β-lactam antibiotics and β-lactamase inhibitors. Furthermore, because of the conserved enzyme activity of V211Cf as the wild-type enzyme, V211Cf may serve as an attractive tool for mechanistic studies of the class C β-lactamase. Last but not least, our study further supported the applicability of utilizing a non-allosteric protein modified with a fluorophore close to the active site as a sensing system for its ligands. This opens up an innovative approach for the development of enzymes into reagentless biosensors.

Acknowledgments

I am deeply indebted to my chief supervisor, Dr. Thomas Y.C. Leung for his guidance, support and encouragement. In addition, I would like to express my sincere gratitude to my co-supervisor, Prof. K.Y. Wong for his advices and valuable comments on this project.

Moreover, I would like to thank Dr. P.H. Chan for his precious comments on the design of the fluorescein-labeled class C β-lactamases. Besides, I would like to thank Prof. C.W. Tsang for his constructive comments on this project and also Mr. P.K. So for his generous assistance in mass spectrometry.

In addition, I would like to express my appreciation to Mr. C.H. Cheng, Dr. M. Yau, Ms. K.L. Yeung and other technical staff at the Biology Section of the Department of Applied Biology and Chemical Technology for their technical assistance.

Enormous thanks were gone to my teammates and friends, especially Ms. H.W. Au, Ms. K.Y. Choy and Ms. W.M. Lam, at the Department of Applied

Biology and Chemical Technology for their friendships and helps.

Furthermore, I would like to acknowledge the Research Committee of the Hong Kong Polytechnic University for offering me a studentship and a tuition scholarship in 2002 – 2006.

Last but not least, love and appreciations are extended to my family for their patience and unceasing support throughout my postgraduate studies.

Abbreviations

[X]	Concentration of solution X
6-APA	6-aminopenicillanic acid
7-ACA	7-aminocephalosporanic acid
Amp C	Class C Amp C beta-lactamase
A_x	Absorbance at wavelength of x nm
B. cereus	*Bacillus cereus*
B. subtilis	*Bacillus subtilis*
BSA	Bovine serum albumin
$CaCl_2$	Calcium chloride
cat	Chloramphenicol acetyl transferase gene
CH_3CN	Methyl cyanide
Cm^R	Chloramphenicol resistant
Cm^S	Chloramphenicol sensitive
dH_2O	Deionized water
DMF	Dimethyl formamide
DNA	Deoxyribonucleic acid
E. cloacae	*Enterobacter cloacae*

E. coli	*Escherichia coli*
EDTA	Ethylene-diaminetetra-acetic acid
*erm*C	Gene conferring erythromycin resistance
Er^R	Erthromycin resistant
Er^S	Erthromycin sensitive
h	Hour(s)
H. influenza	*Haemophilus influenza*
HCl	Hydrochloric acid
IC_{50}	Inhibition constant
kDa	Kilodaltons
LB medium	Luria-Bertani medium
M	Molar
MAPB	3-aminophenyl boronic acid
MeOH	Methanol
min	Minute(s)
MW	Molecular weight
MWCO	Molecular weight cut-off
NaCl	Sodium chloride
NMWL	Nominal molecular weight limit

OD_x	Optical density at wavelength of x nm
ori	Origin of replication
P. vulgaris	*Prunella vulgaris*
PBP	Penicillin binding protein
PCR	Polymerase chain reaction
PenPC	Beta-lactamase I from *Bacillus cereus*
rpm	Revolutions per min
s	Second(s)
S. aureus	*Staphylococcus aureus*
SDS	Sodium dodecyl sulphate
SDS-PAGE	Sodium dodecyl sulphate - polyacrylamide gel electrophoresis
TEMED	N,N,N',N'-Tetramethyl-ethylenediamine
Tris-HCl	Tris(hydroxymethyl)aminomethane
UV	Ultra violet light
v	Velocity
V	Volts
v_0	Initial velocity
α	Alpha

β	Beta
Δ	Delta; change of
ε	Extinction coefficient
Ω	Omega

Table of contents

Chapter I

Introduction

I.1. *β*-lactam antibiotic

β-lactam antibiotics, including penicillins and cephalopsorins, have been effective therapeutics commonly used for combating various bacterial infections (DiPiro and May, 1988; Joshi and Milfred, 1995). They are characterized by a four-membered *β*-lactam ring and classified into four main classes including penams, penems, cephems and monocyclic *β*-lactams according to their specified structures (Figure I.1).

The conserved *β*-lactam ring is a critical feature responsible for their antibacterial effect of interference with cell wall biosynthesis. Bacterial cell wall, which provides structural rigidity to the cell essential for bacterial survival, is made up of a mesh of cross-linked peptidoglycan. The highly reactive amide bond of the *β*-lactam ring is thought to resemble the peptide bond in D-alanyl-D-alanine of the peptide branch of uncross-linked peptidoglycan (Tipper and Strominger, 1965; Lee, 1971). Based on this reason, *β*-lactam antibiotics act as structural analogs of acyl-D-alanyl-D-alanine substrate of transpeptidase (also known as

penicillin-binding protein, PBP), a bacterial enzyme involved in cell wall formation. They inactivate the enzyme by acylating its active site serine to form a stable non-catalytic acyl-enzyme complex (Figure I.2). With the active site covalently-modified by *β*-lactam antibiotic, transpeptidase can no longer catalyze the cross-linking of peptidoglycan which is an essential final step in bacterial cell wall assembly (Lee *et al.*, 2001), resulting in a formation of mechanically weakened cell wall. Finally, the loss of cell wall integrity increases the susceptibility of the bacteria to osmotic stress, eventually causing cell death.

With the mechanistic action of *β*-lactam antibiotics working on bacterial cell wall synthesis, the application of these agents in antibacterial therapy offers several advantages making them successful and popular in the human and veterinary medicine. First, *β*-lactam antibiotics can effectively inactivate proliferation of active growing bacteria which require rapid cell wall biosynthesis. Second, *β*-lactam antibiotics generally ensure safe therapies on mammals by specifically targeting at cell wall assembly which is a process virtually absent in the eukaryotic world (Frère *et al.*, 1992; Projan, 2002). Therefore, in addition to good pharmacokinetic, minimal side effect and cost effectiveness, *β*-lactam antibiotics have been antibacterial agents frequently used in clinical practice and

animal husbandry since their clinical introduction for over 50 years, and nowadays account for more than 65% worldwide antibiotic market (Elander, 2003).

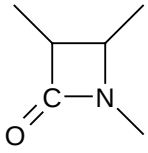

1

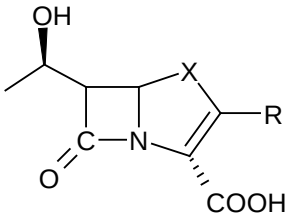

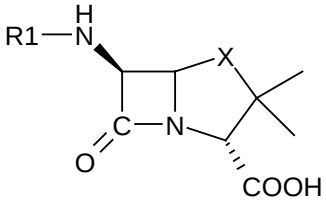

2 **3**

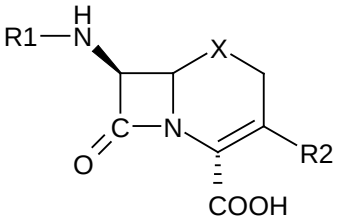

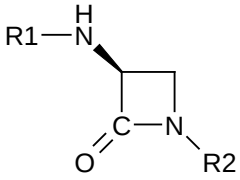

4 **5**

Figure I.1. The generalized structures of *β*-lactam ring **1** that is a basic skeleton of the *β*-lactam antibiotic and the four major classes of *β*-lactam antibiotic including penem **2**, penam **3**, cephem **4** and monocyclic *β*-lactam **5**.

(A)

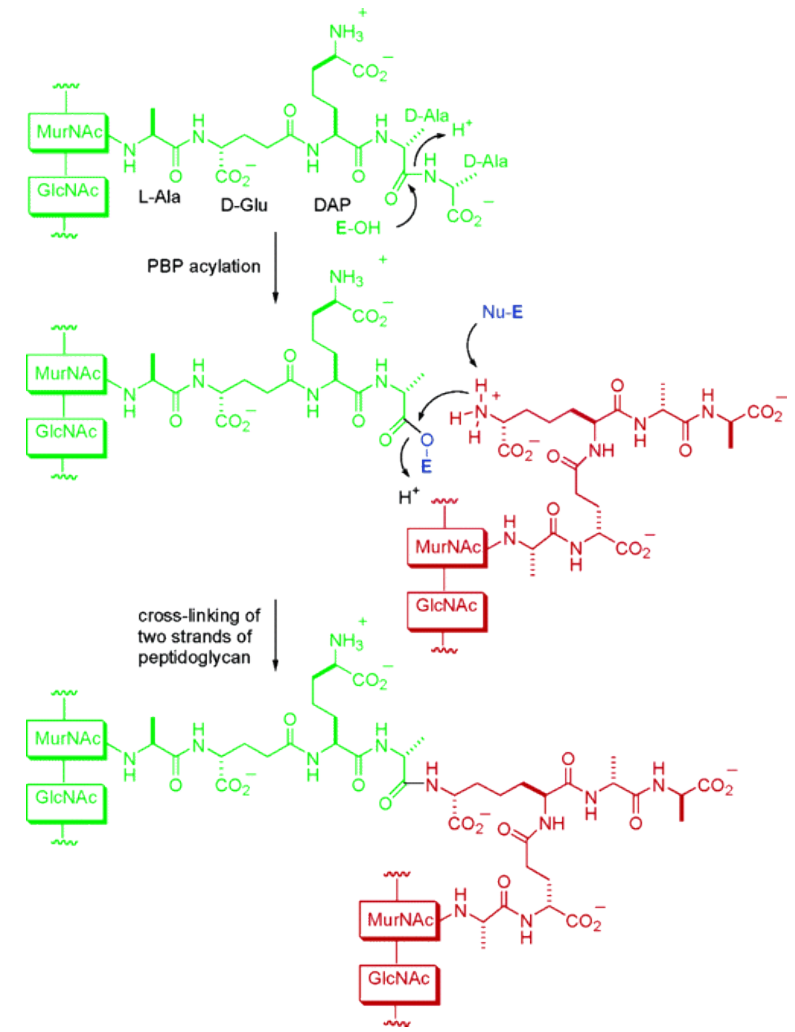

(B)

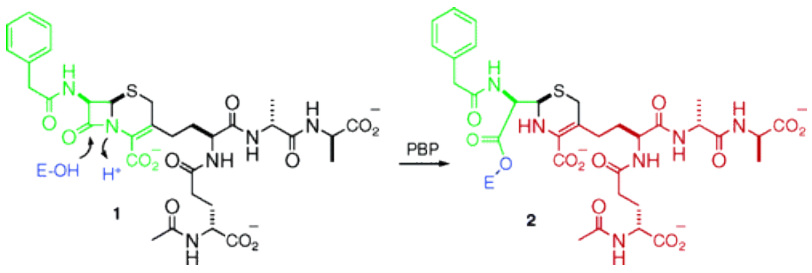

Figure I.2. Cross-linking of peptidoglycan via transpeptidation catalyzed by PBP and its inhibition by a cephalosporin. (A) At the last stage of cell wall

assembly, transpeptidation begins with acylation of the active-site serine of PBP (denoted by E) by the peptide of the first strand of peptidoglycan (in green). The second strand of the peptidoglycan (in red) is then reacted with the ester of the acyl-enzyme intermediate to give rise to a cross-linked cell wall. (B) In the presence of cephalosporin **1**, due to the similarity of the backbone of cephalosporin (in green) with the terminal acyl-D-alanyl-D-alanine portion of the peptide chain of the first strand of the peptidoglycan, the antibiotic acylates the active site of PBP in the way as the peptide from the first strand of peptidoglycan does, resulting in an acyl-enzyme complex **2**. The acyl-enzyme species mimics the geometry of the first enzyme-bound peptidoglycan strand (shown in green) poised to receive the amine of diaminopimete (DAP) from the second strand of peptidoglycan (shown in red). This figure is adapted from Fisher *et al.* (2005).

I.2. *β*-lactamase

I.2.1. Background of *β*-lactamase

β-lactamase (*β*-lactam hydrolase; E.C. 3.5.2.6) is a bacterial enzyme of clinical significance as it is usually the primary cause of *β*-lactam antibiotic resistance (Ogawara, 1981; Neu, 1992; Siu, 2002; Wilke *et al.*, 2005; Tenover, 2006). The resistance mechanism to *β*-lactam antibiotic by *β*-lactamase rests on its catalytic action on the hydrolysis of *β*-lactam antibiotic to give a ring opened and bacterially-inert *β*-amino acid. The hydrolytic action is catalyzed either by extracellular *β*-lactamase with high catalytic efficiency (Christensen *et al.*, 1990) or outnumbered amount of enzyme at the periplasmic space (Hechler *et al.*, 1989). As a result, the antibacterial effect of the antibiotic is abolished as the drug has been destroyed before it can reach its physiological target, the transpeptidase that is located on the membrane.

According to the amino acid sequence, *β*-lactamase is classified from class A to D (Ambler, 1980; Kotra *et al.*, 2002; Majiduddin *et al.*, 2002; Samaha-Kfoury and Araj, 2003). These four classes of enzymes fall into two distinct divisions – metalloenzyme and active-site serine enzyme – regarding to their basis of mechanistic action (Frère *et al.*, 1999). Class B *β*-lactamase is a metalloenzyme

that utilizes a zinc ion as a catalytic centre and its mechanistic action on β-lactams involves the formation of a non-covalently bound intermediate. In contrast, class A, C and D β-lactamases are active-site serine enzymes that proceed the hydrolytic reaction through the transient formation of a covalent acyl-enzyme complex as illustrated in Scheme I.1. After the first encounter with the β-lactam substrate, the catalytic serine attacks the carbonyl carbon of the β-lactam, opening its four-membered β-lactam ring to generate a covalent acyl-enzyme complex. Afterwards, the resultant covalent complex is attacked by an activated water molecule. Consequently, the covalent bond between the serine Oγ atom and the lactam carbonyl carbon is disrupted, subsequently releasing the hydrolyzed product and regenerating a free enzyme.

Of these two mechanistic divisions of β-lactamases, the serine enzymes are more dominant than their zinc-dependent counterparts. In particular, the class A and C enzymes are currently the most and second-most prevalent classes of β-lactamases respectively, representing immediate threats on the antibiotic therapy (Rice and Bonomo, 2000). Therefore, they have been subjected to immense studies for understanding their structure-function relationships.

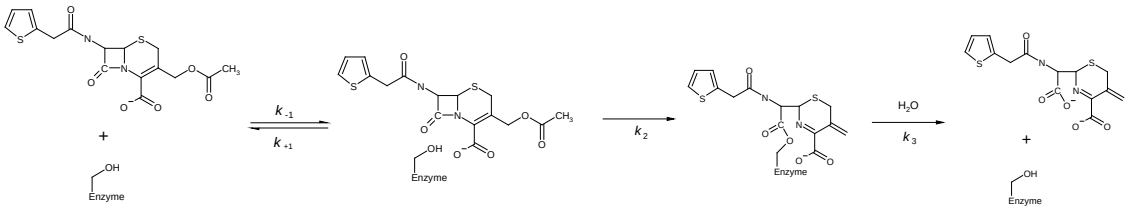

E + S ES ES* E + P

Scheme I.1. The reaction pathway of the serine β-lactamase. Free enzyme, E; substrate, S; pre-covalent substrate-enzyme complex, ES; acyl-enzyme complex, ES*; hydrolyzed product, P.

I.2.2. Class A and class C *β*-lactamases

Class A and class C *β*-lactamases are monomeric proteins with sizes of about 29 kDa and 39 kDa respectively. With their differences in the genetic nature of the structural gene, source of bacteria and also distribution in the cell, discrepancies in site of action and form of protection against the *β*-lactam agents are found between these two classes of *β*-lactamases (as listed in Table I.1).

As revealed by structural information (Lobkovsky *et al.*, 1993; Knox *et al.*, 1996) and phylogenetic studies (Hall and Barlow, 2003 and 2004), they are evolutionarily-related enzymes descended from PBP, sharing topological similarity (Massova and Mobashery, 1998 and 1999). Despite arisen from a common ancestral protein, divergence in the evolutionary paths of class A and class C *β*-lactamases (Bulychev and Mobashery, 1999) resulted in diversification in some of their structural features that may differentiate their catalytic machineries for substrate hydrolysis. Here, the molecular structures, the catalytic mechanisms and the catalytic properties of these two closely-related enzymes are compared and discussed in Section I.2.2.1 – I.2.2.3 respectively.

Table I.1. Comparison of the distribution and dissemination of class A and class C *β*-lactamases (Medeiros, 1997)

	Class A *β*-lactamases	**Class C *β*-lactamases**
Distribution among bacteria	In both gram-negative and gram positive bacteria	Only in gram-negative bacteria
Structural gene	Often on plasmids or transposons	Usually chromosomal
Regulation of production	Rarely inducible, except in *S. aureus* and *P. vulgaris*	Often inducible
Location in cell	Periplasmic space or excreted from the cell	Periplasmic space
Protection against *β*-lactam antibiotics	Protection to a population of cells if it is in a secretory form (e.g. in the case of *S. aureus*) or if cells lack a permeability barrier (e.g. in the case of *H. influenza*)	Protection to single cells

I.2.2.1. Molecular structures of class A and class C *β*-lactamases

The general architecture of these two families of *β*-lactamases is delineated by two structural domains – an all-*α* domain and a mixed *α*/*β* domain. As class C *β*-lactamase has additional loops and secondary structure on its all-*α* domain, it has a larger size than its class A counterpart. The active site of both enzymes is situated at the groove in-between the all-*α* domain and the *α*/*β* domain, forming the core of the catalytic cavity. The geometry of this active site cavity is maintained by several conserved residues that surround the catalytic centre. And the equivalent structural and functional elements of class A and class C *β*-lactamases that defines this cavity are revealed in Figure I.3.

The first structural component to be mentioned here is the Ω-loop. It is a segment of loosely-packed residues that delimits the bottom of the active site cavity. Although it is a common feature in both class A and class C *β*-lactamases, the Ω-loops of the two enzymes are strikingly different (Lobkovsky *et al.*, 1993; Knox *et al.*, 1996). First, the Ω-loop of the class C enzyme is twice the length of that of the class A enzyme. As the Ω-loop forms the border of the active site pocket, the longer Ω-loop in class C enzyme in term gives rise to a larger substrate binding site in the class C enzyme than its class A counterpart. The larger binding

site allows better accommodation of bulky substrate at the class C enzyme, partially accounting for the substrate preference of the class C enzyme on cephalsoporins that are typically larger in size and have bulkier functional groups. Second, the conformation of the Ω-loop of the class C enzyme is distinct from that of the class A enzyme. As illustrated in Figure I.4, this loop structure in class C enzyme is twisted and has an orientation running anti-parallel to that of the class A enzyme. Third, the Ω-loop of class C enzyme does not contain any catalytic important residues while that of class A enzyme does. And this will be further elaborated in the following part.

In addition to the Ω-loop, four structural and functional elements constituting the catalytic cavity are identified (Frère, 1995; Galleni *et al.*, 1995). The first element is a S-X-X-K motif which constitutes a turn in a long helix running from the all-α domain to the α/β domain. The first residue of this motif is the active site serine and it is in close proximity with the side-chain of an invariant lysine residue located at the helix-turn downstream. This element corresponds to the core of the active site cavity. The second element is composed of three residues lied on a short loop in the all-α domain. The side chains of the first and third residues protrude to the active-site cleft, making up one side of the catalytic cavity. The

third element is a triad on the innermost strand of the β-sheet in the α/β domain, forming an opposite edge of the catalytic pocket. Whilst the three elements mentioned above are consensus for both class A and class C β-lactamases, the fourth element, an E166 residue, is indeed a unique feature in class A β-lactamase. It is located on the Ω-loop with its side chain pointing towards the active site. It plays an indispensable role in the catalytic reaction in the class A β-lactamase (Escobar *et al.*, 1991; Leung *et al.*, 1994; Banerjee *et al.*, 1998). It has been suggested that class C β-lactamase lacks a functional acidic residue corresponding to Glu166 in class A enzyme (Nukaga *et al.*, 1993). Although Asp217 in class C β-lactamase has a similar spatial arrangement as Glu166 in the class A enzyme, its side chain is pointing away from the active site cavity and it has been found to be having no functional role in the catalysis (Tsukamoto *et al.*, 1990; Zhang *et al.*, 2001).

Because of the consensus of the structural and functional elements, the local environments of the active site pockets of class A and class C β-lactamases are analogous to each other (Figure I.5). In both enzymes, the conserved residues in the active site pocket are strategically positioned to form a dense array of hydrogen-bonding network systems that participates in the catalysis. In addition,

sites for molecular recognition, for instances, a cationic recognition site for the C(3)4' substrate carboxylate (Fenollar-Ferrer *et al.*, 2003) and an oxyanion hole for the carbonyl group of *β*-lactam ring (Murphy and Pratt, 1988; Usher *et al.*, 1998) are strictly conserved in the active site pocket among the two enzymes. The major difference between the active site pockets of the two *β*-lactamases is the presence of a tightly-bound water molecule with Glu166 residue on the Ω-loop in class A *β*-lactamase. It is proposed that this water molecule forms a bridge between the hydroxyl group of Ser70 and carboxylate side chain of Glu166 and is well-coordinated for nucleophilic attack on the acyl-enzyme complex in the hydrolytic reaction (Guillaume *et al.*, 1997).

(A) **(B)**

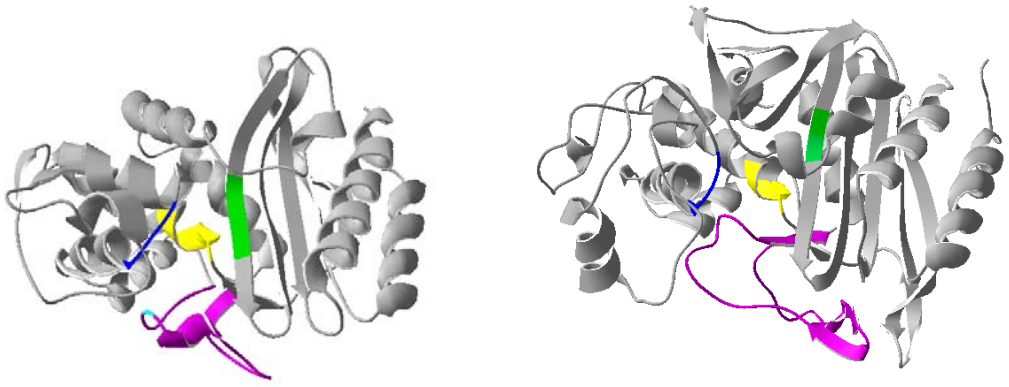

(C)

	Structural element	Structural and functional elements			
	Ω-loop	**Element 1**	**Element 2**	**Element 3**	**Element 4**
Class A	^{160}X – ^{181}X	^{70}S*-X-X-K	^{130}S-D-N ^{130}S-D-S ^{130}S-D-G	^{234}K-T-G ^{234}K-S-G ^{234}R-T-G ^{234}R-S-G	^{166}E
Class C	^{187}X – ^{225}X	^{64}S*-X-X-K	^{150}Y-A-N ^{150}Y-S-N	^{315}K-T-G	No equivalent residue

Figure I.3. Comparison of the tertiary structures of class A *β*-lactamase (A) and class C *β*-lactamase (B). The equivalent structural and functional elements of the two classes of *β*-lactamases are listed (C) and shown as follows: Ω-loop, magenta; element 1, yellow; element 2, blue; element 3, green; and element 4, cyan. The active site serine is marked by an asterisk and "X" refers to a variant amino acid residue. Figure (A) and (B) are generated by SwissPdb Viewer (Guex and Peitsch, 1997).

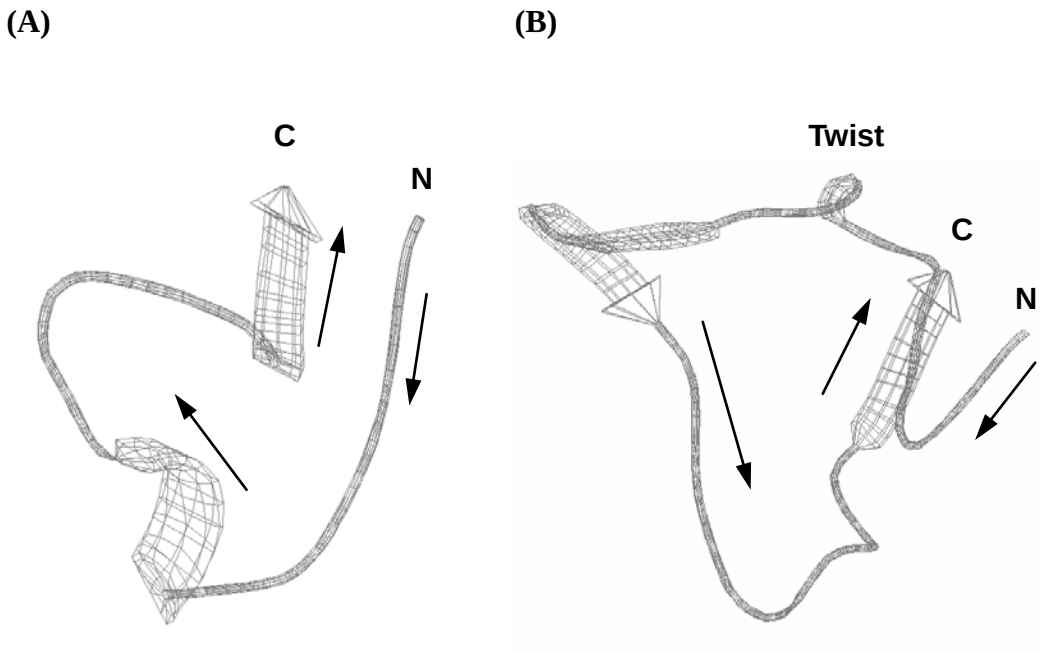

Figure I.4. Comparison of the conformations of the Ω-loop of class A *β*-lactamase (A) and that of class C *β*-lactamase (B). The N-terminal end and C-terminal end of the loop are shown by "N" and "C" respectively. The loop direction is indicated by black arrows. The Ω-loop of class C *β*-lactamase is twisted and extends in a direction reverse to that of the class A *β*-lactamase. Figures (A) and (B) are generated by SwissPdb Viewer (Guex and Peitsch, 1997).

(A)

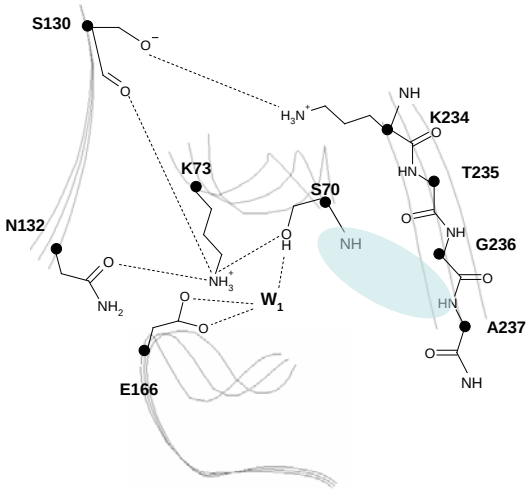

(B)

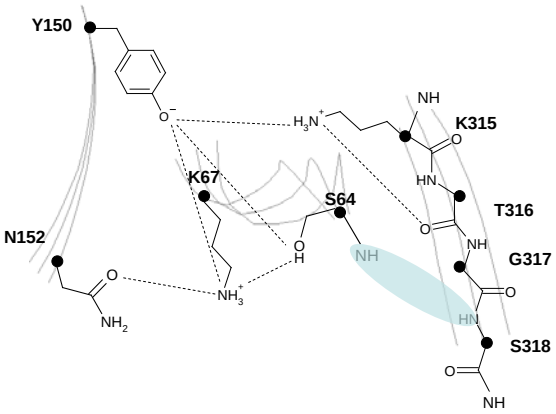

Figure I.5. Comparison of the local environments of the active site pockets of class A *β*-lactamase (A) and class C *β*-lactamase (B). W_1 indicates a water molecule. The shaded area refers to an oxyanion pocket formed by the backbone amides of the active site serine and Ala237 in class A *β*-lactamase or Ser318 in class C *β*-lactamase (Matagne *et al.*, 1998; Beadle *et al.*, 2002; Fenollar-Ferrer *et al.*, 2003). Figures (A) and (B) are generated by SwissPdb Viewer (Guex and Peitsch, 1997).

I.2.2.2. Catalytic mechanisms of class A and class C *β*-lactamases

As described in Section I.2.1, class A and class C *β*-lactamases take the same mechanistic action involving a formation of a covalent acyl-enzyme intermediate in the turnover of *β*-lactam antibiotics. With the utilization of a serine residue as the catalytic centre, they hydrolyze *β*-lactams through a three-step process which is composed of substrate binding, acylation and deacylation (Beadle *et al.*, 2002).

The first step of the reaction is a reversible substrate binding to the active site pocket to form the enzyme-substrate (ES) complex. In this step, *β*-lactamase recognizes its substrate through the electrostatic attractions between the cationic side chains of the residues resided on the active site and the carboxylate of the *β*-lactam substrate. Next, the substrate is positioned within the active site through a network of hydrogen bonds and non-polar interactions that stretch across the entire molecule, leading to the formation of a pre-covalent complex. This complex orients the substrate for the nucleophilic attack by the active site serine in the next acylation step.

Followed by the formation of the pre-covalent complex, acylation, which refers to a general base-catalyzed acyl-transfer from the *β*-lactam to the enzyme,

occurs (Figure I.6.A). First, a general base is recruited for abstracting proton from the hydroxyl group of the active site serine, thereby increasing the nucleophilicity of the serine residue. The activated serine then attacks the carbonyl carbon of the *β*-lactam ring, giving rise to a tetrahedral intermediate. With a subsequent proton transfer back from the general base to the departing *β*-lactam amine, the intermediate collapses followed by a ring cleavage and formation of the acyl-enzyme complex (ES*).

The final step is the deacylation of the acyl-enzyme adduct (Figure I.6.B). This step involves a hydrolytic water molecule, presumably activated by proton removal by a nearby general base. This activated water molecule is responsible for the nucleophilic attack on the acyl-enzyme adduct to give a transient intermediate. Breakdown of this intermediate is then resulted from a proton donation from the base to the departing serine. The turnover of substrate ends up with the release of the hydrolyzed product and the enzyme active site is consequently regenerated.

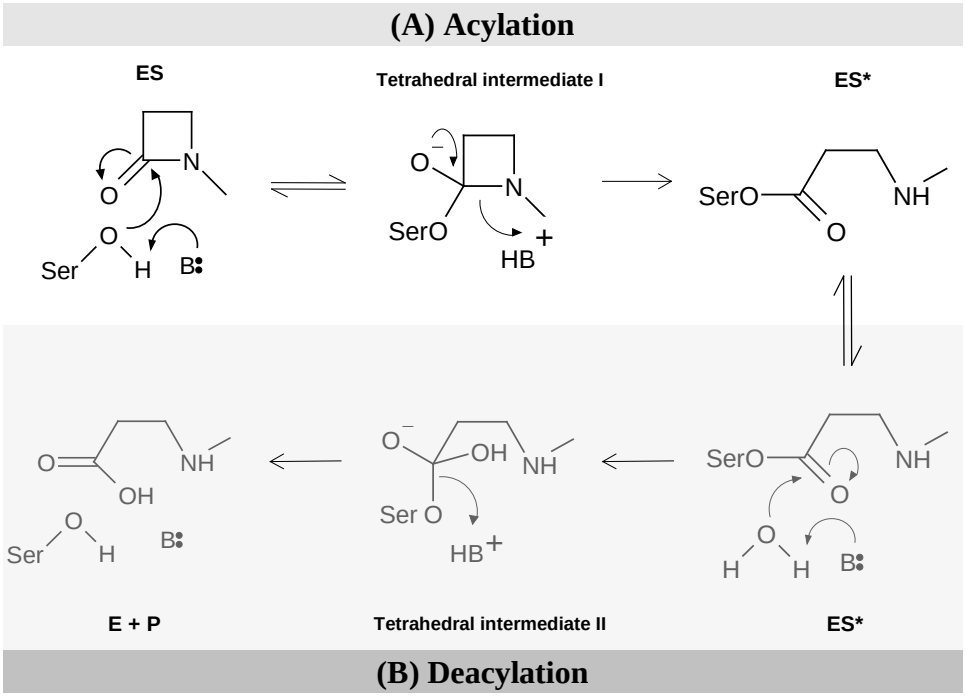

Figure I.6. Steps of acylation (A) and deacylation (B) along the reaction pathway of serine β-lactamase with the participation of the general base. B: general base; E, free enzyme; ES, noncovalent enzyme-substrate complex; ES*, covalent acyl-enzyme complex; P, product. This figure is modified from Page and Laws (1998).

I.2.2.3. Catalytic properties of class A and class C *β*-lactamases

The catalytic efficiency of *β*-lactamase is governed by the steady-state kinetic parameters of k_{cat} and k_{cat}/K_m. Respective to the three-step reaction of serine *β*-lactamase in substrate hydrolysis depicted in Scheme I.1, the turnover number, k_{cat} (= k_2k_3 / k_2+k_3) reflects the deacylation rate, k_3 whereas the specificity constant, k_{cat}/K_m, which is defined by k_2/K' (where $K' = k_{-1}+k_2 / k_{+1}$), is an independent parameter to deacylation rate and corresponds to the second order rate constant for the acylation reaction (Waley, 1992; Page and Laws, 1998; Page, 1999). With the structural differences of the active site pocket and variations in the catalytic apparatus, class A and class C *β*-lactamases display different catalytic properties towards the *β*-lactam substrates.

First of all, they generally demonstrate a very different catalytic performance towards the two main categories of *β*-lactam antibiotics, penicillins and cephalosporins (Table I.2). When comparing the hydrolysis between penicillins and cephalosporins, very often, class A *β*-lactamase has a higher specificity towards penicillins and shows a relatively higher catalytic efficiency in the turnover of penicillins. In contrast, class C *β*-lactamase has a reverse relationship in the substrate preference and kinetic characteristic with its class A counterpart

(Mustafi *et al.*, 2004). This discrimination in catalytic behaviors of class A and class C *β*-lactamases, in term, distinguishes them as penicillinase and cephalosporinase respectively. And both of these enzymes reach catalytic perfection to their preferred substrates as revealed by high turnover number and values of k_{cat}/K_m close to the upper diffusion limit of $10^7 – 10^8$ $M^{-1}s^{-1}$.

In addition, because of the more sophisticated deacylation system developed in class A *β*-lactamase than class C *β*-lactamase (Adachi *et al.*, 1991), class C *β*-lactamase is less effective than its class A counterpart. While deacylation in class A enzyme is highly efficient and so rapid that there is no accumulation of acyl-enzyme intermediate (Bicknell and Waley, 1985), deacylation is rate-limiting ($k_2>>k_3$) in class C *β*-lactamase resulting in a buildup of acyl-enzyme intermediate. The slow deacylation not only implies the low k_{cat} values of class C *β*-lactamase but also contributes to low K_m values due to the accumulation of acyl-enzyme intermediate coming along with it (Knott-Hunziker *et al.*, 1982; Galleni and Frère, 1988a and 1988b). Thus, the high k_{cat}/K_m of class C *β*-lactamase is sometimes the consequence of low K_m value and low k_{cat} value which is different from that of the class A enzyme correlated with high k_{cat} value. Therefore, even though the k_{cat}/K_m values of both classes of *β*-lactamase are sometimes comparable, the catalytic

performances of these enzymes can be significantly different due to their variations in the k_{cat} values.

Table I.2. Kinetic parameters for the turnovers of penicillin G and cephalosporin C by class A and class C *β*-lactamases (Knox *et al.*, 1996).

		Class A *β*-lactamase	**Class C *β*-lactamase**
Penicillin G	k_{cat} (s^{-1})	2200	14
	k_{cat}/K_m ($mM^{-1}s^{-1}$)	29000	23000
Cephalosporin C	k_{cat} (s^{-1})	14	1100
	k_{cat}/K_m ($mM^{-1}s^{-1}$)	150	2700

I.2.3. Perspective of *β*-lactamase-mediated antibiotic resistance

β-lactamase-mediated antibiotic resistance is of an increasing significance. In response to the selective pressure created by intensive and indiscriminate use of *β*-lactam agents, resistant strains of bacteria emerge as consequences of derepression of chromosomal *β*-lactamase production (Normark *et al.*, 1986; Tejedor-Junco *et al.*, 1998) and dissemination of *β*-lactamase encoding gene (Barker, 1999; Petrosino *et al.*, 1998). To date, more than 470 *β*-lactamases have been identified (Bush, 2001; Fisher *et al.*, 2005) and new variants of *β*-lactamases notably plasmid-encoded cephalosporinases (Bauernfeind *et al.*, 1998; Odeh *et al.*, 2002; Alba *et al.*, 2003), metallo-*β*-lactamases (Walsh, 2005) and extended-spectrum *β*-lactamases (ESBL) (Rahal, 2000; Bradford, 2001;) are increasing in number. This rapid emergence of *β*-lactamases results in therapeutic failures of *β*-lactam antibiotics (Finch, 2002; Brook, 2004) that in term contribute to rise in drug cost, untreatable disease and high mortality, thus posing significant clinical challenges.

I.3. Detection of *β*-lactam antibiotics

I.3.1. Significance of *β*-lactam antibiotic detection

Detection of *β*-lactam antibiotics has been an important field in food and pharmaceutical industries with respect to its two main purposes: quantitative analysis of *β*-lactam antibiotics and identification of potential drug candidates.

Determination of *β*-lactam antibiotic level is an important task in food quality control for reducing the incidence of *β*-lactam antibiotic contamination. As *β*-lactam antibiotics are intensively used as antimicrobials, prophylactic agents and growth promoters in livestock (Shea, 2003), they are the most commonly found type of contaminants in poultry and dairy products (Musser *et al.*, 2001). *β*-lactam antibiotic contamination is of particularity concern as it associates risks in various aspects. First of all, it usually comes across with antibiotic allergy in hypersensitive individuals (Ahlstedt, 1984; Saxon *et al.*, 1987; Kim *et al.*, 2002; Fonacier *et al.*, 2005), interference in the intestinal flora and emergence of bacterial resistance (Lee and Maurer, 2000; Tollefson and Karp, 2004). In addition, from the industrial point of view, it gives rise to technological difficulties in dairy product production by which the *β*-lactam residue in raw milk inhibits the bacterial processes involved in the downstream fermentation. To assure the food is

residue-free and safe for consumption, the levels of antibiotics in food are tightly-regulated and set to certain acceptance limit by the international bodies including FDA and EU. This addresses the need of sensitive, quantitative detection of *β*-lactam antibiotics in the food industry.

Whilst detection of *β*-lactam antibiotics would help reduce the incidences of the antibiotic contamination, it is also important for combating the antibiotic resistance by leading to drug discovery. With the fact that the rapid emergence of bacterial resistance limits the lifespan of the currently-using *β*-lactam antibiotics (Bush, 2004), screening for novel *β*-lactam antibiotics and *β*-lactamase inactivators would fulfill the continuing need for cycles of new antimicrobial discovery and development (Matagne *et al.*, 1999; Essack, 2001; Thomson *et al.*, 2004). This probably ensures effective therapy for infectious diseases, thus important for fighting with the *β*-lactamase-mediated resistance.

I.3.2. Current approaches for *β*-lactam antibiotic determination

Presently, a variety of standard test methods have been established to meet the highly desired demands of quantitative *β*-lactam antibiotic detection. Some of the commercially available tests that are intended for routine determination of

β-lactam antibiotics in milk are outlined in Table I.3.

In general, the existing standard methods can be classified into two groups: microbial inhibition assays and rapid tests. Microbial inhibition tests work on the principle of inhibition of the growth of susceptible bacteria in the presence of *β*-lactams in the testing samples. The test results are usually indicated by a color change that is resulted from the microbial growth in the test setup. Owing to reagentless, simplicity, and ease of use, microbiological tests allow day-to-day basis of screening for *β*-lactam compounds. Nevertheless, as these methods work in broad spectrum and require lengthy incubation to allow the microbial growth, they have the drawbacks of lack of specificity and time-consuming. On the contrary, rapid tests are sensitive methods with results typically available within 5 – 10 min. They are immunoassays like Parallux™ (Huth *et al.*, 2002) and receptor assays, including SNAP® Beta-lactam Test, Charm Test™ (Charm and Chi, 1982; Nouws *et al.*, 1999), *β*-STAR, Delvo-X-Press *β*L-II, and Fluorophos BetaScreen E.U. test (Sternesjö and Johnsson, 1998), based on receptor proteins that are specific for the active *β*-lactam antibiotics. Although rapid tests are superior to the microbial inhibition assays in terms of sensitivity and test duration time, in the routine practice, a single step of rapid test is not sufficient and a broad

spectrum microbial inhibition test is also carried out for residue screening of the milk prior to market (Food Safety Authority of Ireland, 2002).

In addition to the conventional methods described above, numerous approaches for determination of the *β*-lactam antibiotic level have been reported.

Several enzymatic and cell-based methods have been described but with limited success. For examples, a colorimetric method based on the release of *β*-galactosidase by *β*-lactam hypersensitive microorganism reported by Quesada *et al.* (1996) had a shortcoming of a long test duration time; and a whole-cell biosensor relying on pH changes attributed to the degraded carboxylic products from *β*-lactamase-mediated hydrolysis of the *β*-lactams prepared by García *et al.* (1998) was unfavorable for detection of *β*-lactam antibiotics either in trace amount or having great stability towards hydrolytic action by *β*-lactamase owing to its low sensitivity (10^{-3} to 10^{-4} M) as well as the possibilities of obtaining false positives due to the inability of *β*-lactamase to hydrolyze *β*-lactamase-stable antibiotics. In addition, a penicillin biosensor coupling penicillinase activity with pH sensitivity of fluorescein fabricated by Healey and Walt (1995) was of low sensitivity (in mM range).

Alternative immunological assays have been developed for detecting *β*-lactam antibiotics (Chambers *et al.*, 2001; Benito-Peña *et al.*, 2005). They usually provide qualitative determination of the antibiotics by showing promising characteristics of fast reaction time and high sensitivity. However, as antibodies are specific to the particular *β*-lactam structure they raised from, immunoassays always fail to detect among various types of *β*-lactam antibiotics.

While the methods mentioned above are based on biomolecular recognitions, the development of analytical methods should also be highlighted. Chromatographic techniques, for instances, high performance liquid chromatography (HPLC) (Pires de Abreu *et al.*, 2003), liquid chromatography-electrospray ionization tandem mass spectrometry (LC-ESI-MS) (Riediker and Stadler, 2001), and liquid chromatography coupled with chemiluminsecence detection (Kai *et al.*, 2003), have been well-established for analysis of *β*-lactam compounds. In addition, other techniques, namely electrochemiluminescence detection (Liang *et al.*, 1996), surface plasmon resonance-based biosensor (Gustavsson *et al.*, 2004) and electrophoretic method (Cutting et al., 1995), were also reported. These methods usually permit reliable

quantitative and qualitative analytical determinations of β-lactam antibiotics. However, some of these methods are laborious, tedious and require complicated sample preparation steps, limiting their uses in examination of routine samples. In particular, chromatographic methods like mass spectrometry involve highly sophisticated instrumentation, making them too expensive in practice and this restricts their application in post-screening test to confirm the positives obtained from preliminary screening by microbiological test (Anderson *et al.*, 1996; Okerman *et al.*, 2001; Holstege *et al.*, 2002; Ghidini *et al.*, 2003).

Table I.3. Commercially available standard tests purposed for detection of *β*-lactam antibiotics in milk (Food Safety Authority of Ireland, 2002).

	Manufacturer	**Time per test**	**Reaction type**
Microbial inhibition assay			
Delvotest SP Kit	Gist-brocades/DSM	2 h 30 min	Color change
Copan test	Copan Italia SpA	2 h 30 min – 3 h	Color change
Charm Farm	Charm Sciences	2 h 30 min – 3 h	Color change
Charm AIM-96	Charm Sciences	4 h	Color change
Rapid test			
Parallux *β*-Lactam	Idexx Inc.	4 min	Fluorescence
SNAP *β*-Lactam	Idexx Inc.	< 10 min	Color change
Charm MRL *β*-Lactam	Charm Sciences	< 9 min	Color change
β-STAR.	UCB-Bioproducts	5 min	Color change
Delvo-X-Press *β*L-II	Gist-brocades/DSM	< 7 min	Color change
Fluorophos BetaScreen E.U. Test	Advanced Instruments Inc.	10 min	Fluorescence

1.4. Fluorescein-labeled class A *β*-lactamase

Recently, the use of a fluorescein-conjugated class A *β*-lactamase I mutant from *B. cereus* designated as E166Cf has been exploited in the design of a fluorescent sensor for detecting *β*-lactam antibiotics (Chan *et al.*, 2004). Although *β*-lactamase can hydrolyze *β*-lactam antibiotics, with the Glu166 residue on the Ω-loop of the class A enzyme cysteine-point mutated, the enzyme became catalytically impaired. The fluorescent sensor was constructed by incorporating a fluorescein molecule into the position at Glu166 of such hydrolytically defective enzyme (Figure I.7.A). Upon the addition of substrate, the entry of the substrate into the enzyme active site pushed the buried fluorescein molecule away from the hydrophobic pocket. The exposure of the fluorescein molecule to the environment modulates a fluorescence increase (Figure I.7.B). And such substrate-induced fluorescence enhancement serves as the basis of E166Cf as a sensing system for *β*-lactam antibiotics.

This E166Cf was promising as a novel sensor for *β*-lactam antibiotics as it demonstrated high specificity and sensitivity in the quantitative analysis of *β*-lactam antibiotics. In addition, its amenability to a micro-titre plate format implied its feasibility to high throughput screening. The potential uses of E166Cf

was not only limited for detecting the level of the antibiotics in milk and screening for new inhibitors but also for screening bacteria for *β*-lactamase against a panel of antibiotic that can help making an appropriate antibiotic choice in the empirical therapies (Chan *et al.*, 2005).

(A)

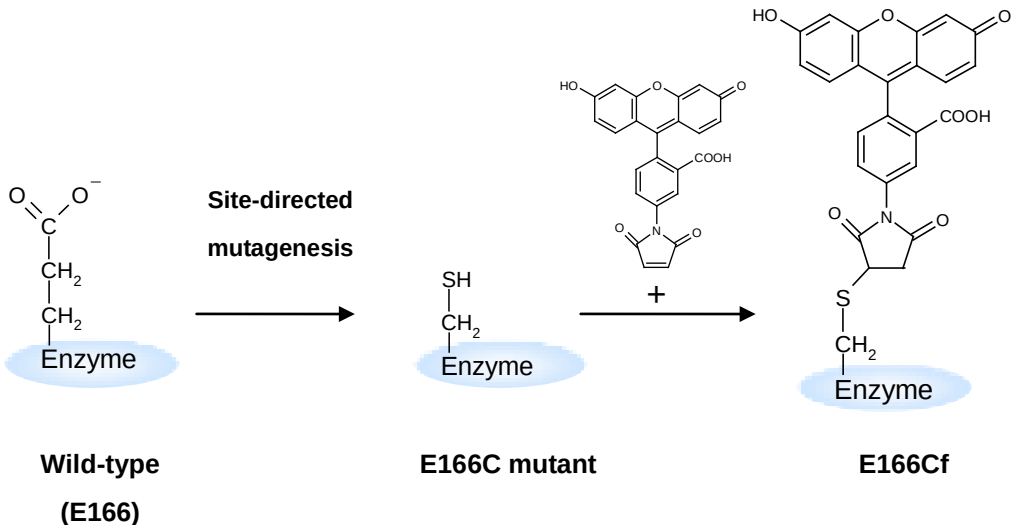

(B)

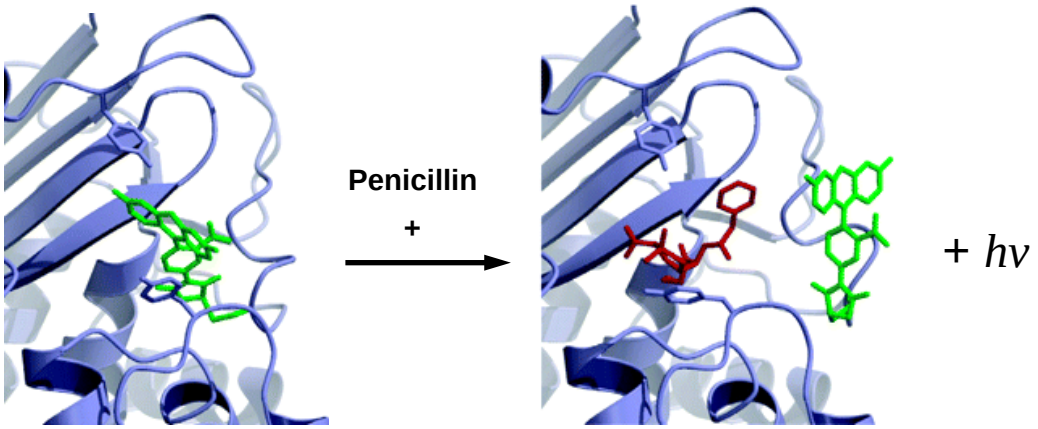

Figure I.7. Construction and working principle of E166Cf. (A) Construction of E166Cf involved two steps: (1) Cysteine substitution at E166 residue of the wild-type enzyme was performed to give an E166C mutant; (2) Conjugation of a fluorescein molecule to the E166C mutant was carried out to give the E166Cf. (B) The rationale of E166Cf for sensing β-lactam antibiotics was formed by the

fluorescence enhancement of E166Cf triggered by the change of the local environment of the fluorescein molecule (green) upon the addition of the substrate (red). Figure (B) is modified from Chan *et al.* (2004).

I.5 Aim of study

With the increasing trends in the development of efficient screening systems for *β*-lactam compounds, the advanced fluorescent biosensor, E166Cf previously described in Section I.4 opened the way to utilize a class A *β*-lactamase tethered to a fluorescein in its active site cavity as a convenient and sensitive sensing tool for *β*-lactam antibiotics and *β*-lactamase inhibitors. As mentioned in Section I.2.2.3, class A *β*-lactamase is a good penicillinase that hydrolyzes penicillins more efficient than cephalosporins. And it was that reason to explain why it exhibited a faster response to penicillins than cephalosporins when it became a fluorescent sensor. Due to the differential substrate profiles between class A and class C *β*-lactamases, we postulated that the better recognition of cephalosporin-type substrates by class C *β*-lactamase than its class A counterpart will make class C enzyme a preferable alternative to be a fluorescent protein for rapid sensing of cephalosporins. Apart from this, searching for potent class C *β*-lactamase inhibitors has been of increasing therapeutic importance owing to the resistance towards the once-dependable third generation cephalosporins attributed to the recent rapid emergence of chromosomal- or plasmid-derived class C *β*-lactamases (Smith, 2000; Nukaga *et al.*, 2004) and the weak inactivation of the class C *β*-lactamase by the existing mechanism-based inhibitors. Therefore, we were

interested in exploring the possibility of turning a class C *β*-lactamase into a sensor for the purpose of detection for *β*-lactam antibiotics and discovery of efficient class C *β*-lactamase inhibitors.

To achieve our goal, in this project, we have prepared a fluorescein-labeled class C *β*-lactamase, V211Cf by introducing a fluorescein molecule to an Amp C *β*-lactamase from *Enterobacter cloacae* P99 (P99 *β*-lactamase) at the position of 211. And this project was divided into five parts. In the first part of the project, we illustrated the structure-based strategy in the rational design of V211Cf. The preparation and characterization of V211Cf were reported in Chapter III.1. The second part of the project focused on the feasibility of V211Cf in the application for sensing *β*-lactam antibiotics. The capability of V211Cf for the detection of penicillins and cephalopsorins was assessed by fluorometric studies as discussed in Chapter III.2. In the third part of the project, studies were performed to investigate the fluorescence properties of V211Cf in the presence of some *β*-lactam-based inhibitors and transition state analogs so as to evaluate the possibility of this fluorescent *β*-lactamase as a probe for inhibitors (Chapter III.3). In addition, in the forth part of the project, attempt to optimize the performance of V211Cf was made by introducing a second mutation (substitution of tyrosine at

the position of 150 with a serine) to the enzyme to give a catalytically impaired Y150S/V211C. This double mutant was then subjected to fluorescein conjugation to give Y150S/V211Cf. The fluorescence properties of this derivative towards β-lactam antibiotics were examined and described in Chapter III.4. The final part of the project aimed for having a comprehensive overview of the fluorescein-labeled class A and class C β-lactamases. Comparisons of the designs and performances among V211Cf, Y150S/V211Cf and the previously reported E166Cf were made and discussed in Chapter IV.

Chapter II

Materials and Methods

II.1. Materials

II.1.1. Bacterial strains and plasmids

E. coli SN03 harboring pNU 354 with *E. cloacae* P99 Amp C *β*-lactamase gene was a kind gift from Dr. M. Galleni of University of Liege, Belgium (Galleni *et. al*, 1988). *E. coli* XL-1 Blue was used as a recipient of the recombinant plasmid. *B. subtilis* 1A304 (ϕ105MU331) was used as a host for the over-expression of the *β*-lactamase wild-type and mutants. *B. subtilis* containing pSG704 was used for the expression of *β*-lactamase I E166C mutant.

Plasmid pSG1113 was a prophage-based vector employed for production of P99 Amp C *β*-lactamase in *B. subtilis* expression system and its map was shown at Figure II.1.

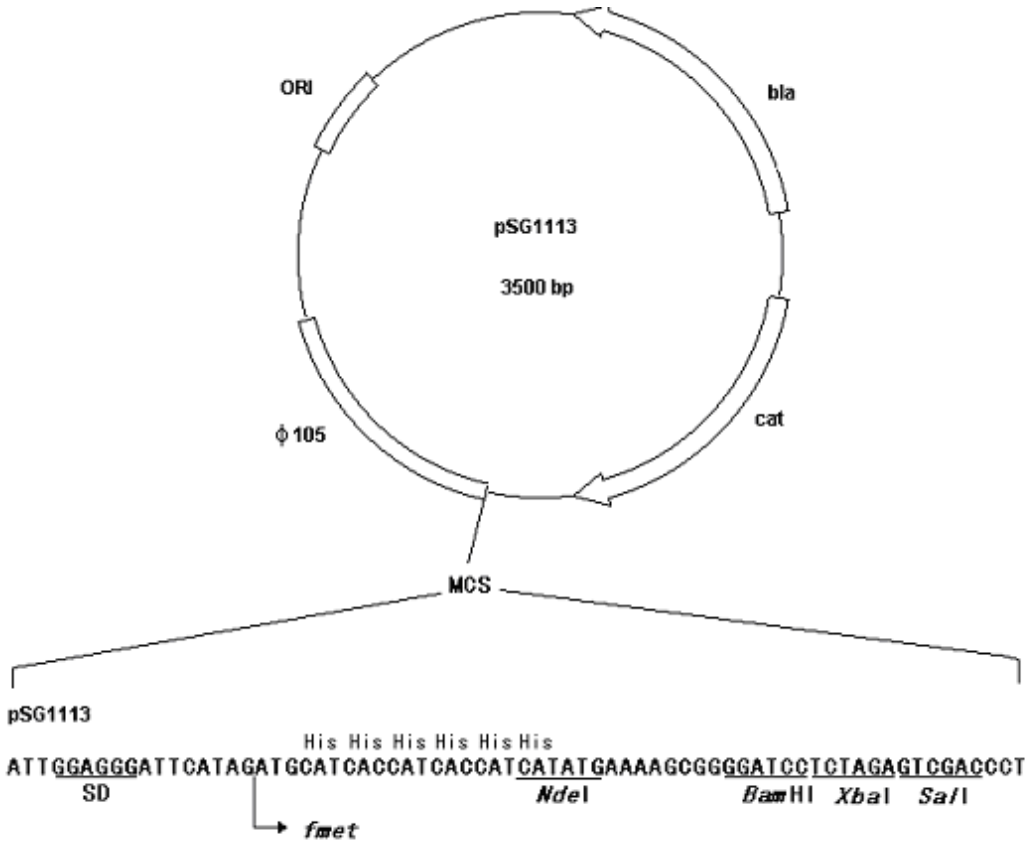

Figure II.1. Plasmid map for integration vector pSG1113. The vector carries a pBR 322 replication origin (ORI) for *E. coli*, the promoter and the Shine-Dalgarno-type ribosome binding site (SD) of prophage ϕ105 MU331. Antibiotic selective markers include *cat* gene for chloramphenicol resistance and *bla* gene for ampicillin resistance. "*fmet*" represents the start codon "ATG" coding for the N-terminal Met residue. Multiple cloning site (MCS) provides the site for insertion of the heterologous gene downstream the sequence encoding for a stretch of six histidine amino acids.

II.1.2. Media

Brain heart infusion, nutrient agar, tryptone and yeast extract were obtained from Oxoid Ltd. (Nepean, Ontario, Canada). For *E. coli* cell cultivation, LB medium was from USB (Cleveland, OH) and 2×TY medium was prepared as listed in Appendix. Spizizen minimal medium, pre-transformation and transformation medium used in the preparation and transformation of *B. subtilis* were prepared as described in the Appendix.

II.1.3. Chemicals

General chemicals were purchased from Amersco, BDH and Sigma Chemical Co. (St. Louis, Mo.). Celite was from BDH. Ampicillin and penicillin G were from USB (Cleveland, OH). 6-APA, 7-ACA, 3-aminophenylboronic acid, 2-thiopheneboronic acid, cephalothin, cefoxitin, ceftriaxone, cefotaxime, chloramphenicol and erythromycin were purchased from Sigma-Aldrich. Nitrocefin was obtained from Becton Dickinson and Company (Cockeyville, Md.). Sulbactam and tazobactam were gifts from Qilu Pharmaceutical Co. Ltd. (Jinan, China). Clavulanic acid was generously provided by Prof. Y. Ishii. 2-(tert-butylamino)sulfonylphenylboronic acid were supplied from Frontier Scientific Inc. (Logan, Utah). Fluorescein-5-maleimide was purchased from

Molecular Probes (Eugene, O.R.).

II.1.4. Proteins

BSA and lysozyme were obtained from Sigma. Restriction enzymes for cloning were purchased from Promega (Madison, WI, USA).

II.2. Preparation and transformation of competent cells

II.2.1. Preparation of *E. coli* competent cells

First, *E. coli* XL-1 Blue strain was cultured in 5 ml sterilized LB medium for 14 – 16 h at 37^{o}C with shaking at 250 rpm. A portion of 200 µl culture was added to 20 ml fresh LB medium and subjected to a further incubation at 37^{o}C with 250 rpm shaking. When OD_{600} reached 0.3 – 0.4, the cells were harvested by centrifugation at 4000 rpm for 20 min at 4 ^{o}C. While the supernatant was discarded, the cell pellet was resuspended in 10 ml of ice-cold 100 mM $CaCl_2$, mixed gently, and kept on ice for 25 min. The cells were again pelleted by centrifugation at 4000 rpm for 20 min at 4 ^{o}C. After that, the cells were resuspended in 0.5 – 1 ml of $CaCl_2$ on ice, mixed gently and held at 4 ^{o}C overnight. Glycerol was added to a final concentration of 15 % (v/v) and the competent cells were aliquoted into eppendorf before a quick freeze by liquid nitrogen. Finally,

the competent cells were stored at - 80 ^{o}C.

II.2.2. *E. coli* transformation and selection

Plasmid and $CaCl_2$ treated-competent cells were mixed in an ice-cold eppendorf tube. It was then incubated on ice for 30 min and heat shocked at 42 ^{o}C for exactly 2 min. Then 200 µl of 2×TY medium was added to the tube, mixed and incubated at 37 ^{o}C for 1 h 30 min. Afterwards, portions of 200 µl of transformed cells were plated on the nutrient agar with appropriate antibiotic and incubated at 37 ^{o}C overnight.

II.2.3. Preparation of *B. subtilis* competent cells

B. subtilis 1A304 (ϕ105MU331) was streaked on nutrient agar plate and incubated at 37^{o}C overnight. A single colony was inoculated into 5 ml pre-transformation medium in a universal bottle. It was then incubated at 37^{o}C with shaking at 280 rpm until its OD_{600} reached 3.0 – 3.3. At this point which was the late exponential phase of *B. subtilis*, the cells had the capability of uptaking DNA and were thus competent for transformation.

II.2.4. *B. subtilis* transformation and selection

About 5 to 10 µg DNA was added to a 100 µl-aliquot of competent cells that were resuspended in 1 ml transformation medium. The suspension was mixed and incubated at 37^{o}C with shaking at 280 rpm for 90 min. During transformation, the target gene was inserted into the *Bacillus* genome by homologous recombination. Positive transformants were selected on nutrient agar plates that were supplemented with chloramphenicol (5 µg/ml) and further screened for erythromycin sensitivity (Er^{S}; 20 µg/ml). Only phenotypic $Cm^{R}Er^{S}$ transformants resulted from the double cross-over (Figure II.2) were isolated for protein expression (Liu *et al.*, 2004).

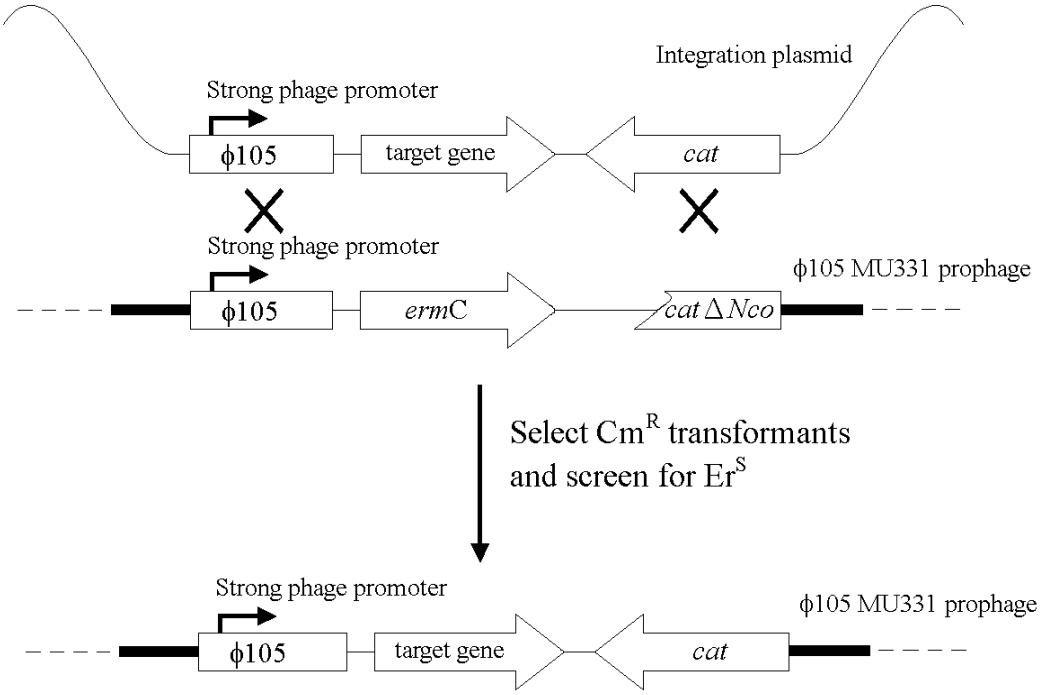

Figure II. 2. Schematic drawing of the construction of a prophage of *B. subtilis* allowing expression of the target gene. The integration plasmid carrying the target gene (shown linearised, as it would be following uptake by a competent cell) was transformed into *B. subtilis* strain 1A304 (ϕ105MU331) with selection for the Cm^R marker, and the transformants were screened for an Er^S phenotype. Such transformants should have arisen from a double-crossover event, as shown, placing the target gene under the control of the strong, heat-inducible ϕ105 phage promoter. Lines: thin line, plasmid; thick line, ϕ105MU331 prophage; and broken line, *B. subtilis* chromosome. Symbols: ϕ105, a *Mun*I-*Nde*I ϕ105 phage DNA

fragment (~600 bp) containing the promoter regions and the Shine-Dalgarno (SD)-type ribosome-binding site from prophage ϕ105MU331 (Leung *et al.*, 1995); *erm*C, gene conferring erythromycin resistance; *cat*, gene conferring chloramphenicol resistance; *cat⊿Nco*, a truncated *cat* gene; and "╳", crossover region of the homologous recombination event.

II.3. DNA manipulation

II.3.1. Subcloning of Amp C gene into pSG1113

Generation of the expression vector for N-terminally His-tagged *E. cloacae* P99 Amp C enzyme was achieved by incorporating the Amp C gene into pSG1113 to give pSG1113/M. Plasmid pNU354 isolated from *E. coli* SN03 by Wizard® Plus SV Minipreps DNA Purification System (Promega) was served as the template for *E. cloacae* P99 Amp C gene amplification. To facilitate the insertion of the target gene into the cloning vector, *Nde*I and *Xba*I sites were incorporated into the 5' and 3' ends of the Amp C gene with forward primer: 5' – CGA CTT CAT ATG ACG CCA GTG TCA GAA AAA CAG CTG – 3' and reverse primer: 5' – CAG ATT TCT AGA TTA CTG TAG CGC CTC GAG GAT ATG – 3' respectively via PCR using Expand™ Fidelity PCR system (Boehringer Mannheim). The PCR profile was set as follows: pre-denaturation at 94°C for 5 min; 25 cycles of denaturation at 94°C for 1 min, annealing at 44°C for 1 min for amplification of Amp C gene, elongation at 72°C for 1 min; and a final step of further elongation at 72°C for 7 min. The vector and amplified PCR product were subsequently subjected to double digestion by *Nde*I and *Xba*I at 37°C overnight. Digested fragments of vector and insert were gel-purified by the Agarose Gel DNA Extraction Kit (Roche) and ligated by Quick Ligation™ Kit (New England

Biolabs, Inc.). $CaCl_2$ -treated *E. coli* XL1-Blue cells (ampicillin sensitive) were transformed with the recombinant plasmid and clones were selected on nutrient agar supplemented with ampicillin (80 μg/ml). The identity of clones was verified by DNA sequencing with specific primers.

II.3.2. Site-directed mutagenesis of Amp C gene

Site-directed mutagenesis of Amp C gene was performed by overlap extension PCR (Ho *et al.*, 1989). This method comprised two rounds of PCR steps. In the first round PCR step, two separate PCR reactions were performed, one amplifying the 5'-portion of the insert using a forward primer: 5' – CGA CTT CAT ATG ACG CCA GTG TCA GAA AAA CAG CTG – 3' and a reverse mutagenic primer, and the other amplifying the 3'-portion of the insert using a reverse primer: 5' – CAG ATT TCT AGA TTA CTG TAG CGC CTC GAG GAT ATG – 3' and a forward mutagenic primer. The PCR products obtained from the first round PCR were gel-purified and then annealed to get a full length of the mutated gene in the second round of PCR reaction. Mutated gene was then subcloned to pSG1113 and sequenced entirely to confirm the introduction of the desired mutations and the absence of the unwanted mutations.

II.4. Expression of β-lactamases in *B. subtilis*

β-lactamases used in this study were over-expressed in *B. subtilis* strain 1A304 (ϕ105MU331). *B. subtilis* cells containing the β-lactamase gene was streaked on a nutrient agar plate with 5 μg/ml chloramphenicol and incubated at 37°C overnight. A few single colonies were inoculated into 25 ml BHY medium (37 g/L Brain heart infusion and 5 g/L yeast extract, pH 7.0) in a 250 ml-flask. It was incubated at 37°C and shaked at 300 rpm for 12 – 13 h. This pre-culture was transferred to a baffled flask containing fresh BHY medium in 1:20 dilution, followed by incubation at 37°C with shaking at 300 rpm. Cell growth was monitored by measuring the optical density at 600 nm of wavelength (OD_{600}). When OD_{600} reached 3.0 – 3.5, protein production was heat-induced at 50°C for 5 min with agitation. Then the culture was subjected to further 5 – 6 h incubation at 37°C with shaking at 300 rpm. Afterwards, centrifugation was performed at 4°C, 9000 rpm for 20 min. For extracellular expression of β-lactamase I, the supernatant of the bacterial culture was collected, adjusted to pH 7.0 with concentrated HCl and immediately subjected to purification. On the contrary, for intracellular His-tagged P99 β-lactamase expression, cell pellet was collected and resuspended in solubilization buffer containing 50 mM Tris-HCl (pH 8.0) and 0.1 M NaCl and stored at – 80°C till subsequent purification steps.

II.5. Purification of β-lactamases

II.5.1. Purification of extracellular β-lactamase I

β-lactamase I was purified on the basis of its affinity with celite. First, absorption of β-lactamase I on celite was accomplished by mixing the supernatant with 40 g of celite for 20 min in an ice bath. After discarding the supernatant, the celite was washed with deionized water so as to remove the unbound proteins. After that, elution of the celite-bound β-lactamase was achieved by mixing the celite with 300 ml of protein elution buffer (100 mM Tris-HCl, 2 M NaCl and 100 mM tri-sodium citrate, pH 7.0). The protein solution was then concentrated to 10 ml at 4 °C using an Amicon concentrator equipped with a piece of YM-1 membrane (Millipore, MWCO = 1000). The concentrated protein solution was exchanged with 20 mM NH_4HCO_3 and then freeze-dried. The freeze-dried protein was kept at –20 °C for storage.

II.5.2. Purification of intracellular His-tagged P99 β-lactamase

Prior to purification of intracellular protein, cell lysis was performed as follows: pellet resuspended in solubilization buffer was incubated with 75 μg/ml lysozyme for 1 h at 30^{o}C, followed by a 30 s-sonication for 5 times with a Soniprep 150 ultrasonic disintegrator (MSE Scientific Instrument, England).

Afterwards, bacterial lysate was cleared of cellular debris by centrifugation at 10,000 g for 1 h at 4^{o}C.

Metal affinity chromatography was performed using an Amersham-Pharmacia ÄKTA FPLC system (Amersham-Pharmacia Biotech Inc., Piscataway, NJ). The clarified supernatant was loaded on a nickel II sulfate charged 5-ml HiTrap chelating column (Amersham-Pharmacia Biotech Inc.) that was pre-equilibrated with start buffer made up of 20 mM sodium phosphate buffer, pH 7.4 containing 0.5 M NaCl. The column was then washed with 6 column volumes of the start buffer and the His-tagged protein was eluted by a linear imidazole gradient from 0 to 0.2 M or 0.5 M. Fractions containing the enzyme activity were pooled and dialyzed against a 20 mM potassium phosphate buffer, pH 7.4. Amp C β-lactamase was purified to more then 95% homogeneity by a single step of this chromatographic procedure. For long-term storage, the purified enzyme was buffer-exchanged with 20 mM NH_4HCO_3, lyophilized and stored at –20^{o}C.

II.6. Labeling of β-lactamases with fluorescein-5-maleimide

II.6.1. Labeling of native β-lactamase

To label the protein in a native condition, lyophilized β-lactamase was first dissolved in 50 mM potassium phosphate buffer (pH 7.0). 10-fold molar excess fluorescein-5-maleimide in DMF was added to the protein solution prior to an overnight-incubation in the dark with stirring. Afterwards, excess dye was removed by buffer exchange with 50 mM potassium phosphate buffer by dialysis or using the device of Amicon Ultra-15 (NMWL = 10,000). The labeled mutant was then stored at –80 °C.

II.6.2. Labeling of unfolded β-lactamase

Lyophilized β-lactamase was dissolved in 6 M guanidinium hydrochloride. The protein solution was incubated at room temperature for 30 min to allow the unfolding of protein. Afterwards, 10-fold molar excess of fluorescein-5-maleimide in DMF was added to the protein solution and the pH of the mixture was adjusted to 7.5 with 0.2 M sodium hydroxide. The labeling reaction was carried out by stirring the mixture at room temperature for 3 h in the dark. After that, removal of excess dye was achieved by buffer exchange with 50 mM potassium phosphate buffer by dialysis or using the device of Amicon Ultra-15 (NMWL = 10,000). The labeled mutant was then stored at –80 °C.

II.7. SDS-polyacrylamide gel electrophoresis (SDS-PAGE)

Protein samples were analyzed on 12 % SDS-PAGE in a Mini-PROTEAN III dual slab cell (Bio-Rad Laboratories) based on the difference in relative molecular weight. The sample was mixed with reducing agent β-mercaptoethanol and SDS. The SDS-PAGE gel comprised of 5 % stacking gel (pH 6.8) and 12 % separating gel (pH 8.8) and was subjected to electrophoresis in 1 × running buffer at 200 V for 50 – 60 min. After electrophoresis, the gel was stained with Coomassie blue stain solution for 30 min. Then the gel was immersed into the destain solution with shaking; and the destain solution was changed until a clear background of the gel was obtained. Afterwards, the gel was air-dried and finally mounted with gel drying film (Promega).

II.8. Determination of protein concentration

A total protein concentration of the samples was determined by Bradford assay (Bradford, 1976). In this assay, 800 µl of sample was mixed with 200 µl of Bradford Reagent Dye (Bio-Rad) and left for a 10-min incubation at room temperature in order to allow the formation of stable protein-dye complexes. Afterwards, the absorbance of the sample was measured spectrophotometrically at

the wavelength of 595 nm. The protein concentration of the sample was determined by the comparison against a protein standard curve constructed by different BSA standards.

II.9. *β*-lactamase activity assay

β-lactamase assay was performed by spectrophotometric method on Perkin Elmer Lambda Bio 20 UV/VIS spectrometer at 25^{o}C in 50 mM potassium phosphate buffer (pH 7.0). Substrate hydrolysis was monitored at wavelength of 232 nm for penicillin G ($\Delta\varepsilon$ = 755 $M^{-1}cm^{-1}$), 263 nm for cephalothin ($\Delta\varepsilon$ = 7,240 $M^{-1}cm^{-1}$) and product formation was determined at wavelength of 500 nm for the hydrolysis of nitrocefin ($\Delta\varepsilon$ = 15,900 $M^{-1}cm^{-1}$).

For kinetic analysis, steady-state kinetic parameters were determined by fitting initial rates at different substrate concentrations to the Michaelis-Menten rate equation with non-linear regression using the program of Enzyme Kinetics version 1.1 (Trinity Software).

II.10. Fluorometric studies

Fluorescence measurements were performed on a Perkin Elmer LS-50B

spectrofluorimeter (Beaconsfield, Buckinghamshire, England). Both excitation and emission slit widths were set at 5 nm. All fluoresecence measurements were performed at 20^{o}C.

For fluorescence measurements in which automatic injection of antibiotic solution was required, a FLUOstar OPTIMA automated microplate reader (BMG Labtechnologies) equipped with two sample injectors was used. The injection speed of the sample injector was set at 310 μl/s. Excitation and emission filters of 485 nm and 520 nm were used respectively. The samples were placed in a 96-well microtitre plate (Corning Costar) in all measurements.

Fluorescence stopped-flow experiments were performed on SX.18MV-R Stopped Flow instrument (Applied Photophysics Ltd., Leatherhead, UK). Both excitation and emission slit widths were set at 5 nm. The emission was observed through a 515 nm cutoff filter. All measurements were carried out at 20^{o}C. 1000 data points were acquired in each stopped-flow trace.

Chapter III.1

Rational design, preparation and characterization of fluorescein-labeled class C *β*-lactamases

III.1.1. Introduction

Fluorescent proteins have always been intriguing molecules for highly sensitive biosensing purposes in various aspects (Giuliano and Taylor, 1998; Sloan and Hellinga, 1998; D'Auria and Lakowicz, 2001; Hahn and Toutchkine, 2002; Chudakovet *et al.*, 2005). Apart from the utilization of intrinsic fluorescent proteins for biosensing applications (Doi and Yanagawa, 1999; Pollok and Heim, 1999; Miyawaki *et al.*, 2003; Miyawaki, 2004; Rizzo *et al.*, 2004; Okumoto *et al.*, 2005; Tsutsui *et al.*, 2005), myriads of fluorescent protein biosensors intended for direct, reagentless ligand detection have emerged from proteins attached with extrinsic fluorophores (Gilardi *et al.*, 1994; Marvin and Hellinga, 1998; Salin *et al.*, 2001). In the fabrication of these biosensors, extrinsic fluorophores are incorporated to the proteins through the chemical reactions of their linker groups with the amino acid residues. Advances in genetic engineering can virtually allow incorporation of these fluorophores at any desired specific sites at the proteins, meriting the rational structure-based biosensor design (Shreatha *et al.*, 2002).

One approach for modifying the protein with fluorophores taking the advantage of the thiol reaction between the reactive sulfhydryl group of a cysteine residue with the thiol-reactive probe is widely applied in the protein-based biosensor construction (Shi *et al.*, 2001 and 2002; De Lorimier *et al.*, 2002). With structure-based approach, fluorescent protein biosensors can be constructed by cysteine point mutation at the desirable location of the protein for the subsequent step of covalent attachment of the fluorescent probe.

Recently, a fluorescent class A β-lactamase, E166Cf, described in Section I.4 has been constructed using the same strategy as above. The preparation procedure involved two steps: A first step of introducing a unique cysteine at a strategic position at 166 of a class A β-lactamase for catalytic impairment and fluorophore attachment; followed by a second step of tethering the fluorescent probe to the E166C mutant via the thiol-reaction with fluorescein-5-maleimide. Thus, a β-lactam hydrolytic enzyme was converted into a fluorescent binding protein for its β-lactam substrates and inhibitors, allowing luminescence detection for β-lactam compounds and β-lactamase inhibitors.

The design concept of E166Cf inspired us to turn a class C *β*-lactamase for biosensing application. In our study, we focused on protein-engineering *E. cloacae* Amp C *β*-lactamase (P99 *β*-lactamase) into fluorescein-conjugated enzyme with a similar approach as E166Cf which is outlined in Figure III.1.1. This chapter reports the rational design, preparation and characterization of three fluorescein-labeled class C mutants, Y150Cf, V211Cf, and Y150S/V211Cf.

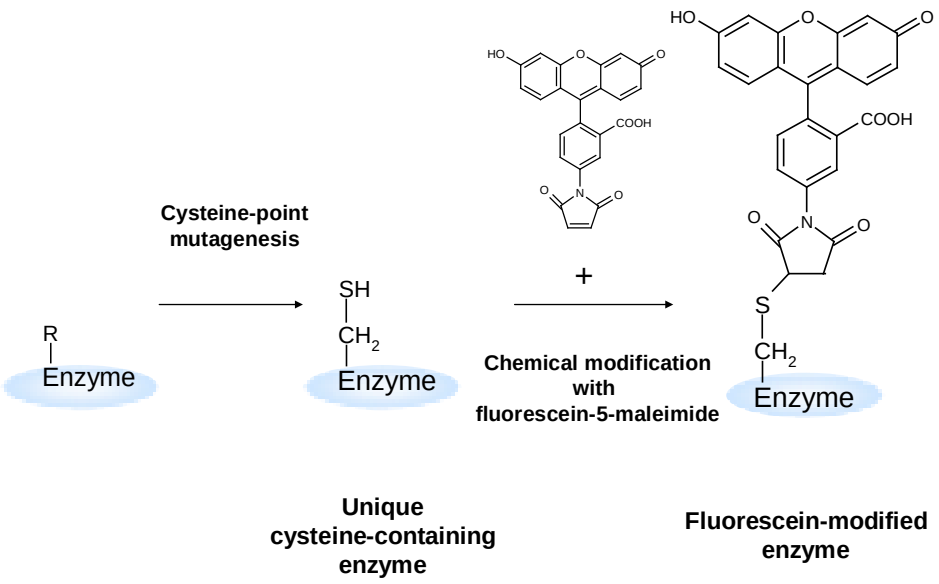

Figure III.1.1. A two-step protocol for the construction of fluorescein-labeled β-lactamases.

III.1.2. Methods

III.1.2.1. Preparation of fluorescein-labeled class C *β*-lactamase mutants

III.1.2.1.1. Construction of class C *β*-lactamase mutants

Three His-tagged P99 *β*-lactamase mutants, including Y150C, V211C and Y150S/V211C were generated by PCR mutagenesis as described in Section II.3.2. Table I.1 shows the template and specific mutagenic primers for each mutant construction. The mutated gene was subcloned into plasmid pSG1113 and sequenced to confirm the identity of the mutant. Afterwards, the resultant plasmid was transformed into *B. subtilis* with the protocol described in Section II.2.2 for subsequent protein expression.

III.1.2.1.2. Production of class C *β*-lactamase mutants

The detailed procedure for expression and purification of class C *β*-lactamase mutants were described in Section II.4 and Section II.5.2 respectively. P99 *β*-lactamase wild-type was also prepared for serving as a control in the subsequent experiments.

III.1.2.1.3. Conjugation with fluorescein-5-maleimide

The detailed procedure for native labeling of Y150C, V211C and

Y150S/V211C was described in Section II.6.1 whereas that for unfolding and labeling of Y150C was described in Section II.6.2.

III.1.2.2. Electrospray ionization-mass spectrometry (ESI-MS)

ESI-mass spectra were obtained with a VG Platform single quadrupole or quadrupole-time of flight (Q-TOF2) mass spectrometer (Micromass, Altrincham, Cheshire, UK) equipped with an electrospray interface. Protein samples were dissolved in H_2O/CH_3CN (1:1 v/v) or H_2O/MeOH (1:1 v/v) containing 0.2% formic acid (v/v) and injected into the electrospray source via a 20 µl-loop injector (Rheodyne 5717) at a flow rate of 10 µl/min. The mass spectrometer was scanned over the m/z 570 – 1600 range. The instrument was calibrated with myoglobin (10 ρmol/µl, average molecular mass 16,951.5).

III.1.2.3. Kinetic analysis

The detailed procedure was described in Section II.9.

Table III.1.1. P99 β-lactamase mutant construction.

	Template	**Mutagenic primers (Sequence from 5' to 3')**	**Resultant plasmid**
Y150C	pSG1113/M	Forward: GGCACAACGCGTCTTT**G**CGCCAACGCCAGCATC Reverse: GATGCTGGCGTTGGCG**C**AAAGACGCGTTGTGCC	pSG1113/Y150C
V211C	pSG1113/M	Forward: GTAAAGCGGTGCGC**TG**TTCGCCGGGTATGCT Reverse: AGCATACCCGGCGA**AC**AGCGCACCGCTTTAC	pSG1113/V211C
Y150S/V211C	pSG1113/V211C	Forward: GCACAACGCGTCTT**AG**CGCCAACGCCAGC Reverse: GCTGGCGTTGGCG**CT**AAGACGCGTTGTGC	pSG1113/Y150SV211C

Remarks:

Mismatched bases for mutagenesis were denoted in boldface.

III.1.3. Results and discussions

III.1.3.1. Design concept of fluorescein-labeled class C *β*-lactamase mutants

In the design of fluorescent protein biosensor, the most critical thing was to decide the attachment site for the fluorophore which would eventually allow reporting of the binding event at the active site. For our construction of the fluorescent class C *β*-lactamase, the rational design of the previously reported E166Cf could guide us for the criteria important for determining the fluorophore attachment site. With respect to its design, the fluorescein molecule was strategically located at the position of 166 based on two rationales. First, considering the location, as *β*-lactamase is a non-allosteric enzyme, the fluorophore should be placed at a position close to the binding site where it could most likely experience the active site's local environment change upon substrate/inhibitor binding. Therefore, Glu166 was chosen to be cysteine-substituted for fluorophore conjugation as it was situated on a flexible Ω-loop, close to the active site. With its side chain protruding towards the active site, the fluorophore tethered at this position also orientated its functional moiety towards the active site as the original residue's side chain did. It was revealed that when a fluorescein molecule was located at this position, the binding event at the active site would induce a change of its microenvironment and concomitantly the

flexibility of the Ω-loop allowed its movement in response to such environment change, thereby switching the fluorescence of E166Cf on. Second, Glu166 is a key residue for the catalysis of *β*-lactam-hydrolytic reaction. Thus cysteine point mutation and fluorophore attachment at this position dramatically impaired the catalytic ability of the enzyme. Without adversely affecting the binding capability with the substrate and inhibitor, this hydrolytic enzyme was, as a result, converted to a fluorescent binding protein, useful for biosensing its *β*-lactam substrates and inhibitors. This system illustrated that considerations about the proximity to the active site, flexibility of the region to be located and the side chain orientation should be taken into account in selecting the site for fluorophore attachment. In addition, it highlighted the importance of suppressing the catalytic activity of the enzyme to minimize the hydrolytic destruction of the *β*-lactam substrates.

With the inspiration from the design of E166Cf, we prepared three class C *β*-lactamase cysteine mutants, namely Y150C, V211C and Y150S/V211C for the modification with fluorescein-5-maleimide to give Y150Cf, V211Cf and Y150S/V211Cf. The design rationale for each mutant is discussed below.

III.1.3.1.1. Rational design of Y150Cf

As illustrated in E166Cf, a wild-type *β*-lactamase was turned into a fluorescent *β*-lactam binding protein by simply introducing a single cysteine point mutation at a catalytically important residue close to the active site for fluorophore attachment and activity suppression. Thus, in our class C *β*-lactamase-based biosensor design, Tyr150, a neighboring residue to the active site serine playing an indispensable role in the enzymatic activity for the class C *β*-lactamases (Dubus *et al.*, 1994 and 1996; Lamotte-Brasseur *et al.*, 2000; Kato-Toma and Ishiguro, 2001), became a potential candidate for the cysteine site-directed mutagenesis for reducing the catalytic efficiency of the enzyme as well as providing a site for fluorophore attachment. This residue is functionally equivalent to Glu166 of the class A *β*-lactamases but located on structural element 2 of the *β*-lactamase which is a constrained short loop on the all-α domain (Figure I.3) instead of residing on the large flexible Ω-loop, spatially different from Glu166 residue in the class A enzymes.

III.1.3.1.2. Rational designs of V211Cf and Y150S/V211Cf

With the realization that signal amplitude would be related to the extent of the movement of the environment sensitive fluorophore, it was worthwhile to

introduce the fluorescent probe on the Ω-loop which is the most flexible region of the enzyme to allow higher degree of resilience for the probe movement. However, when exploring the Ω-loop of the class C *β*-lactamase (Section I.2.2.1), it has no functional residue equivalent to Glu166 in the class A enzyme or any other residues involved in the catalysis. Therefore, we switched our strategy to introduce two mutations to the *β*-lactamase: one on the Ω-loop for the fluorophore attachment and the other on the catalytic important residue to suppress the enzyme catalytic ability.

Visual inspection on the crystallographic structure of the Ω-loop of the class C *β*-lactamase revealed that most of the residues on the loop are too far from the active site or with side chain pointing away from the active site, thus not suitable for locating a fluorophore on them. Conversely, Val211 on the Ω-loop was a good candidate for the fluorophore attachment as it is in close vicinity to the catalytic site with its side chain pointing towards the active site (Figure III.2.A). Investigating further into the molecular surface of the active site cavity, Val211 was a surface residue located in a geometrically well-defined R1 cleft (Figure III.2.B) which is a consensus binding site for the variable amide (R1) side chain at the C6'(7') of the *β*-lactams (Caselli *et al.*, 2001; Tondi *et al.*, 2001; Powers and

Shoichet, 2002). Structural data showed that the ubiquitous R1 group of the substrate appeared to make hydrophobic contacts with Val211, indicating that Val211 is a residue involved substrate recognition (Goldberg *et al.*, 2003). Thus, it would have a high probability for a fluorophore located at the position of 211 in the class C β-lactamase to report the local environment change at the active site, prompting our interest in constructing V211Cf. As mentioned above, a second mutation would be introduced into V211C so as to get a catalytic defective enzyme. As suggested, substituting Tyr150 with a serine would pose a significant effect on the enzyme catalytic ability (Dubus *et al.*, 1994), thus we prepared the Y150S/V211C mutant in parallel for the fluorophore conjugation so as to get a hydrolytic defective fluorescent class C β-lactamase for biosensing purposes.

(A)

(B)

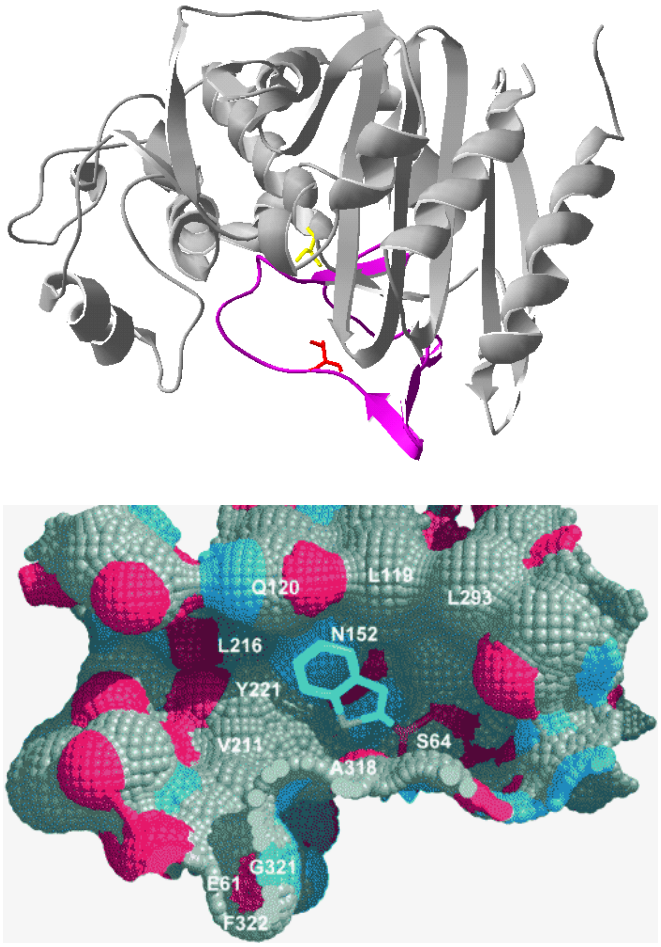

Figure III.1.2. Location of Val211 residue in a class C *β*-lactamase. (A) From the view of the overall structure, Val211 is a residue located on the Ω-loop with its side chain protruding to the active site. Val211, red; Ser70, yellow; Ω-loop, purple. (B) When considering the local environment of the active site pocket, it is a solvent-exposed residue lied at a so-called "R1 cleft" of the enzyme binding site. Figure (A) is generated by SwissPdb Viewer (Guex and Peitsch, 1997) and Figure (B) is adapted from Tondi *et al.* (2001).

III.1.3.2. Preparation of the fluorescein-labeled class C *β*-lactamase mutants

III.1.3.2.1. Preparation of P99 *β*-lactamase wild-type and mutants

As class C *β*-lactamases were expressed intracellularly, 6×His-tag was introduced at the N-terminus of the class C *β*-lactamases to faciliate purification using metal affinity chromatography. In our study, all *β*-lactamase wild-type and mutants including Y150C, V211C and Y150S/V211C were successfully expressed in *B. subtilis* and purified to more than 95% homogeneity with a single metal affinity chromatographic step. The chromatograms for these proteins were shown from Figure III.1.3 to III.1.6. Approximately 15 to 66 mg were usually obtained from 1 L of culture batch.

(A)

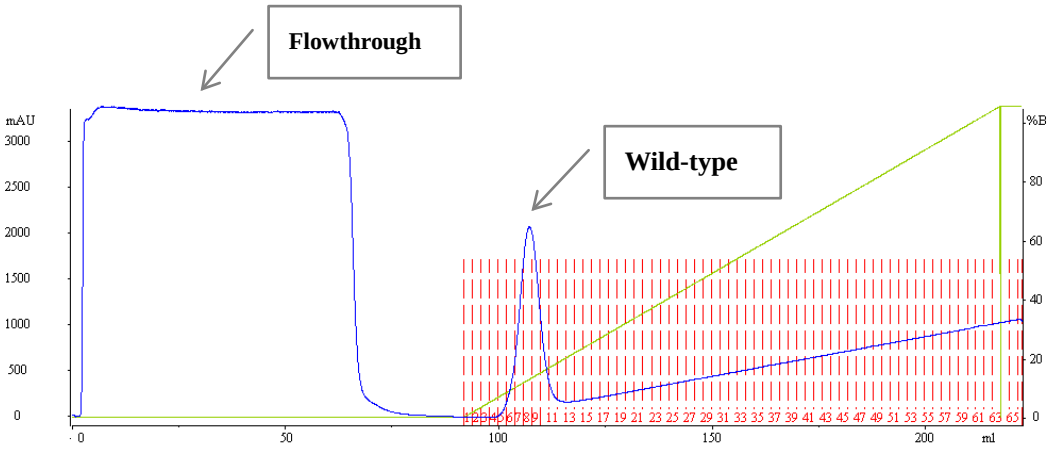

(B)

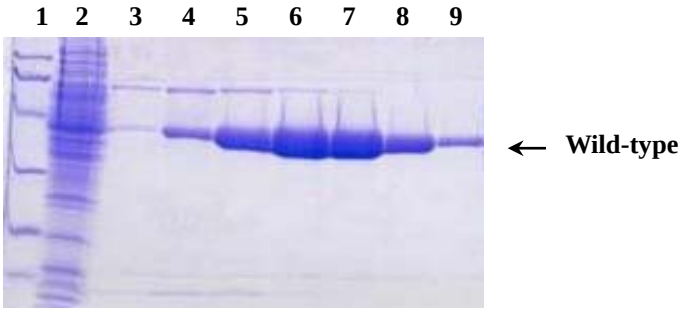

Figure III.1.3. Purification of the wild-type P99 enzyme. (A) Elution profile of the purification of the enzyme from cell lysate obtained from 400 ml-culture by a single step of nickel-charged 5 ml-HiTrap Chelating column. mAU, milli absorption unit; 100 %B = 0.5 M imidazole. (B) SDS-PAGE analysis. Lane 1, low range molecular marker: rabbit muscle phosphorylase b (97,400), BSA (66,200), hen egg white ovalbumin (45,000), bovine carbonic anhydrolase (31,000), soybean trypsin inhibitor (21,500), hen egg white lysozyme (14,400); lane 2, crude cell lysate; lanes 3 – 9, 10 µl of fractions 5 – 11.

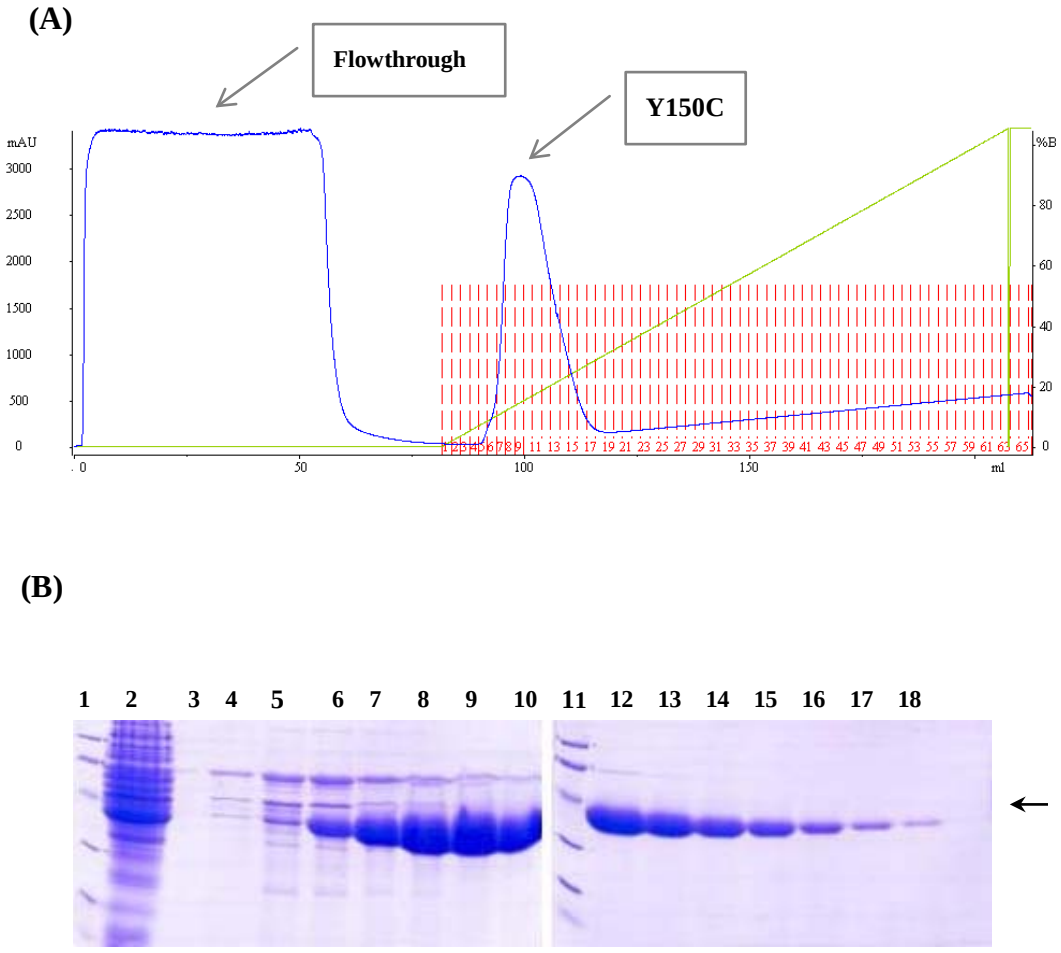

Figure III.1.4. Purification of the Y150C mutant. (A) Elution profile of the purification of the enzyme from cell lysate obtained from 400 ml-culture by a single step of nickel-charged 5 ml-HiTrap Chelating column. mAU, milli absorption unit; 100 %B = 0.5 M imidazole. (B) SDS-PAGE analysis. Lane 1 and 11, low range molecular marker: rabbit muscle phosphorylase b (97,400), BSA (66,200), hen egg white ovalbumin (45,000), bovine carbonic anhydrolase (31,000), soybean trypsin inhibitor (21,500), hen egg white lysozyme (14,400); lane 2, crude cell lysate; lanes 3 – 10 and lanes 12 – 18, 10 µl of fractions 4 – 18.

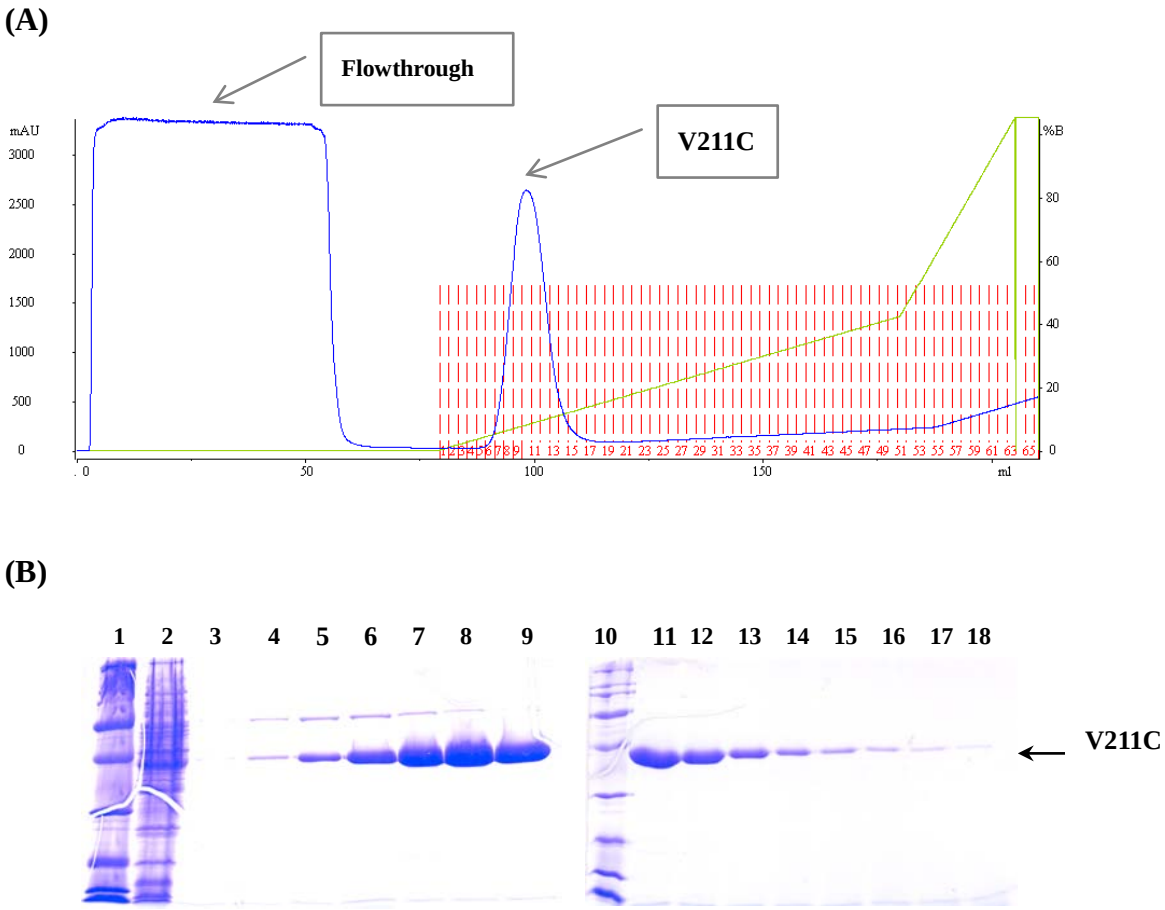

Figure III.1.5. Purification of the V211C mutant. (A) Elution profile of the purification of the enzyme from cell lysate obtained from 600 ml-culture by a single step of nickel-charged 5 ml-HiTrap Chelating column. mAU, milli absorption unit; 100 %B = 0.5 M imidazole. (B) SDS-PAGE analysis. Lane 1, 10, broad range molecular marker: myosin (200,000), *β*-galactosidase (116,250), rabbit muscle phosphorylase b (97,400), BSA (66,200), hen egg white ovalbumin (45,000), bovine carbonic anhydrolase (31,000), soybean trypsin inhibitor (21,500), hen egg white lysozyme (14,400), aprotinin (6,500); lane 2, crude cell lysate; lanes 3 – 9 and lanes 11 – 18, 10 µl of fractions 5 – 19.

(A)

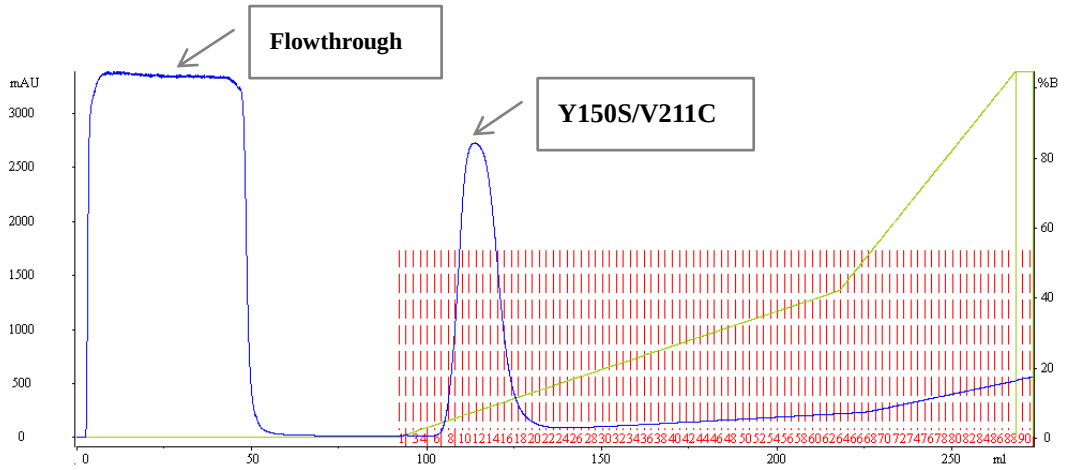

(B)

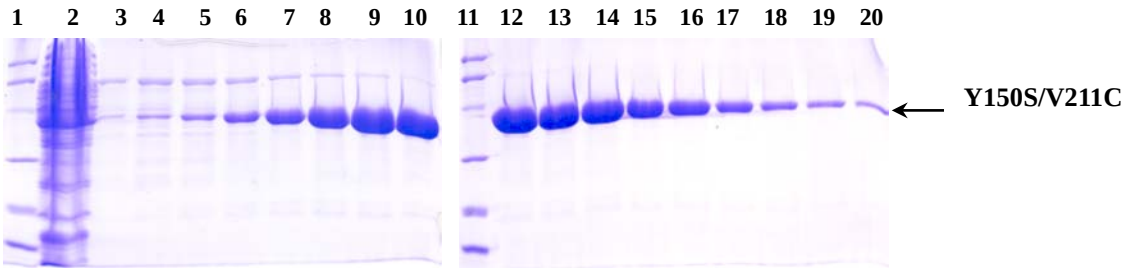

Figure III.1.6. Purification of the Y150S/V211C mutant. (A) Elution profile of the purification of the enzyme from cell lysate obtained from 600 ml-culture by a single step of nickel-charged 5 ml-HiTrap Chelating column. mAU, milli absorption unit; 100 %B = 0.5 M imidazole. (B) SDS-PAGE analysis. Lane 1 and 11, low range molecular marker: rabbit muscle phosphorylase b (97,400), BSA (66,200), hen egg white ovalbumin (45,000), bovine carbonic anhydrolase (31,000), soybean trypsin inhibitor (21,500), hen egg white lysozyme (14,400); lane 2, crude cell lysate; lanes 3 – 10 and lanes 11 – 20, 10 µl of fractions 5 - 21.

III.1.3.2.2. Labeling of P99 *β*-lactamase mutants

Purified Y150C, V211C and Y150S/V211C were subjected to the modification with fluorescein-5-maleimide. V211Cf and Y150S/V211Cf were successfully obtained from labeling the native forms of the mutants as revealed from their fluorescent bands on a SDS-PAGE gel under the UV illumination (Figure III.1.7). However, we failed to obtain Y150Cf because the proteins precipitated after the labeling reaction for both labeling with or without unfolding the protein. This result was consistent with the presence of protein aggregation in the preparation of S130Cf for the class A *β*-lactamase described by Chan (2000) who proposed that the protein was unable to refold back after modified with the fluorescein molecule. Tyr150 in the class C *β*-lactamase was a conserved residue located at a position equivalent to Ser130 in the class A *β*-lactamase (Figure I.3 and Figure I.5), thus the protein precipitation in the preparation of Y150Cf was also postulated as the consequence of the severe structural disturbance on the protein architecture imposed by the bulky fluorescein molecule.

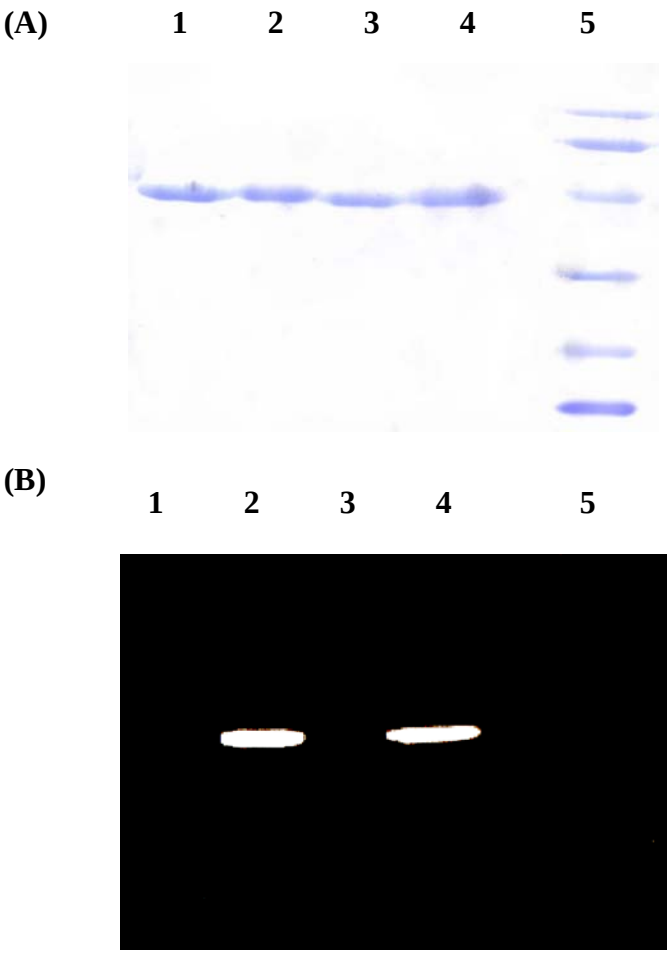

Figure III.1.7. SDS-PAGE of V211C, V211Cf, Y150S/V211C and Y150S/V211Cf mutants stained with Coomassie-blue (A) and under UV illumination (B). Lane 1, V211C; lane 2, V211Cf; lane 3, Y150S/V211C; lane 4, Y150S/V211Cf; lane 5, low range molecular marker: rabbit muscle phosphorylase b (97,400), BSA (66,200), hen egg white ovalbumin (45,000), bovine carbonic anhydrolase (31,000), soybean trypsin inhibitor (21,500), hen egg white lysozyme (14,400).

III.1.3.2.3. Characterization by mass spectrometry

The authenticities of the samples were confirmed by mass spectrometric studies (Figure III.1.8 – III.1.12). The calculated and measured masses of P99 wild-type, V211C, V211Cf, Y150S/V211C and Y150S/V211Cf were compared and summarized in Table III.1.1. It was shown that the molecular masses of the wild-type, V211C and Y150S/V211C mutants determined by ESI-MS were consistent with their corresponding calculated values. In contrast, both measured masses of V211Cf and Y150S/V211Cf differed from their calculated masses. These differences might be due to the association of the fluorescein molecule with a sodium ion which has a mass of 23 (Chan *et al.*, 2004).

Regarding to the mass spectrometric data, almost all V211C and 90% of Y150S/V211C mutants were labeled with fluorescein molecules in a 1:1 ratio, indicating efficient labeling was achieved. This implied that a prior step of protein unfolding for exposing the cysteine residue for labeling reaction was not necessary for efficient labeling of V211C and Y150S/V211C. One possibility was that cysteine introduced at position 211 was a solvent-exposed surface residue, allowing the access of the thiol-sensitive fluorophore to react with its sulfhydryl functional group in the labeling reaction.

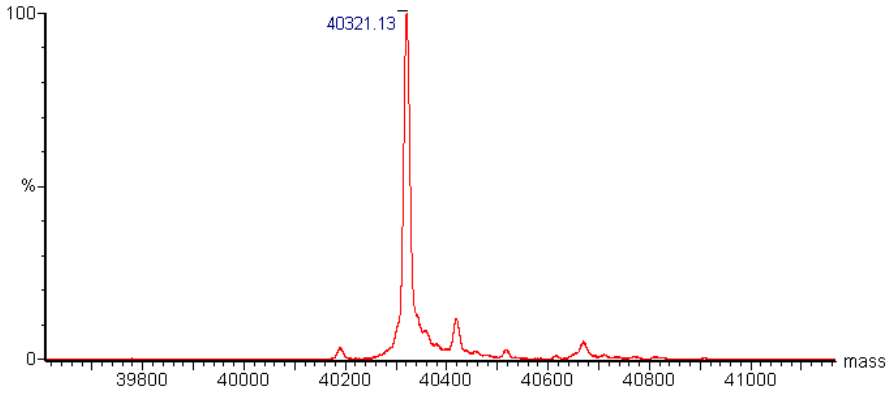

Figure III.1.8. ESI-mass spectra of wild-type P99.

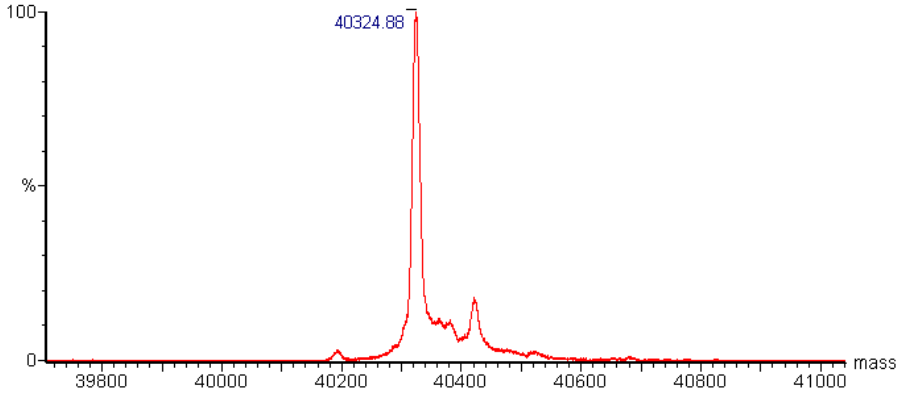

Figure III.1.9. ESI-mass spectra of V211C.

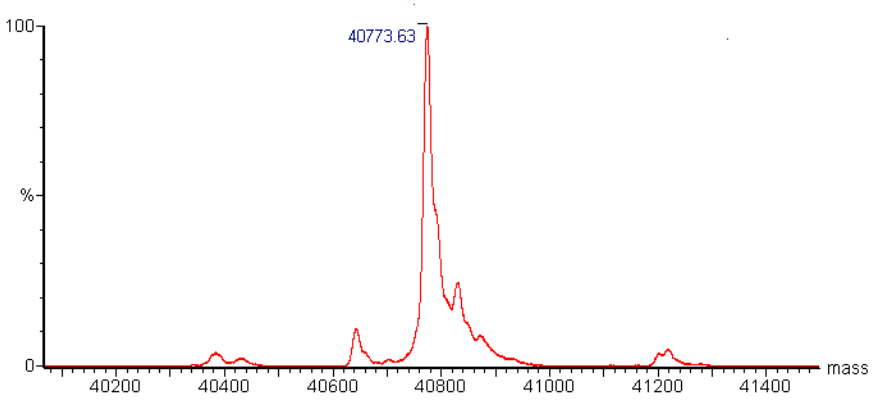

Figure III.1.10. ESI-mass spectra of V211Cf.

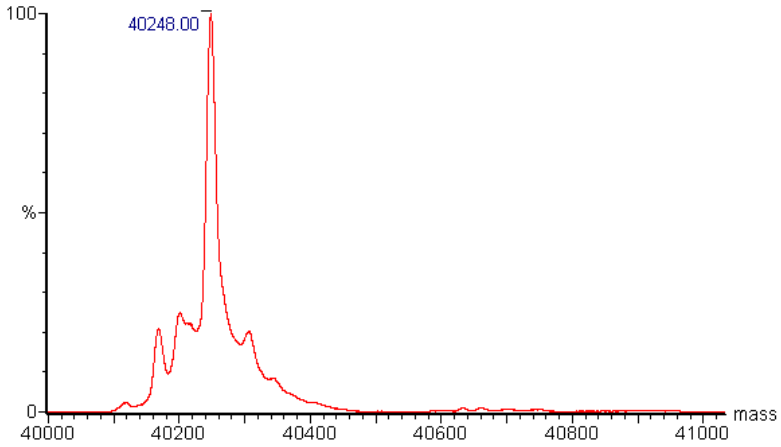

Figure III.1.11. ESI-mass spectra of Y150S/V211C.

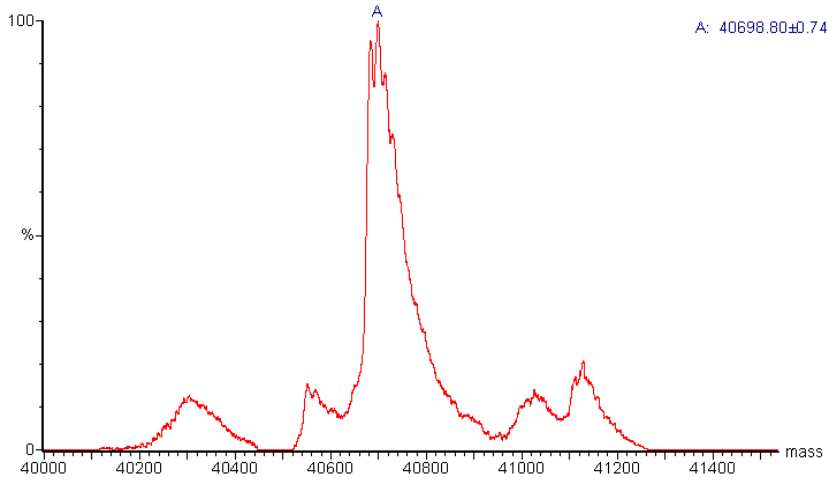

Figure III.1.12. ESI-mass spectra of Y150S/V211Cf.

Table III.1.1. Comparison of the calculated and measured masses of P99 wild-type, V211C, V211Cf, Y150S/V211C and Y150S/V211Cf.

	Calculated mass	Measured mass
Wild-type	40320.2	40320.75 ± 0.8
V211C	40324.2	40323.70 ± 2.62
V211Cf	40751.6	40773.70 ± 3.73
Y150S/V211C	40248.1	40248.00 ± 2.80
Y150S/V211Cf	40675.5	40698.80 ± 0.74

III.1.3.3. Kinetic characterization of fluorescein-labeled class C *β*-lactamase mutants

To evaluate the effects of mutagenesis and fluorophore coupling on the catalytic function of the *β*-lactamase, hydrolytic activities of the fluorescein-labeled class C *β*-lactamases, V211Cf and Y150S/V211Cf were assessed by their hydrolytic degradation of cephalothin, which is a preferred substrate for the class C *β*-lactamases, monitored by spectrometric method and compared with those of their parental wild-type, V211C and Y150S/V211C cysteine-mutants. Their kinetic parameters for the turnover of cephalothin were summarized in Table II.1.1.

In our preparation of the fluorescein-labeled class C *β*-lactamases, the first step was to replace Val211 with a cysteine for fluorophore attachment. As revealed from the kinetic data, V211C displayed a 6-fold lower catalytic efficiency than the wild-type, indicating that *β*-lactamase activity was conserved after the mutagenesis. This result was consistent with the non-functional role of Val211 (Usher *et al.*, 1998; Goldberg *et al.*, 2003), thus mutation at that position showed limited effects on the hydrolytic activity of the *β*-lactamase. Despite the comparable k_{cat}/K_m values between V211C and its parental wild-type enzyme,

V211C mutant had a 2-fold higher in K_m value than the wild-type. As V211 was a residue at the R1 cleft of the enzyme binding site for substrate recognition, such rise in the K_m after substituting valine with a cysteine may be due to the poor substrate recognition resulted from a reduced hydrophobic interaction between the cysteine residue and substrate R1 functional group. For the construction of Y150S/V211Cf, a second mutation of replacing the tyrosine at position 150 with a serine was introduced into the enzyme. Although this mutation did not pose much effect on the K_m value of the enzyme, hydrolytic activity of the enzyme was dramatically reduced (by 3000-fold) with the mutation of Tyr150 into a serine residue. In addition, the significance decrease in the k_{cat} value of Y150S/V211C (around 1800-fold) indicated the strong effect of this mutation on the deacylation rate, consistent with the indispensable role of Tyr150 in the deacylation mechanism (Oefner *et al.*, 1990).

The second step of the preparation was the fluorophore conjugation. Comparable kinetic parameters were observed for the cysteine mutants before and after coupling with the fluorescein molecule. Nevertheless, increase in the K_m value of fluorescein-labeled mutants would probably be the consequence of the steric hindrance introduced by the fluorescein moiety to the binding site that

caused a reduction in the substrate affinity.

In short, for our two fluorescein-modified class C β-lactamases, V211Cf nearly retained the full functional capability as the parental wild-type whereas Y150S/V211Cf lost almost all the hydrolytic activity towards the substrate and was converted into a binding protein for the β-lactams.

Table III.1.2. Turnover of cephalothin by wild-type, V211C, V211Cf, Y150S/V211C and Y150S/V211Cf mutants.

	K_m (μM)	k_{cat} (s^{-1})	k_{cat}/K_m ($\mu M^{-1}s^{-1}$)
Wild-type	9.064 ± 0.692	117.604 ± 2.296	12.974 ± 1.045
V211C	25.556 ± 1.238	53.982 ± 0.985	2.112 ± 0.109
V211Cf	64.492 ± 6.141	47.341 ± 1.902	0.734 ± 0.076
Y150S/V211C	15.306 ± 1.377	0.064 ± 0.002	0.004 ± 0.0004
Y150S/V211Cf	51.718 ± 6.230	0.073 ± 0.002	0.001 ± 0.0001

III.1.4. Concluding remarks

In this chapter, we reported the protein engineering of a class C *β*-lactamase from *E. cloacae* P99 into fluorescent mutant derivatives using structure-based rational design. By the combination of cysteine-point mutation and chemical modification, two fluorescein-labeled mutants, V211Cf and Y150S/V211Cf, were successfully prepared whereas Y150Cf could not be constructed as the protein aggregated after the labeling with the fluorescein-5-maleimide. For the two fluorescein-modified proteins, V211Cf conserved the activity as the parental wild-type whereas Y150S/V211Cf lost its catalytic ability in the substrate hydrolysis. In the next two parts, Chapter III.2 and Chapter III.3, the possibility of V211Cf to report the active site's local environment change and detect *β*-lactamase inhibitors was investigated whereas in Chapter III.4, the perspective of Y150S/V211Cf in biosensing purposes was discussed.

Chapter III.2

Studies on the fluorescence properties of V211Cf towards *β*-lactam antibiotics

III.2.1. Introduction

Molecular recognition between protein and its ligands is very specific and selective process, thus advantageous for providing the fundamental basis of the optical biosensors for the small molecule and ligand detection. The sensing mechanism of these biosensors is often rationalized by the modulation of the signals by the protein global conformational change upon ligand binding experienced by probes located at the distant from the binding sites (Marvin and Hellinga, 1998) or the ligand-binding-induced microenvironment change of the reporter tethered close to the binding sites (Morii *et al.*, 2002; Nagase *et al.*, 2003; Nakata *et al.*, 2004 and 2005; Takaoka *et al.*, 2006). Whilst almost all these biosensors are based on the scaffolds of binding proteins with allosteric properties (Gilardi *et al.*, 1994; Marvin *et al.*, 1997; Hellinga and Marvin, 1998; Salins *et al.*, 2001; Breaker, 2002; De lorimier *et al.*, 2002; Shrestha *et al.*, 2002), the possibility of modifying hydrolytic enzymes for direct sensing systems for their substrates are always neglected with respect to the enzymatic destruction of the substrate analytes. The recent development of fluorescein-labeled class A

β-lactamase, E166Cf (described in Section I.4) pioneered the conversion of a non-allosteric, *β*-lactam-hydrolytic enzyme to be a molecular sensor for detecting its substrates and inhibitors. It functioned with a simple principle of fluorescence enhancement resulted from the change in the microenvironment of the fluorescein reporter on its Ω-loop in close proximity to the active site accompanying binding event. As E166Cf was catalytically defective, the effect of substrate destruction has been minimized.

With the aim of validating the applicability of the concept illustrated by E166Cf for other non-allosteric, hydrolytic enzymes in the generic design of biosensors, in our study, we have employed a similar approach as E166Cf for the rational design of novel fluorescent class C *β*-lactamases, as described in Chapter III.1, for detection for *β*-lactam antibiotics. This chapter will focus on the fluorescence properties of the prepared fluorescein-modified class C *β*-lactamase, V211Cf, which was of restored hydrolytic activity, towards *β*-lactam antibiotics. The possibility of V211Cf to report the local environment change is first going to be discussed. Next, the fluorescence behaviors of V211Cf in the presence of the two main categories of *β*-lactam antibiotics, including penicillins and cephalosporins, are examined. The structures of the tested *β*-lactam antibiotics are

shown in Figure III.2.1. Finally, the potentials of V211Cf for biosensor development and mechanistic studies will be commented.

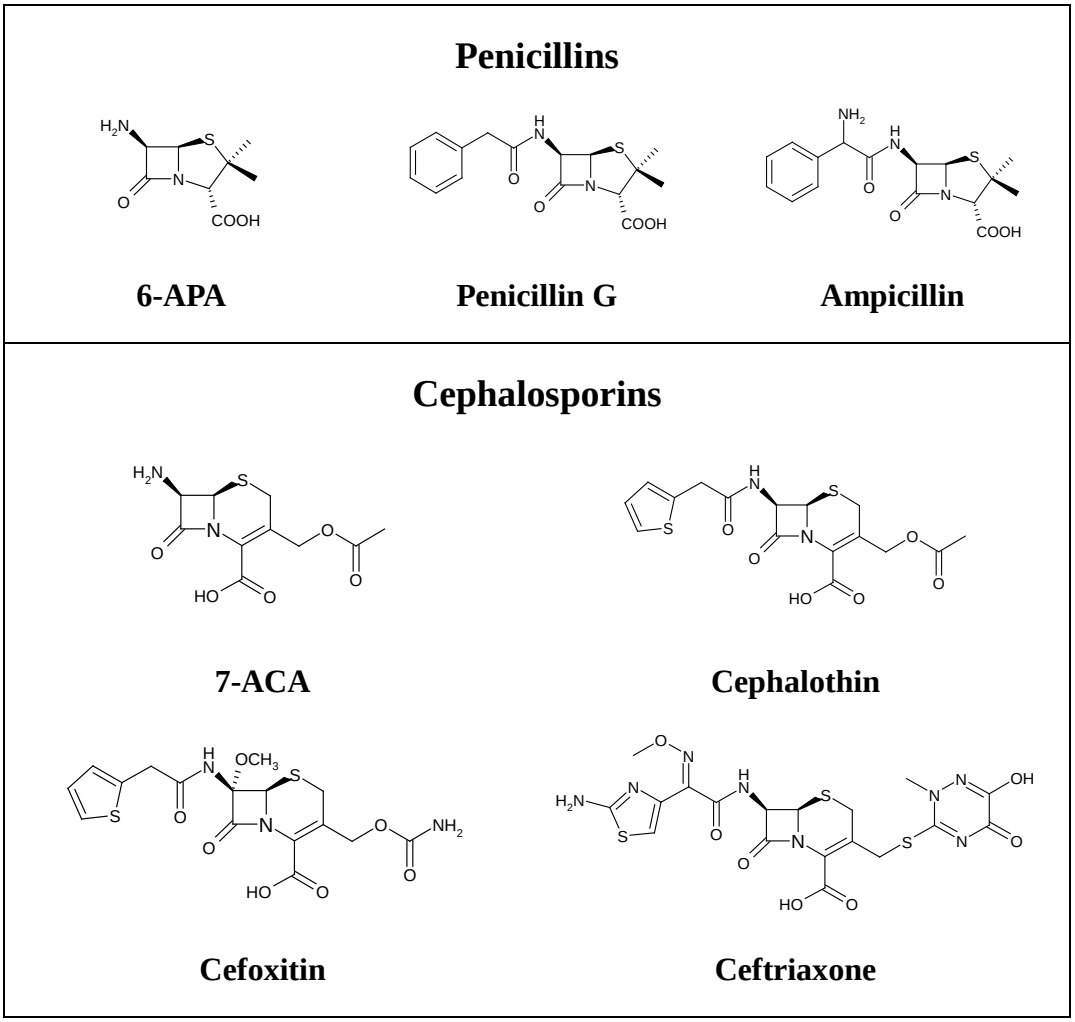

Figure III.2.1. Structures of β-lactam antibiotics involved in this study.

III.2.2. Methods

III.2.2.1. Spectrometric studies

The detailed procedure was described in Section II.9.

III.2.2.2. Fluorometric studies

The detailed procedure was described in Section II.10.

III.2.3. Results and discussions

III.2.3.1. Excitation and emission of V211Cf

Excitation and emission spectra of V211Cf in 50 mM phosphate buffer are shown in Figure III.2.2. The excitation wavelength of V211Cf was 498 nm and the emission wavelength was observed at 517 nm on a 498 nm excitation. In addition, spectroscopic characteristic of V211Cf upon the addition of penicillin G was examined. According to the emission spectra of V211Cf in the presence of various concentrations of penicillin G in Figure III.2.3, addition of the penicillin substrate enhanced the fluorescence of V211Cf at a fixed wavelength at 517 nm in a concentration dependent fashion, indicating that V211Cf could provide intensity sensing for the β-lactam antibiotics.

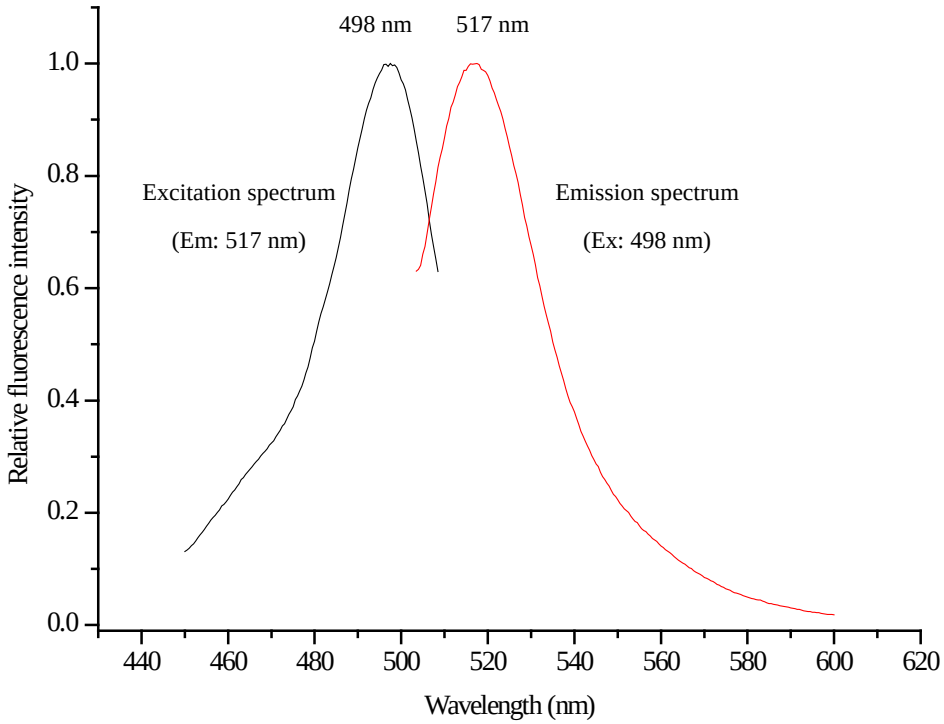

Figure III.2.2. Excitation and emission spectra of 1.0×10^{-7} M V211Cf in 50 mM potassium phosphate (pH 7.0).

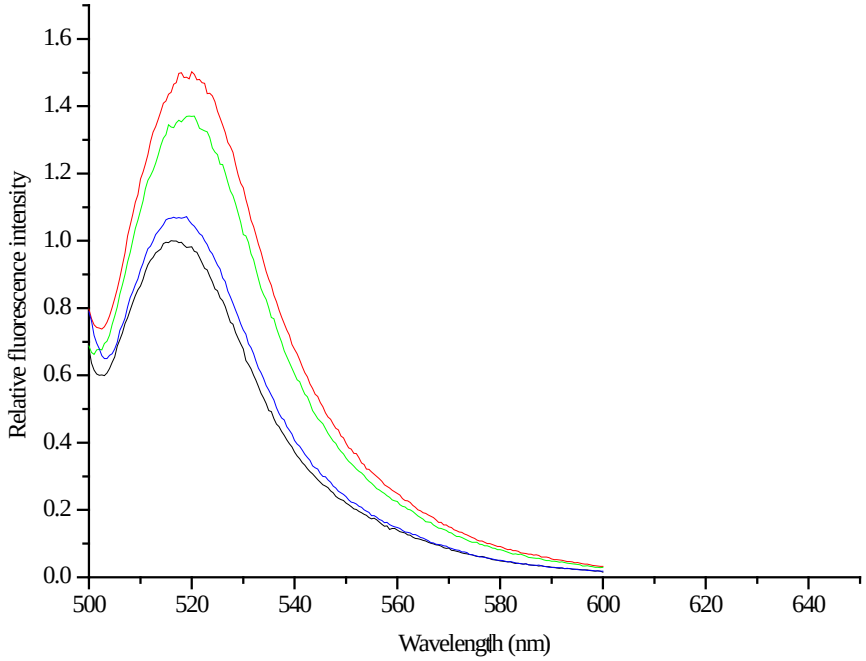

Figure III.2.3. Emission spectra of 1.0×10^{-7} M V211Cf in 50 mM potassium phosphate (pH 7.0) upon the increasing concentrations of penicillin G: 0 M (black), 1.0×10^{-5} M (blue), 1.0×10^{-4} M (green) and 1.0×10^{-3} M (red). All spectra were obtained with excitation at 498 nm.

III.2.3.2. V211Cf as a probe for the local environment of the active site

To assess the capability of V211Cf to report the dynamic local environment change at the active site, time-resolved fluorescence measurement of V211Cf was carried out in the presence of penicillin G which is a good substrate for β-lactamase. As illustrated in Figure III.2.4, when excess penicillin G (1×10^{-3}M) was added to V211Cf, there was a modulation of an increase in fluorescence intensity of V211Cf to a plateau level and this fluorescence signal declined gradually to its basal level. This fluorescence signal was in good agreement with the three-step model of the hydrolytic action catalyzed by β-lactamase:

$$E + S \rightleftharpoons ES \longrightarrow ES^* \longrightarrow E + P$$

The initial phase of fluorescence enhancement of V211Cf upon the addition of penicillin G matched our hypothesis that the entry of the substrate to the active site cavity (E + S) would trigger a dislocation of the fluorescein moiety in close proximity to the active site of V211Cf from the original hydrophobic region to a more solvent exposed environment, resulting in an increase in the fluorescence intensity. Followed by the initial binding of the substrate to the active site, the formation of the pre-covalent enzyme-substrate complex (ES) and the subsequent

acyl-enzyme complex (ES*) sustained the increased fluorescence intensity, leading to the plateau phase of the signal. After the collapse of the acyl-enzyme complex during the deacylation step, the hydrolyzed product was released, thus leaving the active site free (E + P). And this regeneration of active site was demonstrated by the reversibility of the fluorescence signal at the second addition of penicillin G after the signal decline due to the first addition of the substrate as shown in Figure III.2.5. As the enzyme active site was no longer occupied by the substrate, the fluorescein molecule moved back to its original position, leading to the recovery of the fluorescence intensity to its basal level. Therefore, the decline and return of the fluorescence signal to the baseline level was the consequence of the turnover of penicillin G. This can be further supported by the finding that under the same enzyme (1.0×10^{-7}M) and substrate (1.0×10^{-4}M) concentrations, the time required for the abolishment of fluorescence signal (350 s) was consistent with that for the disappearance of penicillin G monitored by the absorbance change at 232 nm (~325 s) (Figure III.2.6). The above results revealed that the fluorescein molecule located nearby the active site of V211Cf was able to report the local environment change at the active site by giving a measurable fluorescence signal, demonstrating the capability of V211Cf to track the reaction occurred at its active site.

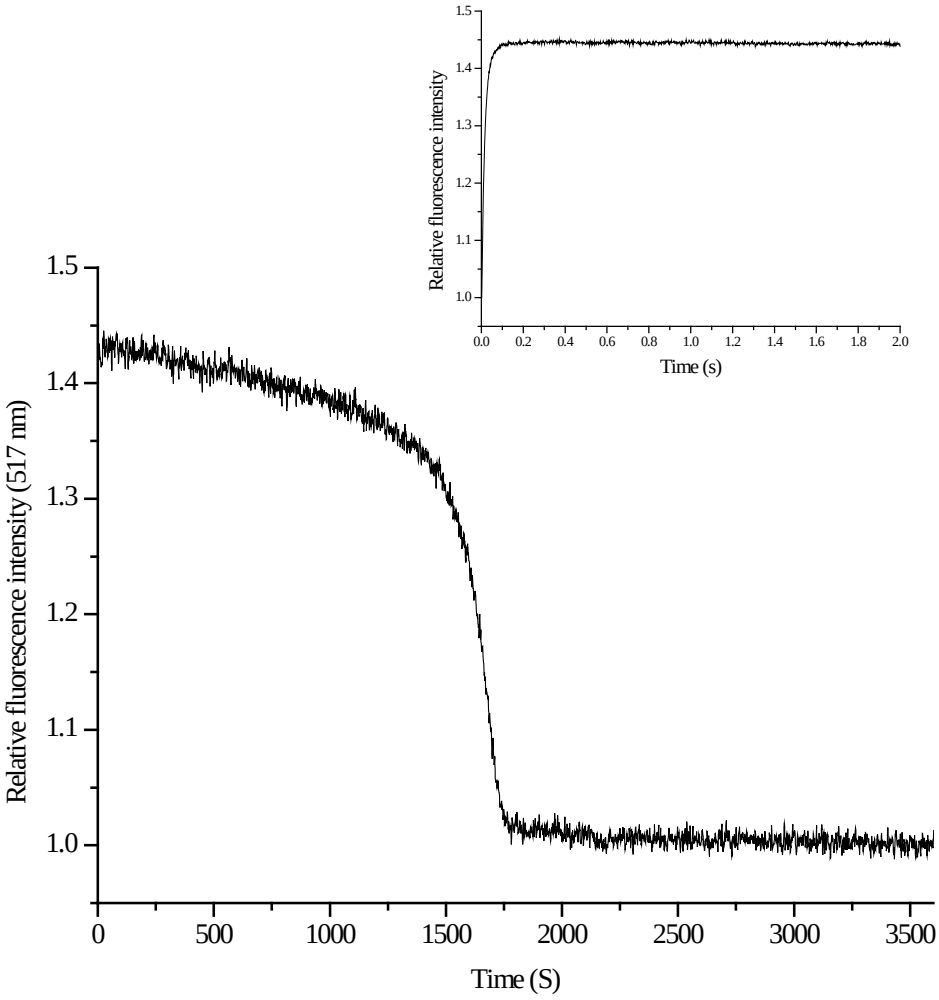

Figure III.2.4. Time-resolved spectrum of 1.0×10^{-7} M V211Cf in 50 mM phosphate buffer with the addition of 1×10^{-3}M penicillin G. Excitation wavelength: 498 nm. The inset shows the initial time-course of the fluorescence signal at the same condition observed through a 515 nm cut-off filter in the stopped-flow experiment. The fluorescence signal was normalized by dividing its reading with that of the background fluorescence.

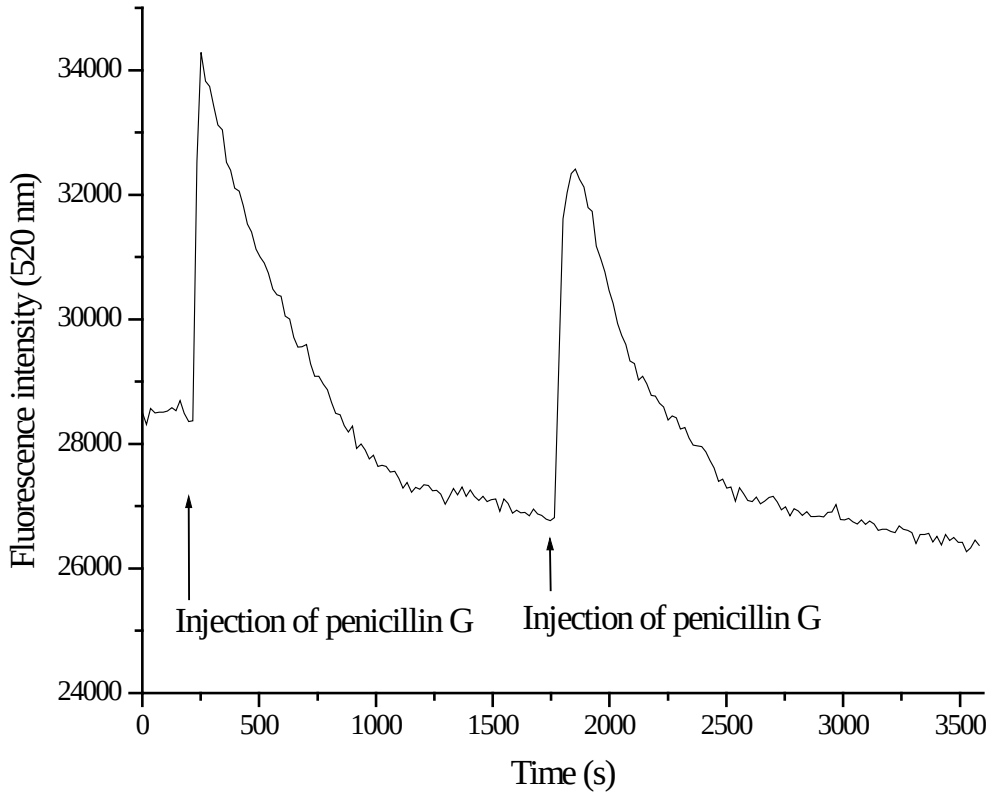

Figure III.2.5. Time-resolved spectrum of V211Cf in 50 mM phosphate buffer with addition of penicillin G by auto-injector at different time points. Excitation wavelength: 485 nm.

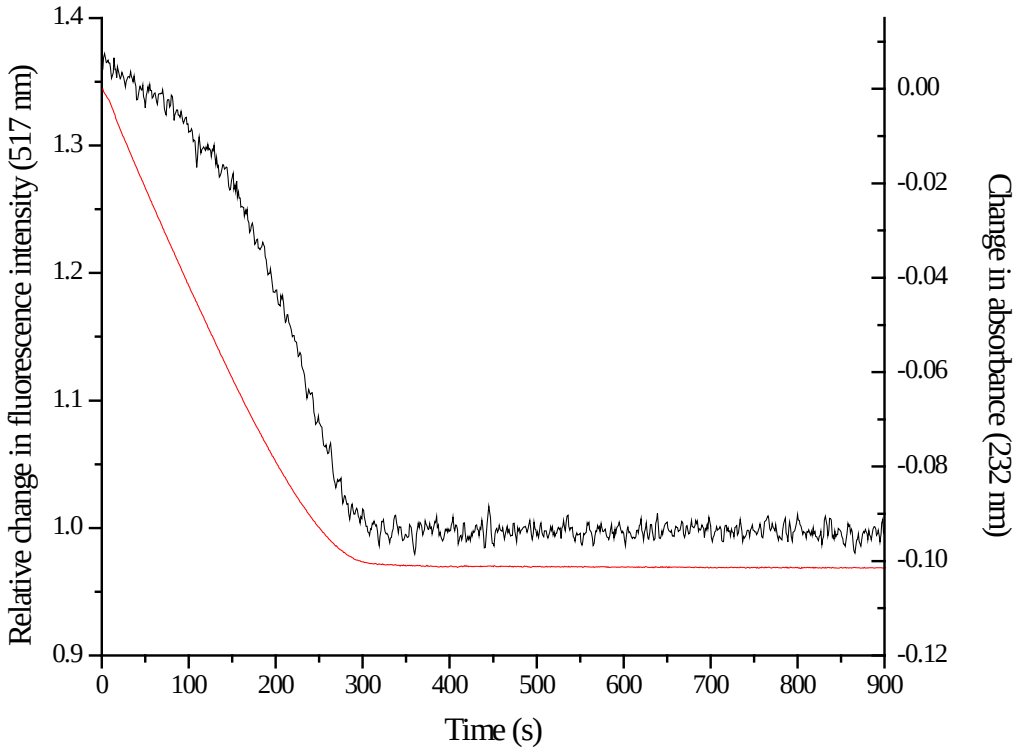

Figure III.2.6. A plot overlying the time-resolved fluorescence signal at 517 nm (with excitation at 498 nm; in black line) and the time-resolved UV absorbance at 232 nm (in red line) obtained from the hydrolysis of 1×10^{-4}M penicillin G by 1×10^{-7}M V211Cf in 50 mM phosphate buffer (pH 7.0) at 20^{o}C.

III.2.3.3. Fluorescence properties of V211Cf towards *β*-lactam antibiotics

To further evaluate the feasibility of V211Cf for the applications for studying interaction between the enzyme and substrate as well as detecting *β*-lactam antibiotics, fluorometric studies of V211Cf in the presence of penicillins and cephalosporins, were conducted. Three penicillins, including penicillin G, ampicillin, and 6-APA, and four cephalosporins, including 7-ACA, cephalothin, cefoxitin and ceftriaxone, were subjected to our study. As revealed by their time-resolved fluorescence spectra from Figure III.2.7 – III.2.13, detectable fluorescence signals were observed for all the tested *β*-lactam compounds. In the following, the fluorescence properties of V211Cf towards these *β*-lactam antibiotics will be discussed in terms of the concentration and type of substrates.

III.2.3.3.1. Effects of substrate concentration on the fluorescence of V211Cf

As mentioned in Section III.2.2, the fluorescence signal of V211Cf corresponded to the hydrolytic reaction of the substrate, thus with fixed amount of enzyme (1.0×10^{-7} M in our experiments), concentration of substrate, as a critical parameter for determining the number of substrate molecules involved in the reaction as well as the turnover rate, will affect the signal intensity and pattern

displayed in the time-resolved measurement.

To determine the effects of the substrate concentration on the signal intensity of V211Cf, dose-response curves were constructed by plotting the peak fluorescence change versus the substrate concentration. Regarding to the dose-response curves (as shown in the inset of each fluorescence spectrum), V211Cf generally responded to the substrates in a concentration-dependent manner. Within the linear region of these sigmoid curves, the intensity of fluorescence increased proportionally to the substrate concentration. Out of these ranges were the conditions of either substrate in excess or in trace amount. In the case of saturated substrate concentration, as all the active sites have been occupied by the substrate molecules and/or coordinated with the transition-state intermediates, further increase in substrate amount would have no effects on the fluorescence intensity. On the contrary, in the situation of very low substrate concentration, the fluorescence-contributing species, ES and ES* are formed in too low quantities to give a detectable signal.

A characteristic fluorescence signal for substrate hydrolysis as illustrated in Figure III.2.4 is composed of three phases: an initial rising phase, a plateau phase,

and a final declining phase to baseline. Substrate concentration is one of the factors determining the duration of each phase, thus deviating the pattern of a substrate at various concentrations. This can be further explained by taking again penicillin G as an example (Figure III.2.14 and Table III.2.1). First, for the initial rising phase which reflected the binding of the substrate to the active site, the higher substrate concentration contributed to a more rapid binding reaction, thus shortening the length of the signal to reach the maximal level (Figure III.2.14.A). After the fluorescence intensity reached its maxima, it is the second plateau phase of the reaction. The stability of this maximal fluorescence signal at this phase is attributed to the lifetime of the formed complexes of ES and ES*. Higher concentration of substrate would probably fuel ES and ES* for more rounds of substrate turnover and maintained a longer duration of the plateau phase. When all the substrates were hydrolyzed, it reaches the final phase of signal decline. More substrate would delay the disappearance of signal which is consistent with the rate of the hydrolysis (Figure III.2.14.B). Besides, the difference in the peak fluorescence signals between the situations of excess substrate and limiting substrate should be highlighted. When substrate was in excess amount, the peak fluorescence signal was entirely attributed to the ES and ES* complexes at the equilibrium state whereas under the condition of limiting substrate, the peak

fluorescence was resulted from a compromise between the rates of formation and dissociation of the ES and ES* intermediates.

III.2.3.3.2. Effects of substrate type on the fluorescence of V211Cf

Other than substrate concentration, the type of substrate is another factor for determining the fluorescence signal pattern of V211Cf. As substrate hydrolysis is an interactive process between the substrate and enzyme, the chemical structures of the substrates and the catalytic properties of the enzyme towards the substrates should be taken into account in the analysis of the effects of the substrate type on the fluorescence of V211Cf. How well the functional groups of the substrate interact with the residues of the enzyme would be a determinant for the binding of the substrate and also the stability of the transient intermediates, thus affecting the length of the various phases in the fluorescence signal. In addition, the ease of the substrate to be hydrolyzed would determine the longevity of signal. As V211Cf conserved the enzyme activity of the wild-type enzyme (Section III.1.3.3), Table III.2.2 showing the kinetic parameters of the turnover of penicillins and cephalosporins by the wild-type P99 β-lactamase would give us a good idea of the catalytic performances of our V211Cf towards the tested β-lactam antibiotics.

Considering the three tested penicillins, penicillin G is a typical good substrate to the class C β-lactamase. Its fluorescence signal (Figure III.2.7) could serve as a guide for us to investigate the effects of the structure of penicillins on the fluorescence properties of V211Cf. Ampicillin, as a modified version of penicillin G, possessed an additional side chain of an amine group to the structure of penicillin G. This modified moiety makes ampicillin less sensitive to hydrolysis by class C β-lactamase than its penicillin G template by reducing the value of k_{cat} to about 20-fold. As deacylation for ampicillin is less efficient than that for penicillin G (due to high k_{cat} value), accumulation of the signal-contributing ES* would be in a larger extent in the case of the hydrolysis for ampicillin, yielding a more stable signal with lengthened plateau phase (Figure III.2.8). Among the three penicillins in this study, 6-APA is the poorest substrate for the class C β-lactamase. Although it has the simplest structure, it lacks the side chain at its C6 position for interacting with the residues at the active site cavity, resulting in its weak binding with the enzyme. The fluorescence signal for 6-APA was made up of an initial spike followed by a long-lasting level-off phase (Figure III.2.9), differing from the typical fluorescence signal mentioned above. As reported by Matagne *et al.* (1990) that the hydrolytic reaction of 6-APA by P99 β-lactamase did not follow the simple three-step model for substrate hydrolysis, this atypical signal pattern of

6-APA may be due to the presence of the complexes formed in the branched pathway along the reaction.

To evaluate the effects of the cephalosporin-type substrates on the fluorescence of V211Cf, four cephalosporins with different reactivity towards class C β-lactamase were used in our study. 7-ACA, a starting compound for the semi-synthesis of cephalosporin derivatives, is a poor substrate to class C β-lactamase with high K_m and low k_{cat} values. Referring to Figure III.2.10, poor affinity of the enzyme with 7-ACA (as reflected by high value of K_m) resulted in a slow increase in the fluorescence intensity at the rising phase whereas low deacylation contributed to a slow decline of the fluorescence signal. This signal pattern is remarkably different from that for the cephalothin which is a first-generation cephalosporin. Cephalothin, as a preferred substrate for the class C β-lactamase, exhibited a comparably short-lived signal with rapid rising phase (which is too fast to be monitored by the steady-state fluorescence measurement) and a sharp decreasing phase (Figure III.2.11). Unlike cephalothin, the second-generation compound, cefoxitin gave rise to more stable signal owing to its low k_{cat} value (3000-fold lower than that for cephalothin) (Figure III.2.12). These results indicated that the more complex the structures derived along the

higher generation of cephalosporins, the lower the sensitivity of the compounds towards the destruction by *β*-lactamase, thus giving signal with greater stability. In contrast, it was another story for ceftriaxone, a third-generation cephalosporin that it contributed to a signal with distorted plateau phase (as shown in Figure III.2.13) as a consequence of the slow formation of the intermediates and complicated branched pathway as suggested by Monnaie *et al.* (1992).

In addition, with respect to good substrates, V211Cf displayed more stable signal for penicillin G than cephalothin, implying that V211Cf hydrolyzed cephalothin more efficiently than penicillin G. This result was in a good agreement with the substrate preference of the class C *β*-lactamase on cephalosporins than penicillins, further demonstrating that the effects of the substrate profile of the enzyme on the fluorescence behaviors of the enzyme modified with a fluorescein close to its active site.

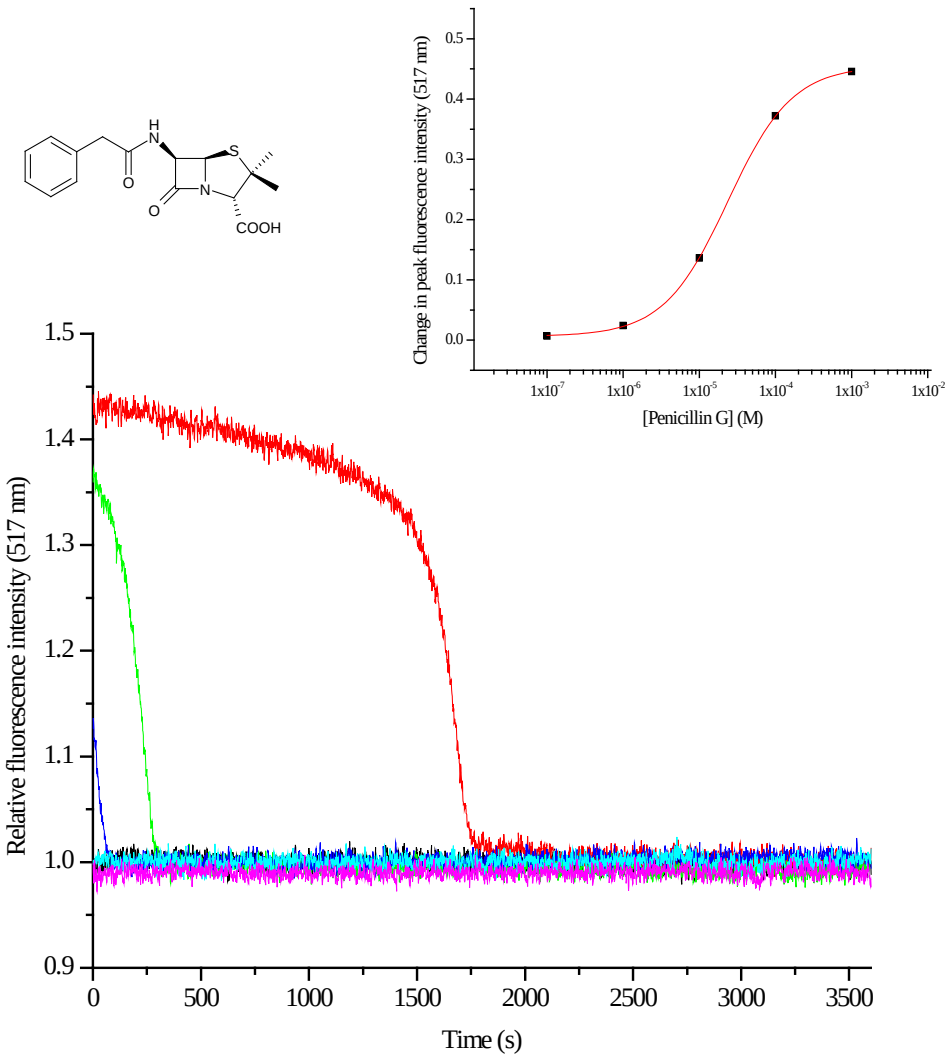

Figure III.2.7. Time-resolved fluorescence spectra of 1.0×10^{-7} M V211Cf in 50 mM potassium phosphate (pH 7.0) with penicillin G at the concentrations of 0 M (black), 1.0×10^{-7} M (magenta), 1.0×10^{-6} M (cyan), 1.0×10^{-5} M (blue), 1.0×10^{-4} M (green), and 1.0×10^{-3} M (red). Excitation wavelength: 498 nm. The inset shows the plot of change in peak fluorescence intensity as a function of concentration of penicillin G.

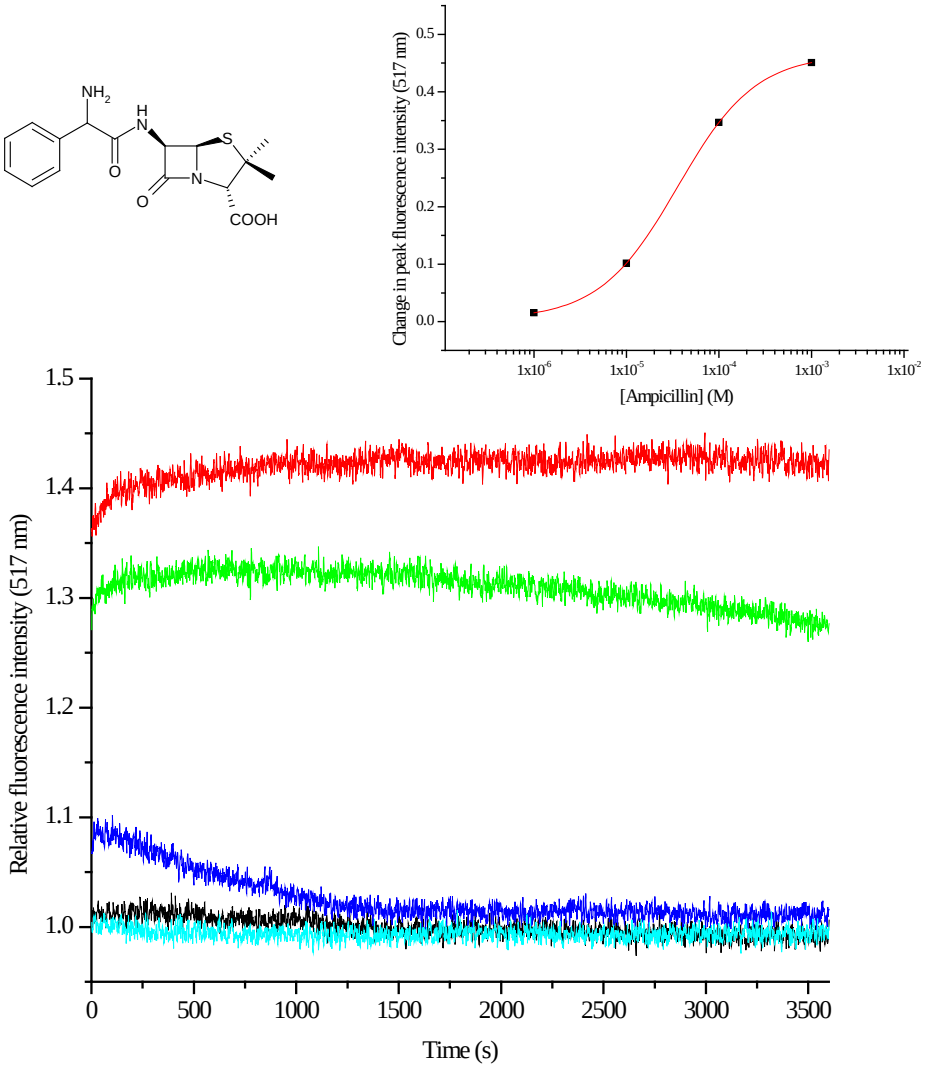

Figure III.2.8. Time-resolved fluorescence spectra of 1.0×10^{-7} M V211Cf in 50 mM potassium phosphate (pH 7.0) with ampicillin at the concentrations of 0 M (black), 1.0×10^{-6} M (cyan), 1.0×10^{-5} M (blue), 1.0×10^{-4} M (green), and 1.0×10^{-3} M (red). Excitation wavelength: 498 nm. The inset shows the plot of change in peak fluorescence intensity as a function of concentration of ampicillin.

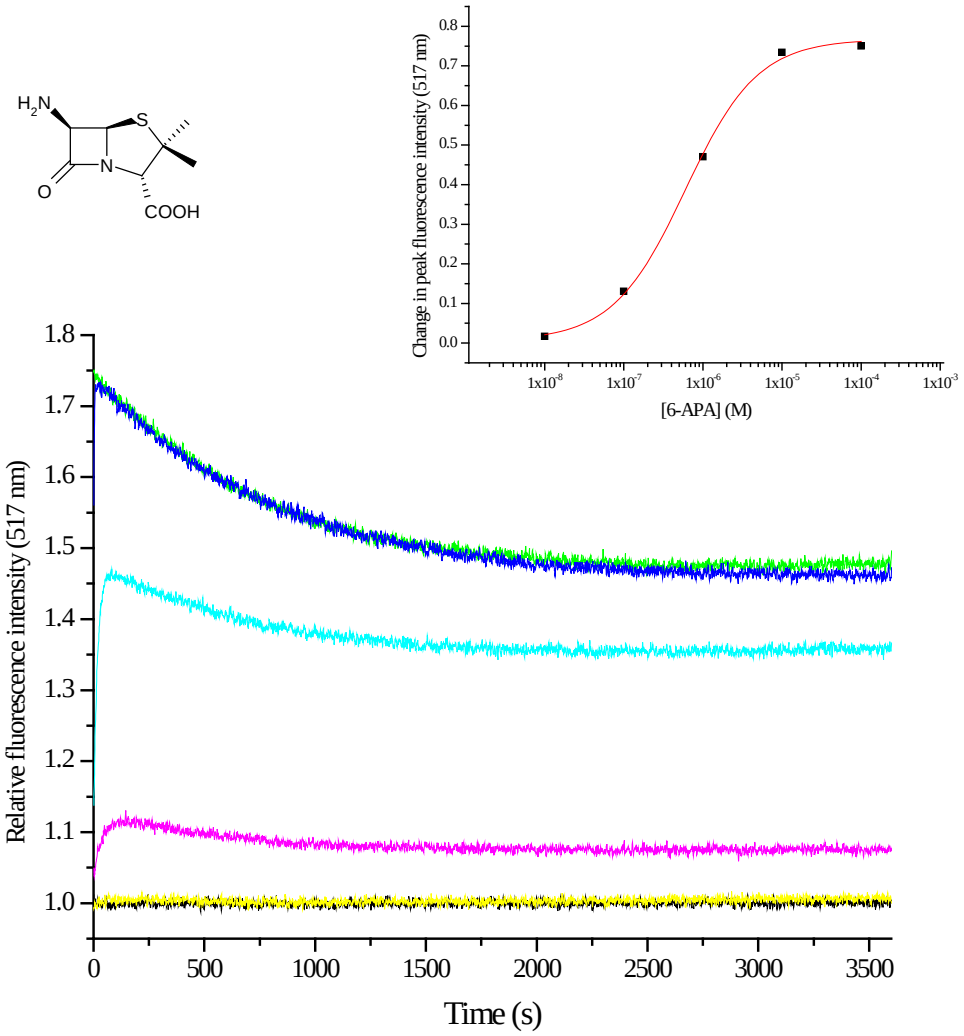

Figure III.2.9. Time-resolved fluorescence spectra of 1.0×10^{-7} M V211Cf in 50 mM potassium phosphate (pH 7.0) with 6-APA at the concentrations of 0 M (black), 1.0×10^{-8} M (yellow), 1.0×10^{-7} M (magenta), 1.0×10^{-6} M (cyan), 1.0×10^{-5} M (blue), and 1.0×10^{-4} M (green). Excitation wavelength: 498 nm. The inset shows the plot of change in peak fluorescence intensity as a function of concentration of 6-APA.

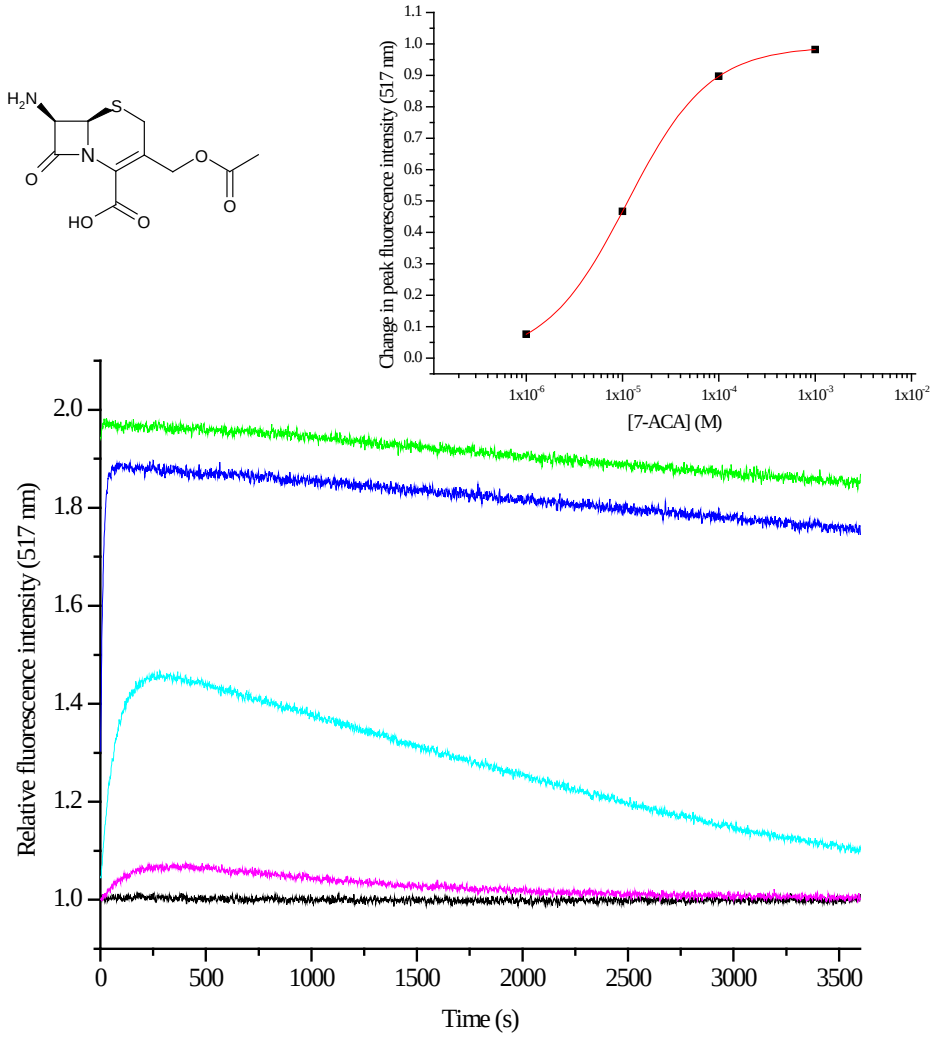

Figure III.2.10. Time-resolved fluorescence spectra of 1.0×10^{-7} M V211Cf in 50 mM potassium phosphate (pH 7.0) with 7-ACA at the concentrations of 0 M (black), 1.0×10^{-7} M (magenta), 1.0×10^{-6} M (cyan), 1.0×10^{-5} M (blue), and 1.0×10^{-4} M (red). Excitation wavelength: 498 nm. The inset shows the plot of change in peak fluorescence intensity as a function of concentration of 7-ACA.

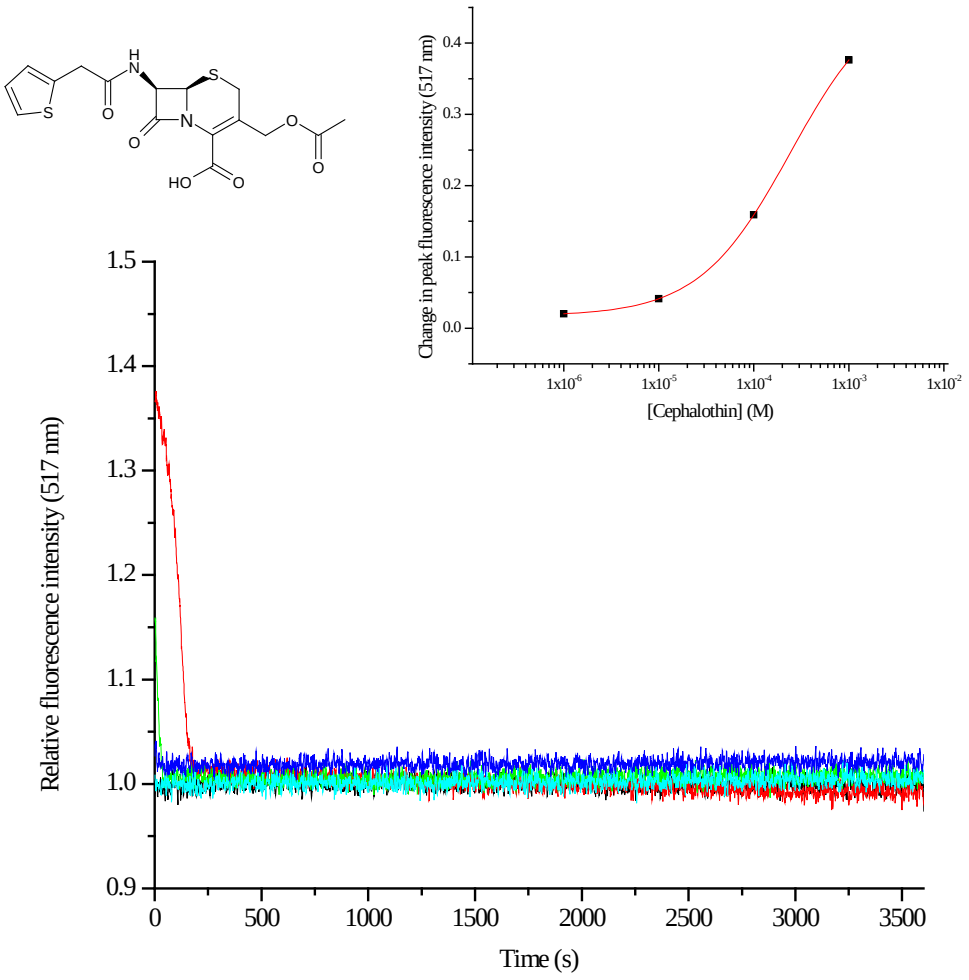

Figure III.2.11. Time-resolved fluorescence spectra of 1.0×10^{-7} M V211Cf in 50 mM potassium phosphate (pH 7.0) with cephalothin at the concentrations of 0 M (black), 1.0×10^{-6} M (cyan), 1.0×10^{-5} M (blue), 1.0×10^{-4} M (green), and 1.0×10^{-3} M (red). Excitation wavelength: 498 nm. The inset shows the plot of change in peak fluorescence intensity as a function of concentration of cephalothin.

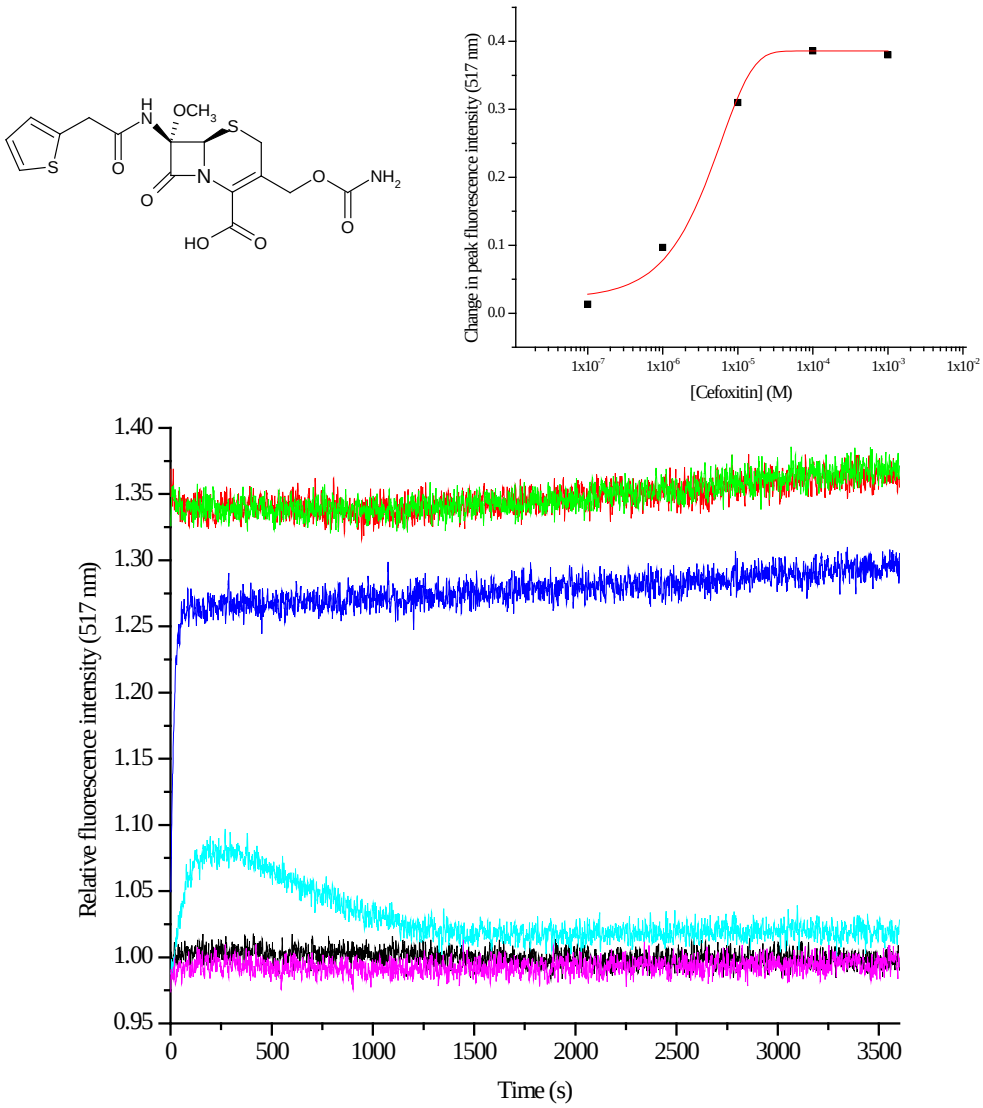

Figure III.2.12. Time-resolved fluorescence spectra of 1.0×10^{-7} M V211Cf in 50 mM potassium phosphate (pH 7.0) with cefoxitin at the concentrations of 0 M (black), 1.0×10^{-7} M (magenta), 1.0×10^{-6} M (cyan), 1.0×10^{-5} M (blue), 1.0×10^{-4} M (green), and 1.0×10^{-3} M (red). Excitation wavelength: 498 nm. The inset shows the plot of change in peak fluorescence intensity as a function of concentration of cefoxitin.

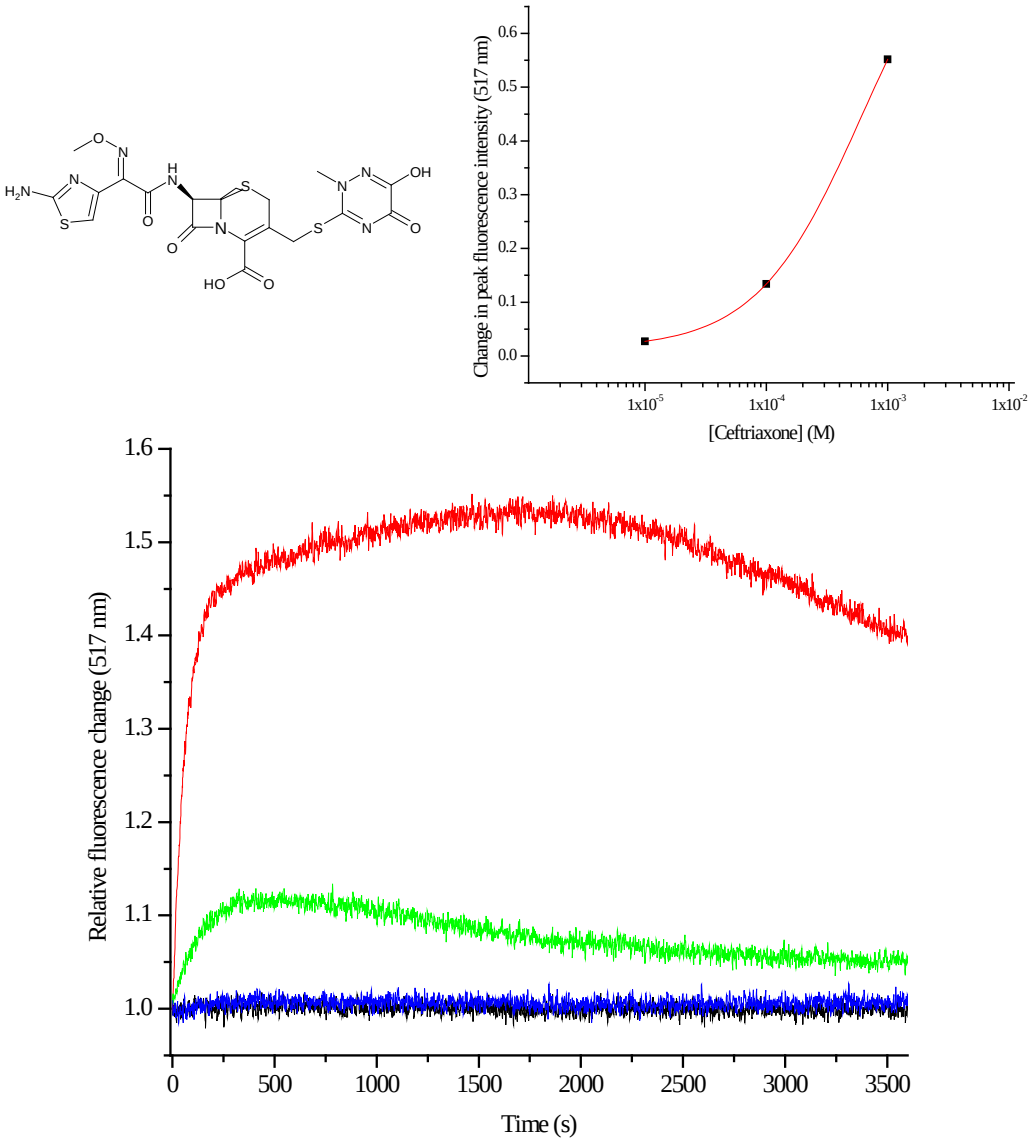

Figure III.2.13. Time-resolved fluorescence spectra of 1.0×10^{-7} M V211Cf in 50 mM potassium phosphate (pH 7.0) with ceftriaxone at the concentrations of 0 M (black), 1.0×10^{-5} M (blue), 1.0×10^{-4} M (green), and 1.0×10^{-3} M (red). Excitation wavelength: 498 nm. The inset shows the plot of change in peak fluorescence intensity as a function of concentration of ceftriaxone.

(A)

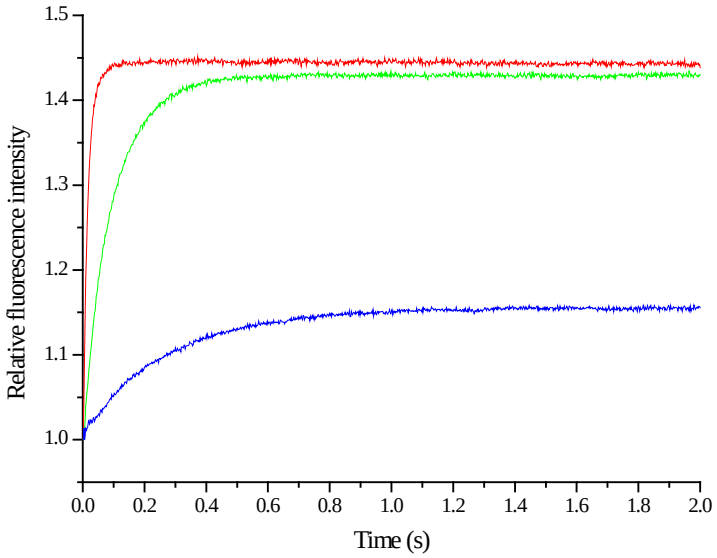

(B)

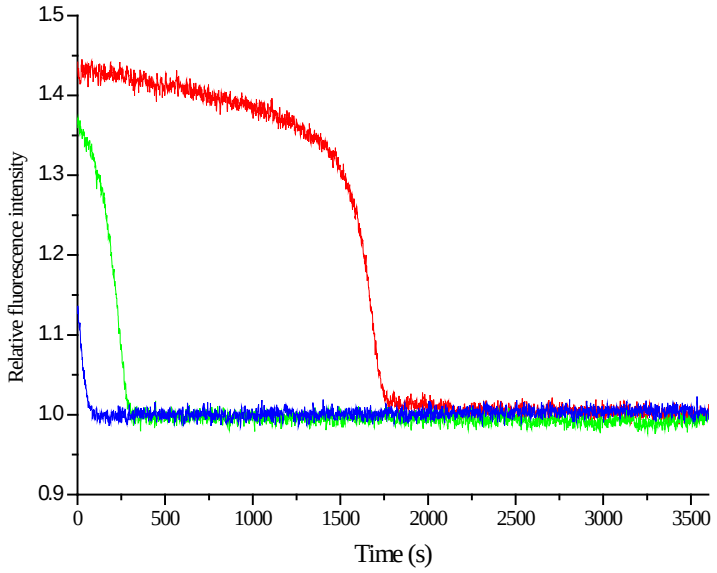

Figure III.2.14. Time-resolved fluorescence spectra of 1.0×10^{-7} M V211Cf in 50 mM potassium phosphate (pH 7.0) in the presence of penicillin G at the concentrations of 1.0×10^{-5} M (blue), 1.0×10^{-4} M (green), and 1.0×10^{-3} M (red) obtained by stopped-flow experiment (A) and fluorometric measurement (B; detailed spectra were shown in Figure III.2.7).

Table III.2.1. Comparison of the signal duration of penicillin G at various concentration.

	Initial rising phase	**Declining phase**
Substrate concentration	**Time required for reaching the maximal fluorescence intensity (s)**	**Time required for the returning to the basal fluorescence intensity (s)**
1.0×10^{-5} M	1.2	200
1.0×10^{-4} M	0.6	350
1.0×10^{-3} M	0.2	1900

Table III.2.2. Kinetic parameters of wild-type P99 β-lactamase for penicillins and cephalosporins.

	Kinetic parameters		
	K_m (µM)	**k_{cat} (s^{-1})**	**k_{cat}/K_m ($\mu M^{-1}s^{-1}$)**
Penicillins			
6-APA	***[a]	***[a]	***[a]
Penicillin G	0.6 ± 0.1[b]	14 ± 1.5[b]	23 ± 5[b]
Ampicillin	0.4 ± 0.05[b]	0.74 ± 0.05[b]	1.8 ± 0.4[b]
Cephalosporins			
7-ACA	950 ± 30[a]	0.2 ± 0.05[a]	0.0002 ± 0.00005[a]
Cephalothin	9 ± 0.7[c]	200 ± 8[c]	20 ± 1[c]
Cefoxitin	0.024 ± 0.002[c]	0.06 ± 0.005[c]	2.5 ± 0.1[c]
Ceftriaxone	0.007[d]	11[d]	0.0033[d]

Remarks:

***. Complex branched pathway.

a. Matagne *et al.*, 1990.

b. Galleni and Frère, 1988a.

c. Galleni and Frère, 1988b.

d. Nukaga *et al.*, 1998.

III.2.3.4. Implications of V211Cf for the sensor development and mechanistic studies

From our data, V211Cf has demonstrated the feasibility of probing the local environment of the active site with a fluorescein reporting group close to the catalytic region and also the ability to convert its recognition with β-lactam substrates into fluorescence signal. Having fluorescence responses according to substrate profile and concentration, V211Cf met the basic requirement for being a biosensor for quantitative analysis of β-lactam compounds. However, the conserved catalytic activity as the wild-type enzyme of V211Cf would contribute to hydrolytic destruction of the substrate analytes (especially the good substrates), thus reducing the signal stability and sensitivity of V211Cf. Therefore, at this stage, instead of being a practical biosensor, it was much more illustrative to make use of V211Cf as a starting framework for future development for sensing molecules for β-lactam antibiotics. The works we have attempted to improve the biosensor performance will be described in Chapter III.4.

From the mechanistic point of view, V211Cf demonstrated desirable fluorescence properties for being a versatile tool for studying kinetic and mechanistic actions of β-lactamase. As β-lactamase-catalyzed hydrolytic reaction

proceeds with the involvement of acyl-enzyme intermediates, tremendous interests have been arisen in capturing these transient substrate-enzyme intermediates from the mechanistic studies of β-lactamase. As V211Cf exhibited fluorescence turn-on following the formation of ES and ES* along the catalytic reaction by β-lactamase, time-resolved fluorescence spectra represented the progress curves for the ES and ES* complexes, thus tracking the trajectory of these intermediates. Since the intermediates often transiently appear as shorted-lived species in the cases of good substrates, studies on these complexes have also always been restricted to the reactions with poor substrates and inhibitors at which there would be accumulation of the intermediate complexes (Fisher *et al.*, 1978; Fisher *et al.*, 1980). In contrast, there was no such limitation on V211Cf as revealed by our fluorometric results of penicillin G and cephalothin which were good substrates susceptible to β-lactamase hydrolysis. When comparing with other methods for tracing the enzyme-substrate complexes, V211Cf showed higher sensitivity over the traditional absorbance monitoring of the intermediate chromophores (Charnas *et al.*, 1978; Knott-Hunziker *et al.*, 1980); and provided higher flexibility than the approaches that utilized the fluorogenic enzyme substrates (Anderson and Pratt, 1981 and 1983; Pratt *et al.*, 1988). Therefore, it was inspiring that V211Cf could become a powerful tool for

studying pre-steady state β-lactamase kinetics with the combination of the stopped flow fluorescence technique, providing better understandings of the enzyme mechanism.

III.2.4. Concluding remarks

To conclude, with a fluorescein molecule strategically located nearby the catalytic site, V211Cf could serve as a probe for the local environment of the active site. The fluorescein reporter was able to give meaningful fluorescence signals in response to the substrate-induced local environment change at the active site depending on the substrate nature and concentration. The capability of V211Cf to sense β-lactam antibiotics further demonstrated the adaptability of the strategy of engineering a non-allosteric hydrolytic enzyme for the biosensor purpose, providing new direction to biosensor research. Furthermore, time-resolved fluorescence measurement of V211Cf not only allows detection for the presence of β-lactam compounds but also offers real-time monitoring of the formation of intermediates along the hydrolytic reaction, helping unravel the mechanistic action of β-lactamase.

Chapter III.3

Utilization of V211Cf as a probe for *β*-lactamase inhibitors

III.3.1. Introduction

β-lactamase has been of particular therapeutic interest owing to its prominent role in the mediation of bacterial resistance. Two general strategies to encounter the *β*-lactamase-producing pathogens are to introduce *β*-lactamase-stable antibiotics and co-administrate enzyme-susceptible *β*-lactam antibiotics with *β*-lactamase inhibitors (Livermore, 1998; Williams, 1999; Walsh, 2000). Basically, the first strategy involves inventions of *β*-lactam antibiotics that are insensitive to the enzymatic hydrolysis, whereas the latter one potentiates the effectiveness of the *β*-lactamase-susceptible antibiotics with the use of *β*-lactamase-targeting inhibitors to protect them from enzymatic inactivation. Of these two strategies, the strategy of combination therapy with inhibitors is generally more welcomed practically since it demonstrates a simple concept of preserving the existing once-dependable, simple antibiotics rather than complicating the situations by introducing new antibiotics which will also have desirable pharmacodynamic and pharmacokinetic properties as the current compounds did. Currently, only three

β-lactamase inhibitors, namely clavulanic acid, sulbactam and tazobactam, which are *β*-lactam-based compounds (**1-3**, Figure III.3.1), are of clinical approval and they are formulated into combinations with various *β*-lactam partners for different clinical settings (Lee *et al.*, 2003).

At present, class C *β*-lactamases have rapidly emerged as the second-most prevalent classes of *β*-lactamases, thus addressing immediate needs of effective therapeutic strategies to combat the causative pathogens containing these *β*-lactamases. Whilst the clinically approved inhibitors in the combination therapy usually allow effective disease controls as they specifically target at the most clinically-encountered class A *β*-lactamases, neither of them are effective agents against the class C *β*-lactamases (Maiti *et al.*, 1998; Payne *et al.*, 2000) (Table III.3.1). This highlighted the demands for searching potent class C *β*-lactamase inhibitors. With the ultimate goal of developing effective class C *β*-lactamase inhibitors, many projects are thus in progress for deriving new *β*-lactam-based inhibitors (Richter *et al.*, 1996; Bitha *et al.*, 1999a and 1999b; Sandanayaka and Yang, 2000; Vilar *et al.*, 2001; Buynak *et al.*, 2002; Sandanayaka *et al.*, 2003; Phillips *et al.*, 2005; Tsang *et al.*, 2005) as well as seeking novel non-*β*-lactam-based inhibitors including boronic acids (Powers *et al.*, 1999; Tondi

et al., 2001; Morandi *et al.*, 2003; Buzzoni *et al*., 2004), phosphonates (Kaur *et al.*, 2003), other organic compounds (Bonnefey *et al.*, 2004) and inorganic complexes (Bell and Pratt, 2002).

Concomitant with the immense interests in the novel inhibitor discovery are the needs for efficient approaches for screening and characterizing a vast array of potential candidates that comes from the nature (Peláez, 2006) or is generated from structure-guided in-parallel synthesis. Conventional approaches for identifying the potential drug candidates are microbial susceptibility testing (Banic, 2006) and *β*-lactamase inhibition assay (Yamaguchi *et al.*, 1983; Perilli *et al.*, 1999; Bethel *et al.*, 2004). These methods determine the minimal inhibitory concentration (MIC) and inhibition constants (IC_{50} or K_i) of the candidates respectively, thus providing indices for the drug potency. In addition, characterization techniques like radioactive labeling of inhibitors (Bush *et al.*, 1993), UV difference spectral studies (Rizwi *et al.*, 1989; Sulton *et al.*, 2005), mass spectrometry (Tabei *et al.*, 2004; Sulton *et al.*, 2005) and crystallographic studies (Chen and Herzberg, 1992; Crichlow *et al.*, 2001; Nukaga *et al.*, 2003; Schmid, 2006), which provide kinetic and structural analyses on the enzyme-inhibitor complexes, are well-established to advance a better

understanding of the inactivation chemistry of the candidates with desirable efficacy for further drug design and lead compound optimization.

Apart from the above techniques, to keep pace with the increasing loads of potential candidates and to shorten the time-investment for the drug development, it is still northworthy to have efficient systems that can allow rapid exploration for the novel therapeutics. This prompted our interests in exploring the potential of our V211Cf for being a versatile tool for novel drug screening and characterization. As revealed in Chapter III.2, our V211Cf with a fluorescent probe conjugated at the proximity to its active site could permit detection of the β-lactam antibiotics and allow on-line monitoring of the enzyme-substrate intermediates. Therefore, we postulated that V211Cf, as a sensing molecule without the loss of the parental wild-type activity, may also find its potential in the applications for identifying novel class C β-lactamase inhibitors as well as characterizing the inactivation mechanism of the inhibitors. This chapter will investigate this feasibility by examining the fluorescence properties of V211Cf towards several β-lactamase inhibitors including clavulanic acid, sulbactam, tazobactam and boronic acids. The structures of these inhibitors are shown in Figure III.3.1.

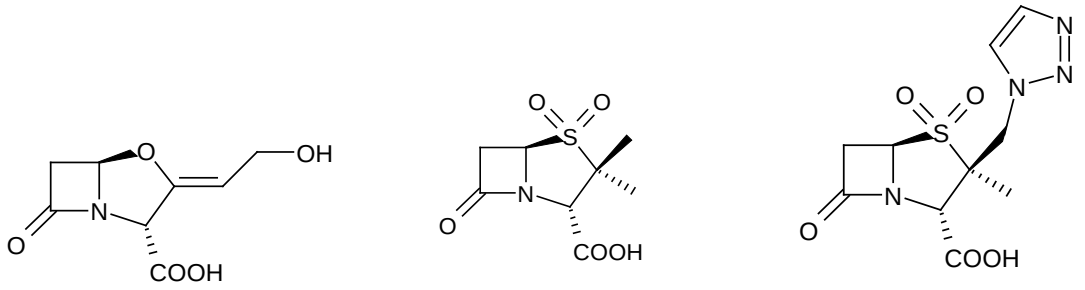

1 **2** **3**

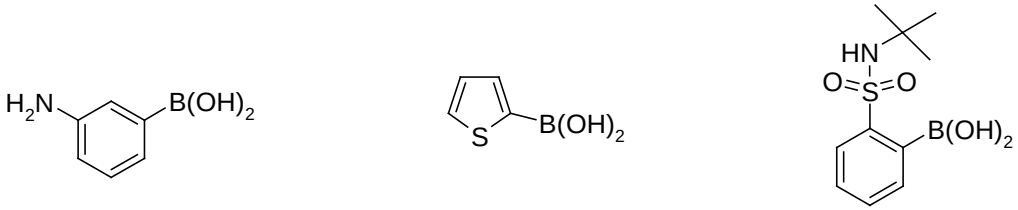

4 **5** **6**

Figure III.3.1. Structures of *β*-lactamase inhibitors involved in this study. *β*-lactam based inhibitors include clavulanic acid **1**, sulbactam **2**, and tazobactam **3**, whereas boronic acids include 3-aminophenylboronic acid **4**, 2-thiopheneboronic acid **5** and 2-(tert-butylamino)sulfonylphenylboronic acid **6**.

Table III.3.1. Effective concentration ranges of clavulanic acid, sulbactam and tazobactam towards the class A and class C β-lactamases (Page, 2000). The ranges are covered by grey color with the most effective concentrations in dark grey color.

	IC_{50}(µM)	0.001	0.01	0.1	1	10	100
Clavulanic acid	**Class A**						
	Class C						
Sulbactam	**Class A**						
	Class C						
Tazobactam	**Class A**						
	Class C						

III.3.2. Methods

III.3.2.1. IC_{50} determination

Inhibitor and enzyme were incubated at 25^{o}C for 5 min at their final concentration. Afterwards, enzymatic reaction was initiated by the addition of 100 µM nitrocefin. Product formation due to hydrolysis of nitrocefin was monitored at 500 nm over 2 min. The fractional activity remaining at each given inhibitor concentration was calculated by dividing the initial velocity in the presence of inhibitor (v_i) by the initial velocity in the absence of inhibitor (v_o). The inhibitor concentration that gave a 50% reduction in enzyme activity (IC_{50}) was determined from a plot of fractional activity as a function of inhibitor concentration which was obtained by fitting the experimental data to the respective equations using Origin 6.0 Professional.

III.3.2.2. Fluorometric studies

The detailed procedure was described in Section II.10.

III.3.3. Results and discussions

III.3.3.1. Inhibitory effects of *β*-lactam-based inhibitors on the class C *β*-lactamases

As a chemically-modified mutant, how similar of V211Cf to its wild-type parent in the functional properties would be directly related to its performances in qualitative drug screening and studies of the enzyme-drug interaction. Previously, V211Cf has shown to be having similar catalytic properties as the wild-type enzyme and here would assess its inactivation by the *β*-lactam-based inhibitors.

Figure III.3.2 shows the inhibitory effects of the clavulanic acid, sulbactam and tazobactam on wild-type, V211C and V211Cf. All of these inhibitors showed concentration-dependent inhibitions on the two enzyme mutants. Their corresponding IC_{50} values were listed in Table III.3.2. Among the three inhibitors, while tazobactam was the best inhibitor inactivating the class C *β*-lactamases in micromolar ranges, clavulanic acid showed poorest inhibitory activity towards the enzymes by exhibiting IC_{50} values higher in one- to two-orders of magnitude than the other two penicillanic acid sulfones did. Furthermore, it was noted that those values for V211C and V211Cf were comparable with those for the wild-type enzyme reported in the literature, indicating that the genetic and chemical

modifications at the position of 211 for the β-lactamase posed no effects on the enzyme's properties towards the inhibitors. And this high similarity in the characteristics between V211Cf and its wild-type towards the inhibitor activities implied the likeliness of V211Cf to reflect the real situation of the enzyme inactivation by the inhibitors. This preliminarily underlined the potential of V211Cf as a useful system for determining the enzyme-inhibitor interaction which is the fundamental basis of inhibitor screening as well as providing important information for inhibition mechanistic studies.

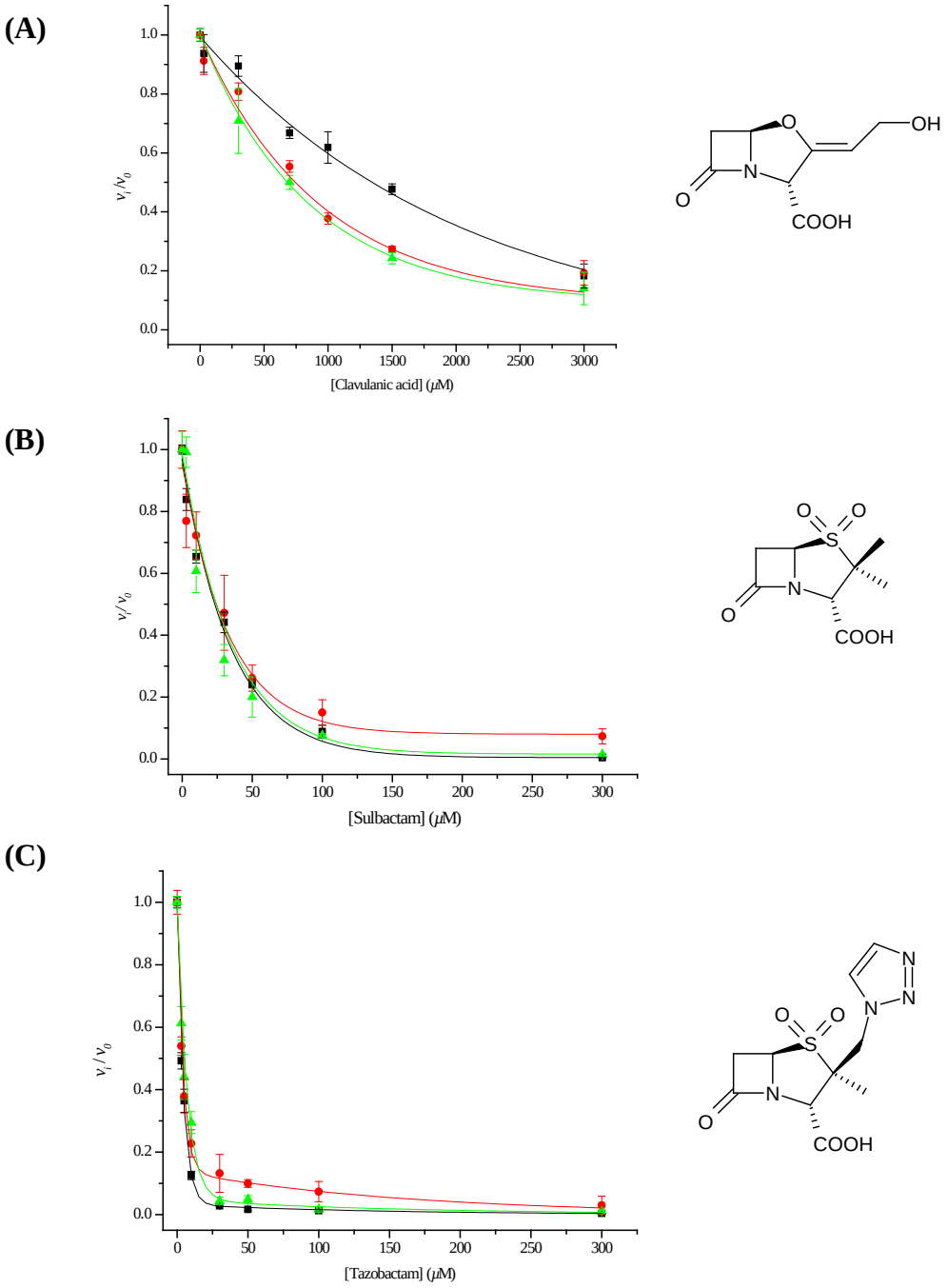

Figure III.3.1. Plots of fractional activity as a function of concentration of clavulanic acid (A), sulbactam (B) and tazobactam (C) for wild-type (in black line), V211C (in red line) and V211Cf (in green line).

Table III.3.2. Inhibition of P99 *β*-lactamase wild-type, V211C and V211Cf mutants by clavulanic acid, sulbactam and tazobactam.

	IC_{50} (μM)		
	Wild-type	**V211C**	**V211Cf**
Clavulanic acid	1322	722	651
Sulbactam	22.4	23.9	17.4
Tazobactam	3.5	3.5	4

III.3.3.2. Fluorescence properties of V211Cf towards *β*-lactam-based inhibitors

Clavulanic acid, sulbactam and tazobactam are suicide inhibitors for *β*-lactamase, inactivating the enzyme through the covalent modification at the enzyme active site. As depicted in Scheme III.3.1, the inhibition mechanism follows complicated branched pathway (Bush, 1988; Therrien and Levesque, 2000). The inhibitors first get bound with the enzyme-active sites and then undergo acylation to give the covalent acyl-enzyme adducts (EI*). Before inactivation, some of these complexes would dissociate through deacylation, thus a small portion of inhibitor molecules would sacrifice in this normal enzyme turnover. The remaining acyl-enzyme complexes would either convert into various transiently inhibited forms of enzymes (E-T) or yield irreversibly inactivated enzymes (EI**) through the rearrangement events, eventually leading to either transient or irreversible inhibition of the enzyme. Despite the general inactivation mechanism shared by the clavam and the penicillanic acid sulfones, slight differences in the partition of the branched pathways leading to inhibition were found between these two groups of inhibitors. And the specific detailed mechanisms proposed for clavulanic acid and the penam sulfones are illustrated in Figure III.3.3 and Figure III.3.4 respectively.

To explore the application of V211Cf for detecting the inhibitors, the fluorescence properties of V211Cf towards these *β*-lactam inhibitors were studied. Figure III.3.5 – III.3.7 showed the time-resolved fluorescence traces of V211Cf towards clavulanic acid, sulbactam and tazobactam respectively. As revealed, V211Cf displayed distinct fluorescence signals for the clavulanic acid and the two penam sulfone compounds observed over a 1-h time-course. For clavulanic acid, there was a gradual increase in the fluorescence intensity followed by the addition of the inhibitor. As shown in the trace for the concentration of 1.0×10^{-3}M of clavulanic acid, the fluorescence signal tended to level-off to a plateau level after its rise to its fluorescence maximum. In contrast, for sulbactam and tazobactam, fluorescence intensities instantaneously increase after mixing V211Cf with the inhibitors and the signals subsided rapidly after the initial fluorescence spikes.

The above fluorescence results indicated that V211Cf could give rise to characteristic signals towards two groups of *β*-lactam inhibitors, the clavam and the penam sulfone which operate their own specific inactivation mechanisms according to different partitions in the routes to inhibition. However, because of the various possible forms of the inhibitor-enzyme adducts along the specific

inactivation pathways for each class of inhibitors, the exact components ascribed to the distinct fluorescence signals for these inhibitors could not be resolved by interpreting these fluorescence traces. Indeed, as the fluorescence signals were due to the synergistic effects of the reaction products formed from each branching reaction in the inactivation process, the traces presented here reflected the integrated dynamics of various branched pathways along the inhibition event. Thus, in conjunction with other characterization techniques, valuable information about the inactivation mechanism would be obtained.

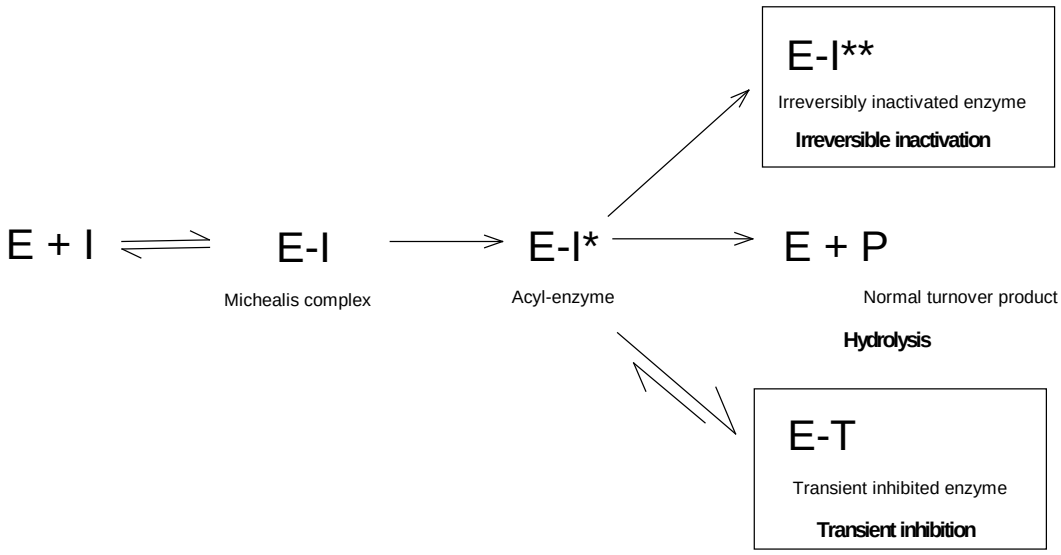

Scheme III.3.1. Generalized branched pathways for inhibition of serine-reactive *β*-lactamase followed by clavulanic acid, sulbactam and tazobactam (Yang *et al.*, 1999).

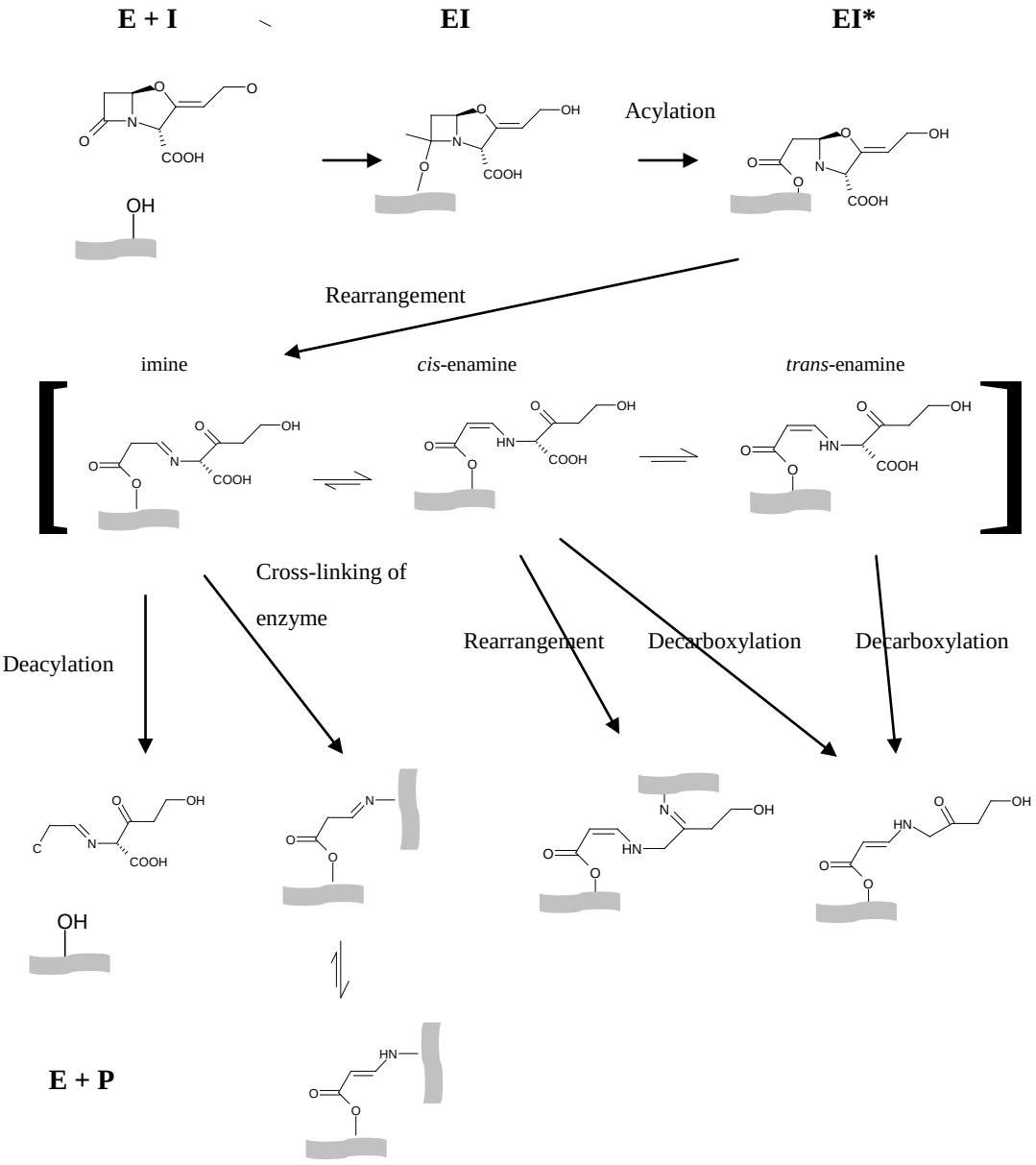

Figure III.3.3. Proposed mechanism of inactivation of serine *β*-lactamase by clavulanic acid (Brown, 1986; Chen and Herzberg, 1992; Padayatti *et al.*, 2005).

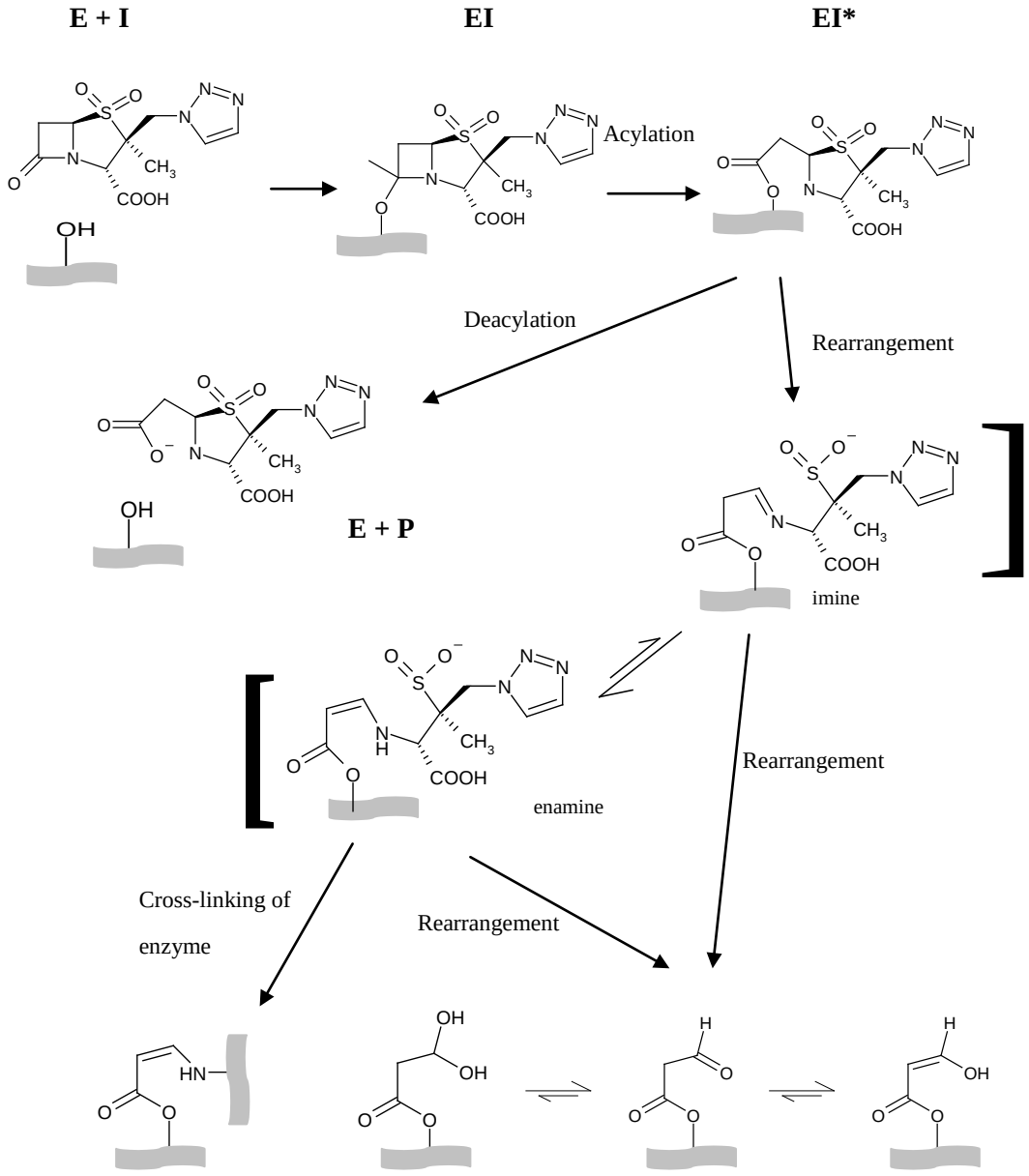

Figure III.3.4. Proposed mechanism of inactivation of serine *β*-lactamase by tazobactam. The inhibition by sulbactam has been suggested in a similar fashion as tazobactam does (Bush *et al.*, 1993; Yang *et al.*, 2000; Bonomo *et al.*, 2001).

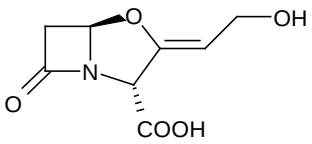

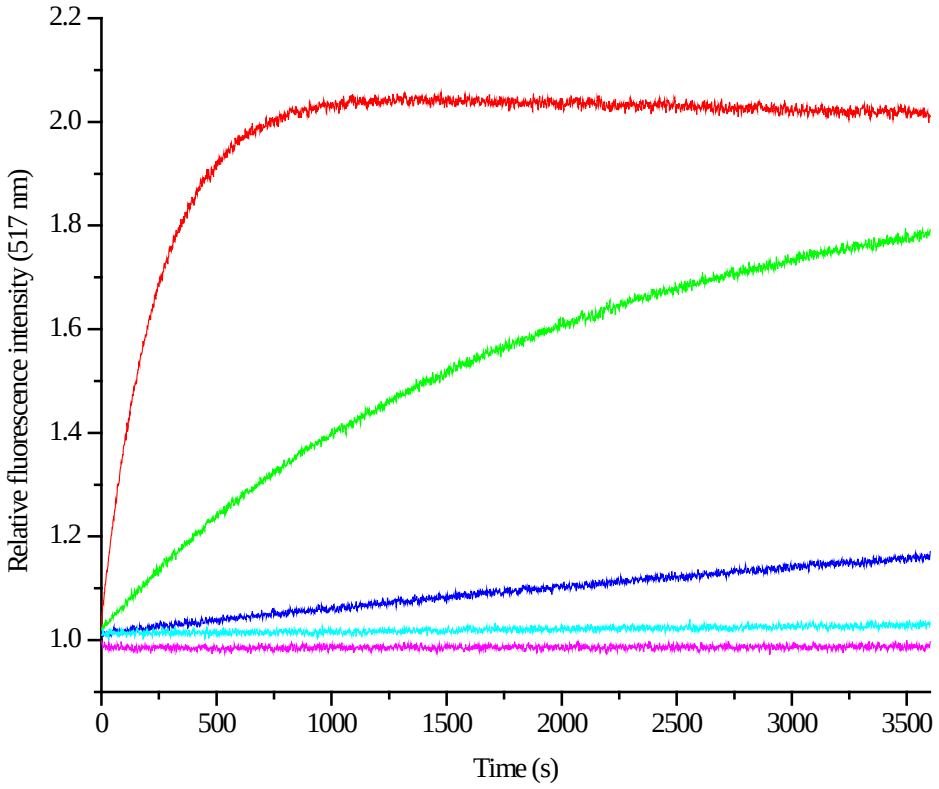

Figure III.3.5. Time-resolved fluorescence spectra of 1.0×10^{-7} M V211Cf in 50 mM potassium phosphate (pH 7.0) with clavulanic acid at the concentrations of 1.0×10^{-7} M (magenta), 1.0×10^{-6} M (cyan), 1.0×10^{-5} M (blue), 1.0×10^{-4} M (green), and 1.0×10^{-3} M (red). Excitation wavelength: 498 nm.

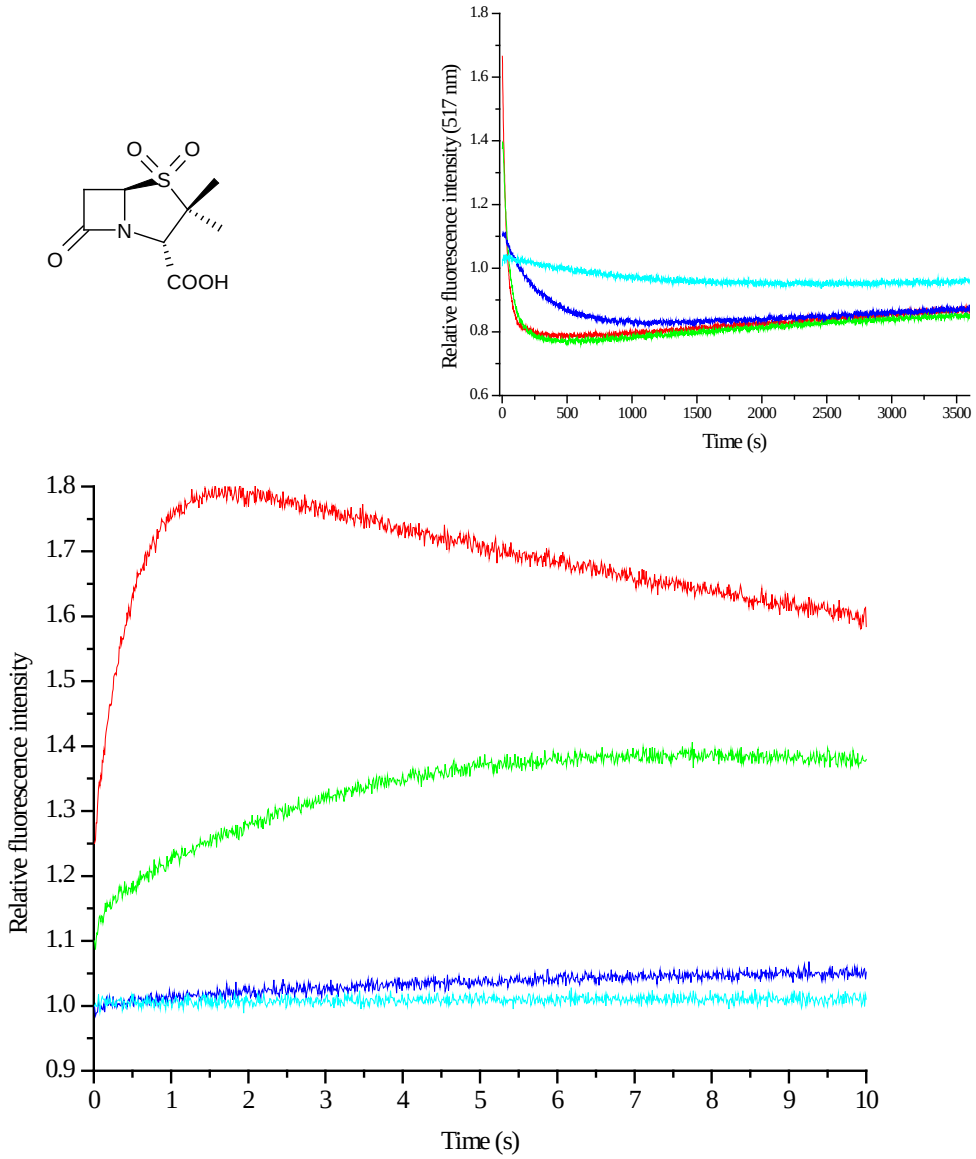

Figure III.3.6. Time-resolved fluorescence spectra of 1.0×10^{-7} M V211Cf in 50 mM potassium phosphate (pH 7.0) with sulbactam at the concentrations of 1.0×10^{-6} M (cyan), 1.0×10^{-5} M (blue), 1.0×10^{-4} M (green), and 1.0×10^{-3} M (red) obtained by stopped-flow experiment. Excitation wavelength: 498 nm. The inset shows the corresponding spectra obtained over 1 h-measurement.

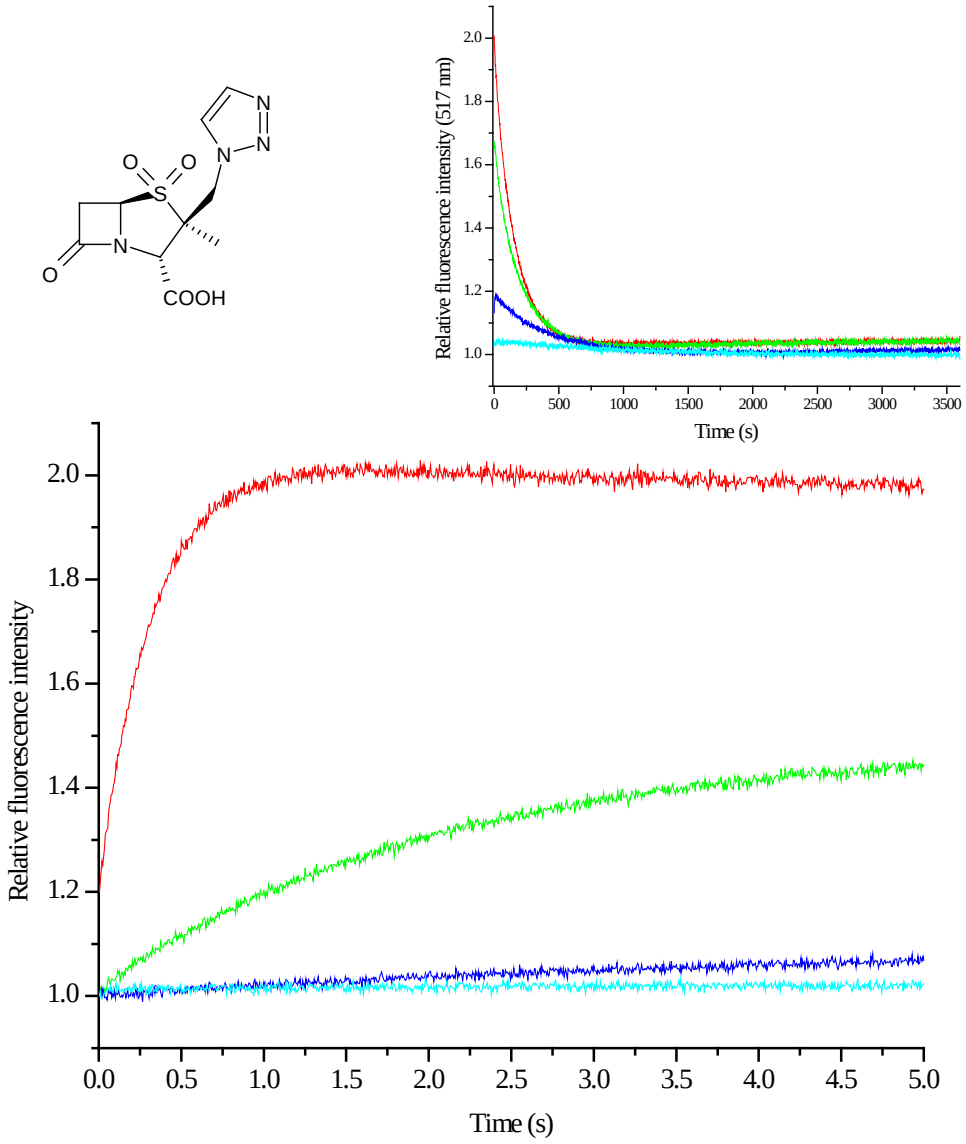

Figure III.3.7. Time-resolved fluorescence spectra of 1.0×10^{-7} M V211Cf in 50 mM potassium phosphate (pH 7.0) with tazobactam at the concentrations of 1.0×10^{-6} M (cyan), 1.0×10^{-5} M (blue), 1.0×10^{-4} M (green), and 1.0×10^{-3} M (red) obtained by stopped-flow experiment. Excitation wavelength: 498 nm. The inset shows the corresponding spectra obtained over 1 h-measurement.

III.3.3.3. Fluorescence properties of V211Cf towards boronic acids

Boronic acid is an intriguing class of non-*β*-lactam compounds that can inactivate serine *β*-lactamases by acting as transition-state analog. Scheme III.3.2 shows its two step inactivation mechanism on a serine-reactive *β*-lactamase. Inactivation process proceeds with an initial binding of a boronic acid to the enzyme active site and a subsequent step of dative covalent bond formation between the active site serine hydroxyl group and the boronic acid to give a reversible adduct (Crompton *et al.*, 1988). This resultant adduct, which adopts a geometry resembling to that of high energy tetrahedral intermediates along the hydrolytic reaction pathway (Figure III.3.8), occupies the active-site of the *β*-lactamase, thus deactivating the enzyme.

With an interest in investigating the capability of V211Cf to probe for these non-*β*-lactam inhibitors, the effects of three boronic acids including 3-aminophenylboronic acid (MAPB), 2-thiopheneboronic acid and 2-(tert-butylamino)sulfonylphenylboronic acid on the fluorescence of V211Cf were examined in our study. The fluorescence traces for these three boronic acids were shown from Figure III.3.9 – III.3.11 respectively.

At the first glance, the fluorescence signals for boronic acids were generally comprised of 2 phases: an initial rising or decreasing phase and a succeeding plateau phase. Moreover, it was observed that the plateau phases of all these three boronic acids were stable over the 1 h-fluorescence detection (shown at the inset for each spectrum). These results were in a good agreement with the two step inhibition mechanism of boronic acid on serine-type β-lactamase that the initial phase corresponded to the binding of the boronic acid to the active site whereas the plateau phase coming afterwards referred to the stage at which all the active sites were saturated with the transition-state analogs.

Inspecting the signal for each boronic acid individually, it was shown that fluorescence quenching was resulted from the addition of MAPB whereas fluorescence enhancement was triggered by adding 2-thiopheneboronic acid and 2-(tert-butylamino)sulfonylphenylboronic acid to V211Cf. This discrimination in the fluorescence behaviors of V211Cf could be ascribed to the different binding orientations of the boronic acid ligands in the active site pocket.

Unlike β-lactam substrates which usually position their side chains at well-defined regions in the active site pocket, boronic acids fit into the enzyme

binding site in various orientations owing to their smaller sizes. Figure III.3.12 illustrates the two categories of possible orientations of the boronic acid in the enzyme active site, the "MAPB-like" and "phosphonate-like" binding modes, which were observed from the co-crystal structures of class C *β*-lactamase with a series of boronic acids (Weston *et al.*, 1998). "MAPB-like" binding mode is so-called as it was illustrated by the crystallographic orientation of MABP inside the enzyme active site (Usher *et al.*, 1998). In this scenario, the MAPB makes favorable interactions with the residues near the oxyanion pocket and positions its 3-amino group towards the hydrophobic groove at the active site pocket (Figure III.3.12.A). Conversely, many of the aryl boronic acids adopt reverse orientations in which they interact well with the residues located at the surface-exposed cleft, protruding their functional groups towards a more hydrophilic environment (Figure III.3.12.B). As these orientations look similar to that observed in the complex formed by a phosphonate with the class C *β*-lactamase (Lobkovsky *et al.*, 1994) (Figure III.3.12.C), they are collectively known as "phosphonate like" mode.

Considering the binding orientations of our three tested boronic acids, MABP, which was the one quenching the fluorescence of V211Cf, was actually the model

of “MABP-like” binding mode whereas the other two fluorescence enhancing boronic acids seemed to orient in “phosphonate-like” configuration. The latter was reasoned by the suggested quadrupole-dipole interaction of the thiophene ring of 2-thiopheneboronic acid with electropositive Asn152 located at the R1 cleft (Weston *et al.*, 1998) as well as the orientation preference demonstrated by bulky sulfonyl boronic acids having large size and high solubility (Tondi *et al.*, 2001) for 2-(tert-Butylamino)sulfonylphenyl-boronic acid.

Correlating the ligand binding orientation with our fluorescence data, it was apparent that the boronic acids which adopt “MAPB-like” binding mode would quench the fluorescence of V211Cf whereas those orient in a “phosphonate-like” manner would modulate fluorescence enhancement of V211Cf. At this stage, although the exact mechanism of the quenching effect of MABP was unclear, the enhancing effects of the boronic acids demonstrating the “phosphonate-like” mode would be rationalized by the positioning of the functional entities of these ligands into the R1 cleft, eventually changing the local environment of the fluorescein reporter tethered on the same site to a more solvent exposed environment, thus increasing the fluorescence intensity.

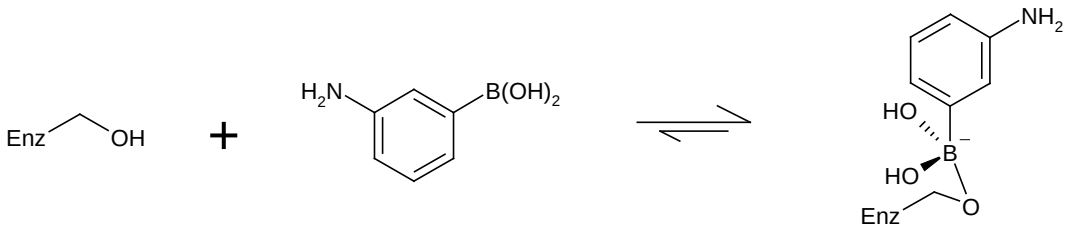

Scheme III.3.2. Inhibition mechanism of boronic acid on serine β-lactamase.

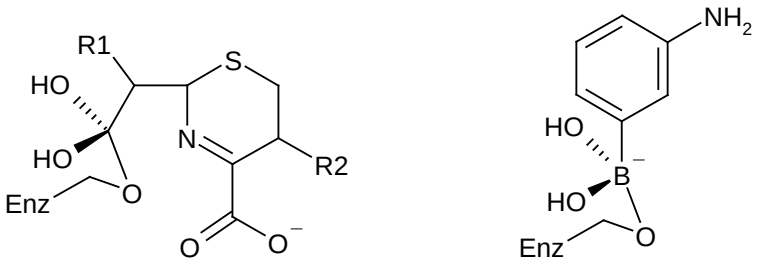

Figure III.3.8. Structures for the high-energy tetrahedral intermediate along the deacylation pathway for *β*-lactamase and the adduct formed between the boronic acid and *β*-lactamase (Usher *et al.*, 1998).

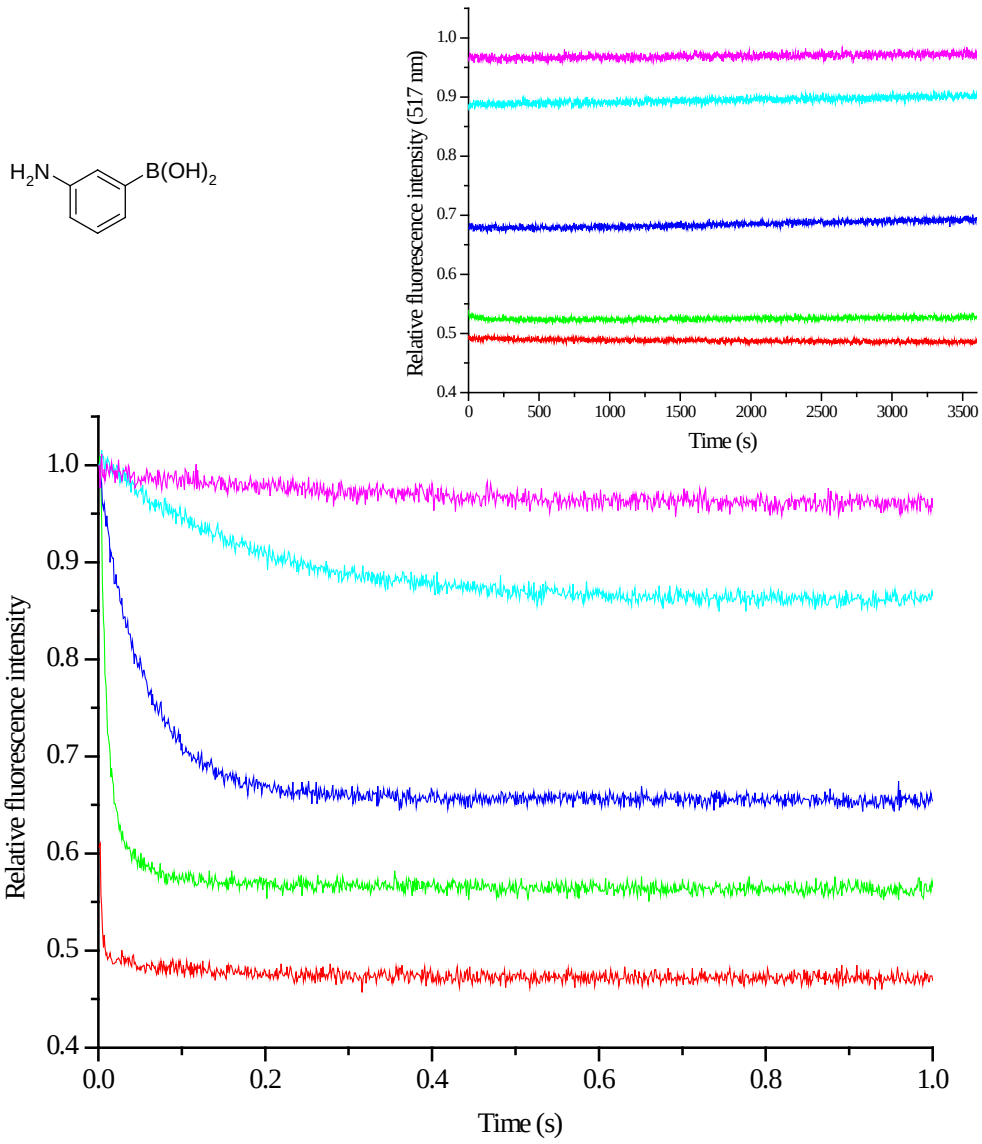

Figure III.3.9. Time-resolved fluorescence spectra of 1.0×10^{-7} M V211Cf in 50 mM potassium phosphate (pH 7.0) with 3-aminophenylboronic acid at the concentrations of 1.0×10^{-7} M (magenta), 1.0×10^{-6} M (cyan) 1.0×10^{-5} M (blue), 1.0×10^{-4} M (green) and 1.0×10^{-3} M (red) obtained by stopped-flow experiment. Excitation wavelength: 498 nm. The inset shows the corresponding spectra obtained over 1 h-measurement.

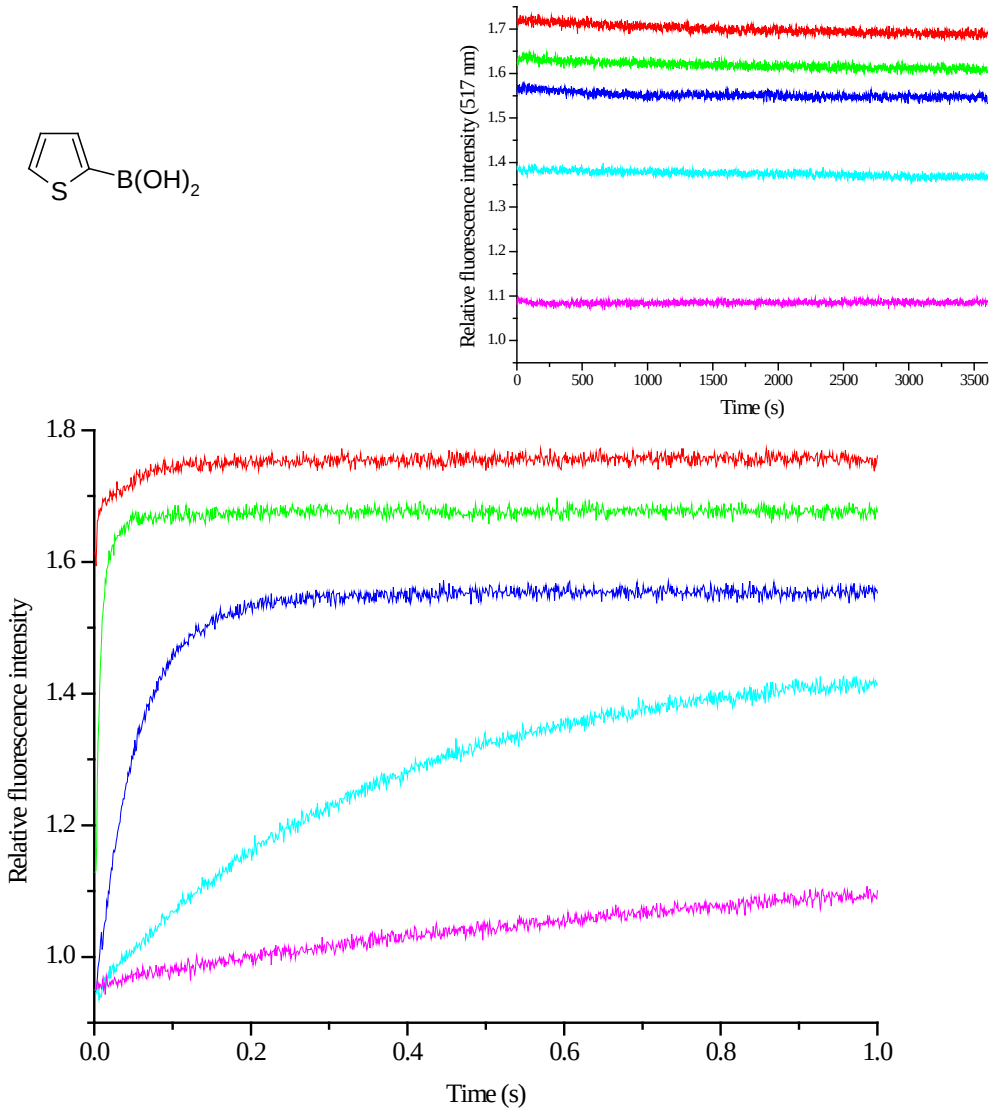

Figure III.3.10. Time-resolved fluorescence spectra of 1.0×10^{-7} M V211Cf in 50 mM potassium phosphate (pH 7.0) with 2-thiopheneboronic acid at the concentrations of 1.0×10^{-7} M (magenta), 1.0×10^{-6} M (cyan), 1.0×10^{-5} M (blue), 1.0×10^{-4} M (green) and 1.0×10^{-3} M (red) obtained by stopped-flow experiment. Excitation wavelength: 498 nm. The inset shows the corresponding spectra obtained over 1 h-measurement.

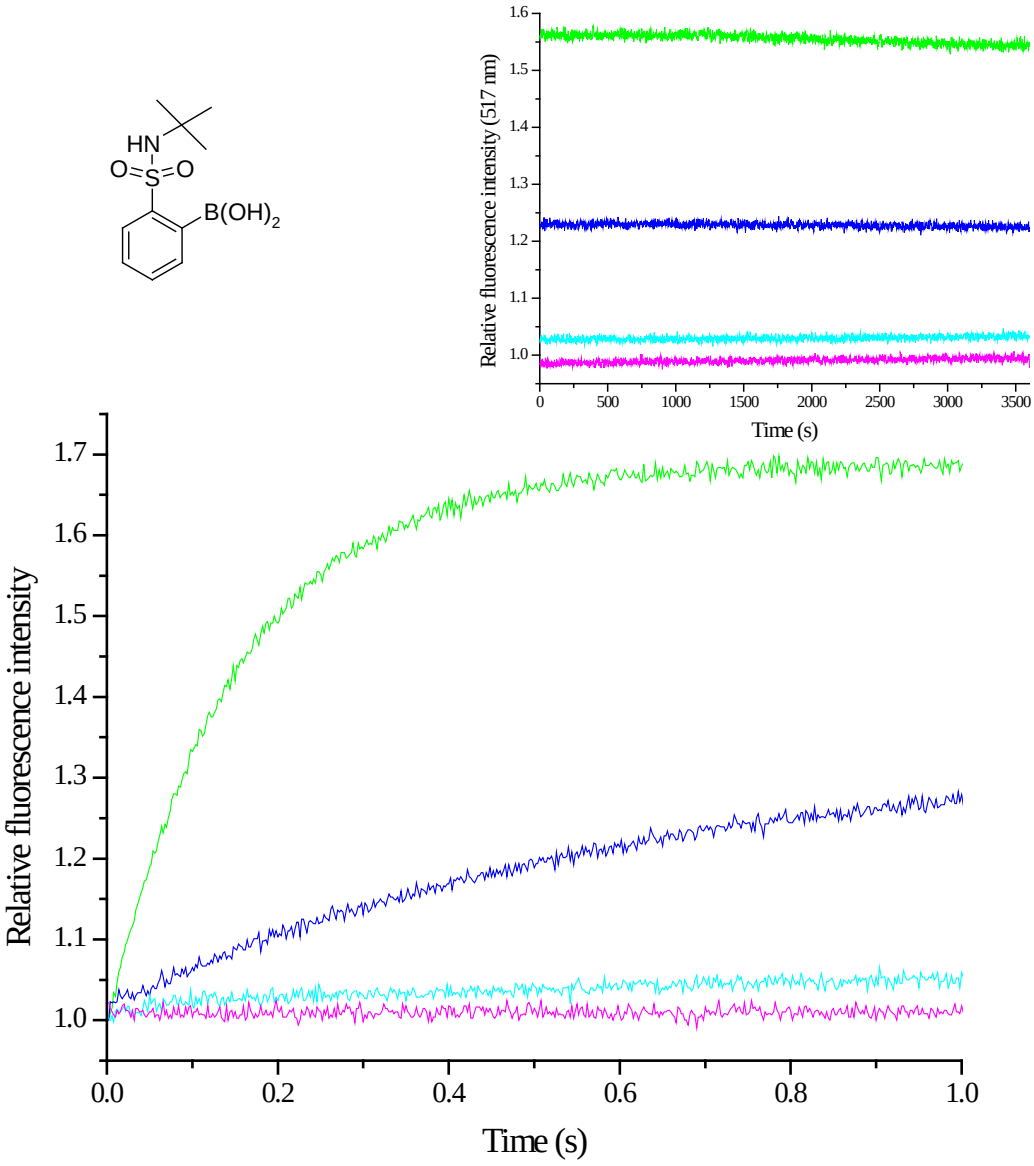

Figure III.3.11. Time-resolved fluorescence spectra of 1.0×10^{-7} M V211Cf in 50 mM potassium phosphate (pH 7.0) with 2-(tert-Butylamino)sulfonylphenyl-boronic acid at the concentrations of 1.0×10^{-7} M (magenta), 1.0×10^{-6} M (cyan), 1.0×10^{-5} M (blue), and 1.0×10^{-4} M (green) obtained by stopped-flow experiment. Excitation wavelength: 498 nm. The inset shows the corresponding spectra obtained over 1 h-measurement.

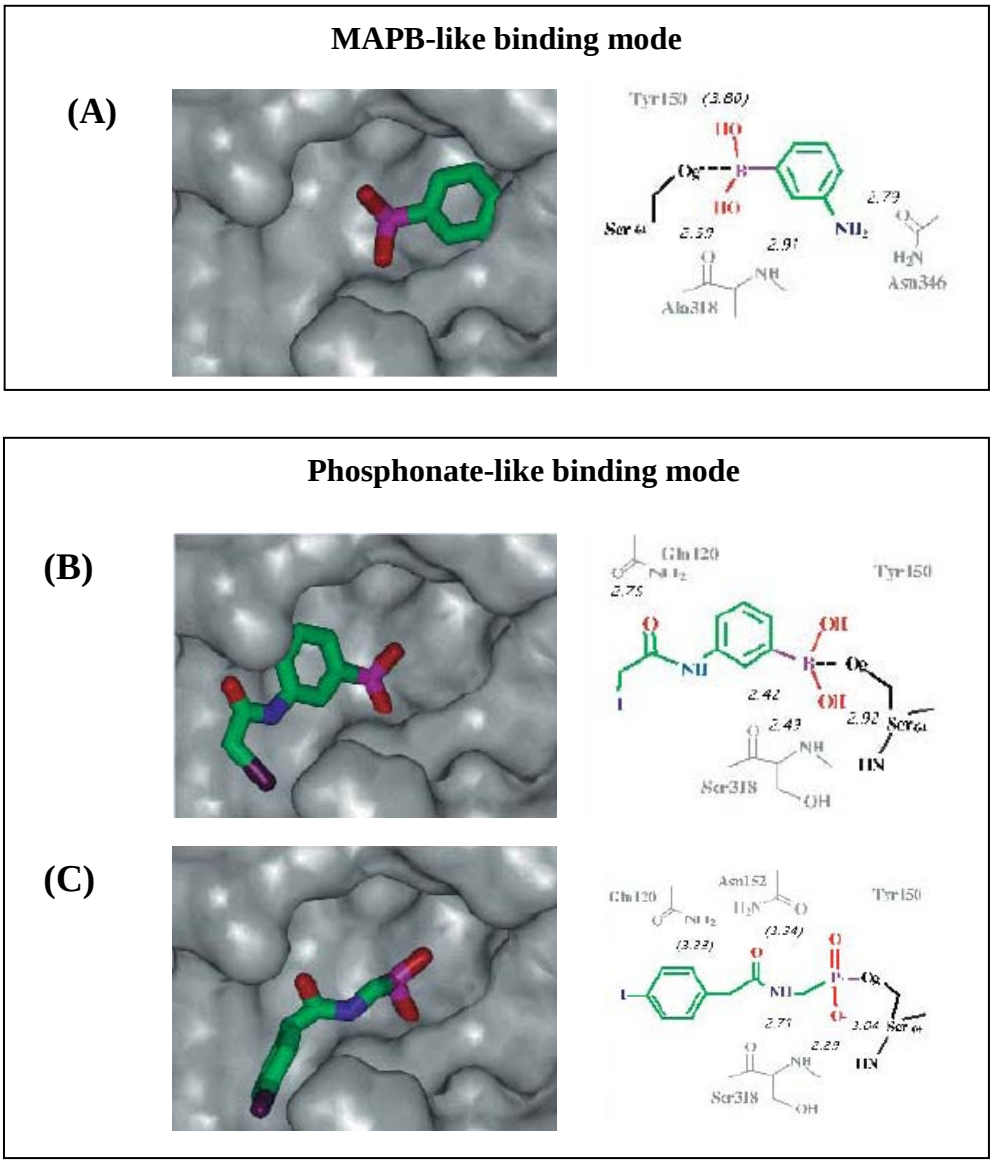

Figure III.3.12. The two most possible boronic acid ligand of orientations. One is the MABP-like binding mode as illustrated by the crystal structure of a MABP-AmpC complex (A); and the other one is the "phosophonate-like" binding mode (B) which is so-called because of its orientation similarity with that of phosphonate ligand-AmpC complex. This figure is adapted from Wouters *et al.*, 2003.

III.3.4. Concluding remarks

At present, a lack of effective controls for pathogens with the rapidly emerging class C β-lactamases pose a pressing need for the discovery of potent class C β-lactamase inhibitors. However, drug discovery process has always been impeded by a lack of efficient high throughput screening system as well as the complexities in the optimization program for the drug lead (Walsh, 2003; Payne and Tomasz, 2004). Here, our V211Cf may help ease these bottlenecks by offering a new approach for monitoring the interaction between the enzyme and the inhibitor. As revealed by the fluorescence data, V211Cf could give responses to the tested inhibitors, demonstrating its feasibility to report the presence of the inhibitors. Interestingly, V211Cf displayed characteristic signals towards different classes of inhibitors which may serve as the fingerprints for the particular groups of inhibitors. In addition, because of its ability to report the dynamic reactions inside the active site, time-resolved measurement of V211Cf allowed a simple method of direct, real-time monitoring of the enzyme-inhibitor interaction. This undoubtedly helps provide valuable information important for optimizing the lead compounds in the structure-based drug design. Although for inhibitors with complicated inactivation pathways, for examples, clavulanic acid, sulbactam and tazobactam in our study, their inhibition mechanisms may not be directly

deciphered from the fluorescence spectra, these fluorescence traces did provide complementary information in the comprehensive mechanistic analyses which make use of a series of techniques like mass spectrometric analyses and crystallographic studies. Furthermore, as demonstrated in Section III.2.3.2, V211Cf was amenable to a micro-titre plate format, shedding light on its potential for high-throughput inhibitor screening. Taken together, V211Cf illustrated attractive features for being an efficient tool for inhibitor screening and mechanistic studies, meriting the discovery for class C β-lactamase inhibitors.

Chapter III.4

Development of Y150S/V211Cf as a biosensor for *β*-lactam antibiotic detection

III.4.1. Introduction

Biosensors derived from natural binding proteins have always provided platforms for reagent-independent biosensing applications because of the non-destructive nature of the binding proteins to their native ligands. On the contrary, the story from E166Cf opened another opportunity of getting a catalytic defective hydrolase modified into a molecule sensor for direct, reagentless detection for its hydrolytic-susceptible substrates. Our first version of the fluorescent class C *β*-lactamases, V211Cf (described in Chapter III.2 and Chapter III.3) was a fluorescent hydrolytic enzyme capable of probing the local environment of the active site. Although it was demonstrated that V211Cf could report the presence of *β*-lactam antibiotics, it rapidly hydrolyzed its preferred substrates, thereby giving transient signals. Therefore, V211Cf was probably not a suitable candidate for sensing the *β*-lactam antibiotics. As a consequence, in our study, Y150S/V211Cf, a fluorescent-labeled enzyme with suppressed activity, was designed for optimizing the performance of V211Cf by reducing the deleterious

effects of the enzyme to the substrate analytes. This chapter aims at reporting the fluorescence properties of Y150S/V211Cf towards the β-lactam antibiotics as well as illustrating the perspective of Y150S/V211Cf for biosensing purposes.

III.4.2. Methods

III.4.2.1. Fluorometric studies

The detailed procedure was described in Section II.10.

III.4.3. Results and discussions

III.4.3.1. Excitation and emission of Y150S/V211Cf

Prior to the investigation of the fluorescence properties of Y150S/V211Cf in the presence of β-lactam antibiotics, the excitation and emission spectra of Y150S/V211Cf were obtained (Figure III.4.1). The excitation wavelength was at 496 nm whereas the emission wavelength was 517 nm upon excitation at 496 nm.

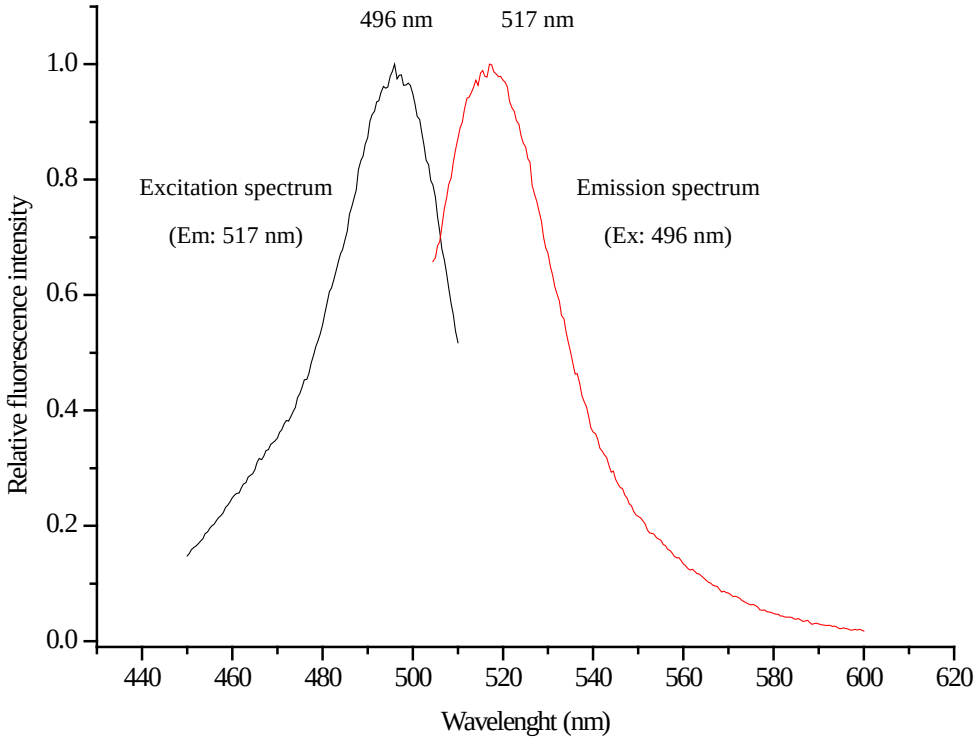

Figure III.4.1. Excitation and emission spectra of 1.0×10^{-7} M Y150S/V211Cf in 50 mM potassium phosphate (pH 7.0).

III.4.3.2. Fluorescence properties of Y150S/V211Cf towards *β*-lactam antibiotics

The fluorescence behaviors of Y150S/V211Cf towards a panel of *β*-lactam antibiotics, including penicillins and cephalosporins, were investigated by time-resolved fluorescence measurement. It was found that Y150S/V211Cf only gave fluorescence signals in the presence of cephalosporins instead of penicillins. Fluorescence traces of Y150S/V211Cf in the presence of cephalosporins, including cephalothin, cefuroxime, cefotaxime and ceftazidime were illustrated from Figure III.4.2 – III.4.5.

Generally speaking, the observed signals of Y150S/V211Cf for cephalosporins were characterized by a first rising or declining phase coming after with a level-off plateau phase. The first rising or declining phase referred to the signal generated by the movement of the fluorophore in response to the approach of the substrate into the active site pocket. The subsequent plateau phase was the state at which the extent of the fluorophore movement reached its maximum. With severe catalytic impairment in Y150S/V211Cf, for both rapidly-hydrolyzed substrate (cephalothin and cefuroxime) and slowly-hydrolyzed substrate (cefotaxime and ceftazidime) for the class C *β*-lactamases, the substrate stayed

long at the active site pocket, resulting in a stable level-off signal.

It was observed that addition of cephalothin, a first generation cephalosporin, and cefuroxime, a second generation cephalosporin, modulated fluorescence enhancement of Y150S/V211Cf whereas addition of two third generation cephalosporins, cefotaxime and ceftazidime, resulted in quenching of fluorescence signal. It was postulated that the rationale of the fluorescence enhancement for cephalothin and cefuroxime was the same as that for V211Cf which was due to a push of the fluorophore moiety outward from the hydrophobic cleft of the active site to a more solvent-exposed environment upon the substrate binding. However, the quenching mechanism of cefotaxime and ceftazidime on the fluorescence of Y150S/V211Cf has not been resolved yet. Perhaps, possibilities like reallocation of the fluorophore to a more hydrophobic environment or fluorescence quenching by the bulky functional group of the third generation cephalosporin would cause the fluorescence quenching observed.

Regarding to the dose-response curves (as shown in the inset of each spectrum), Y150S/V211Cf gave signal corresponding to the concentration of the cephalosporins. It generally demonstrated a 30% change in the fluorescence

intensity with the saturated concentration of cephalosporin (1.0×10^{-3} M). In addition, it displayed fluorescence signal at the lowest concentration at 1.0×10^{-6} M for all of our tested cephalosporins.

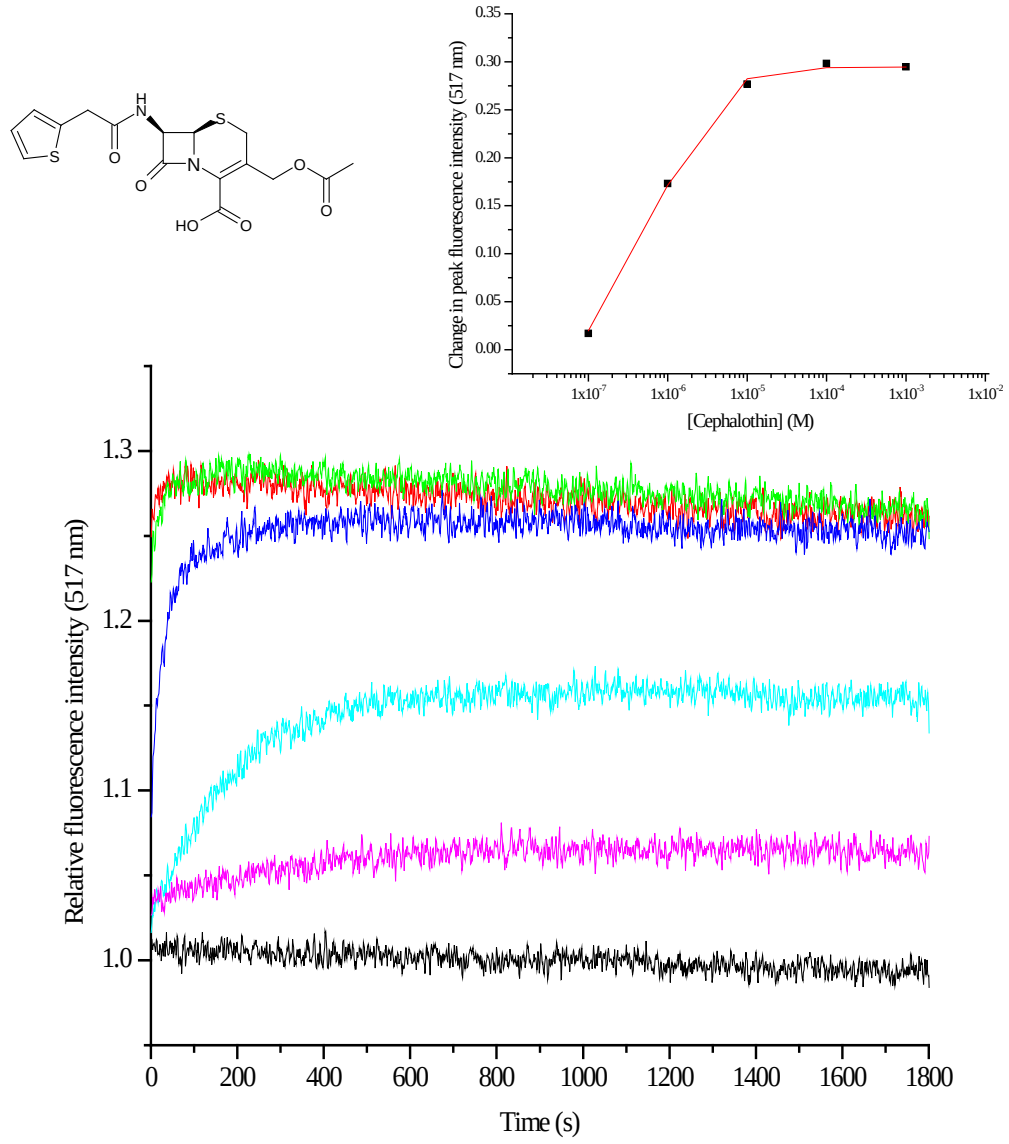

Figure III.4.2. Time-resolved fluorescence spectra of 1.0×10^{-7} M Y150S/V211Cf in 50 mM potassium phosphate (pH 7.0) with cephalothin at the concentrations of 0 M (black), 1.0×10^{-7} M (magenta), 1.0×10^{-6} M (cyan), 1.0×10^{-5} M (blue), 1.0×10^{-4} M (green), and 1.0×10^{-3} M (red). Excitation wavelength: 496 nm. The inset shows the plot of change in peak fluorescence intensity as a function of concentration of cephalothin.

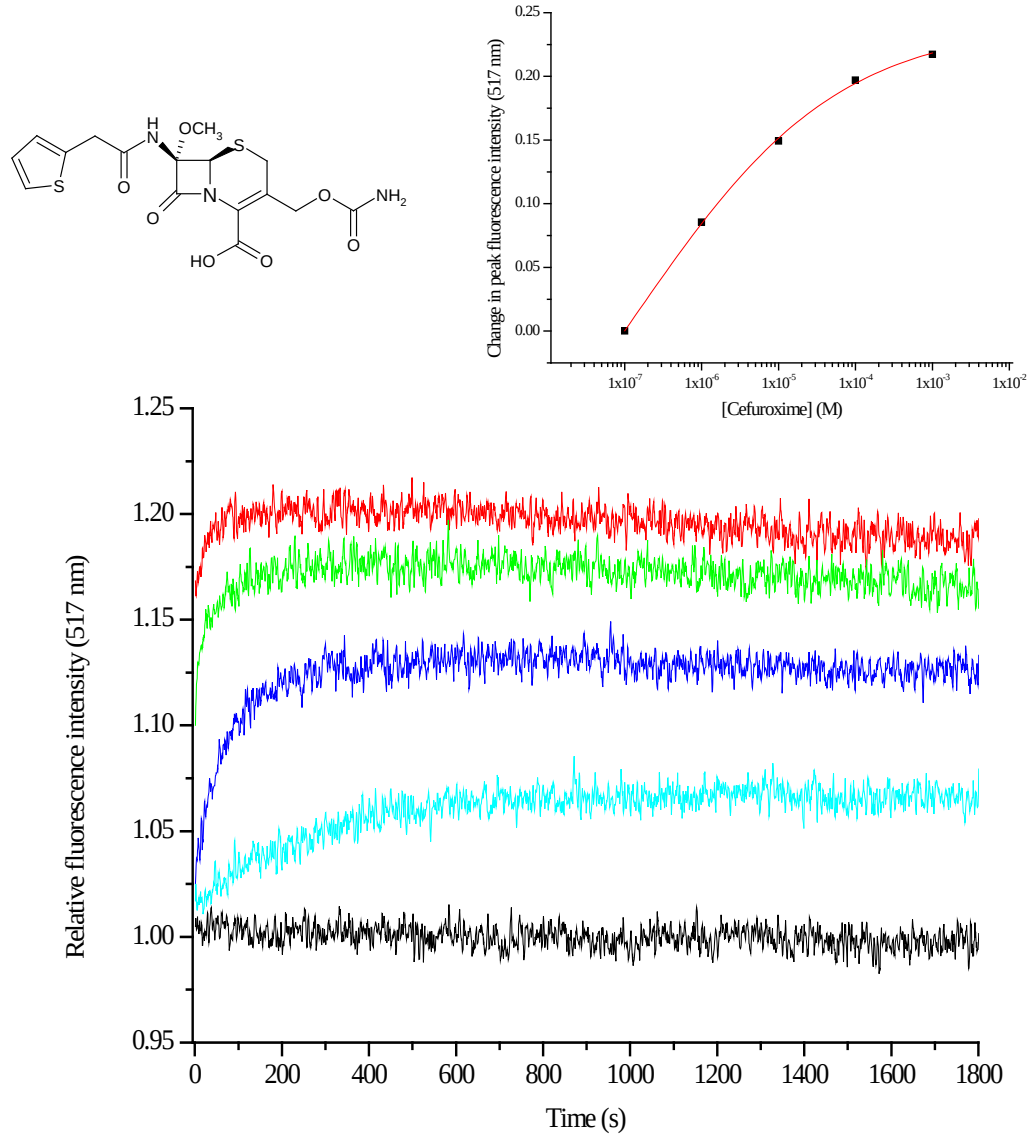

Figure III.4.3. Time-resolved fluorescence spectra of 1.0×10^{-7} M Y150S/V211Cf in 50 mM potassium phosphate (pH 7.0) with cefuroxime at the concentrations of 0 M (black), 1.0×10^{-6} M (cyan), 1.0×10^{-5} M (blue), 1.0×10^{-4} M (green), and 1.0×10^{-3} M (red). Excitation wavelength: 496 nm. The inset shows the plot of change in peak fluorescence intensity as a function of concentration of cefuroxime.

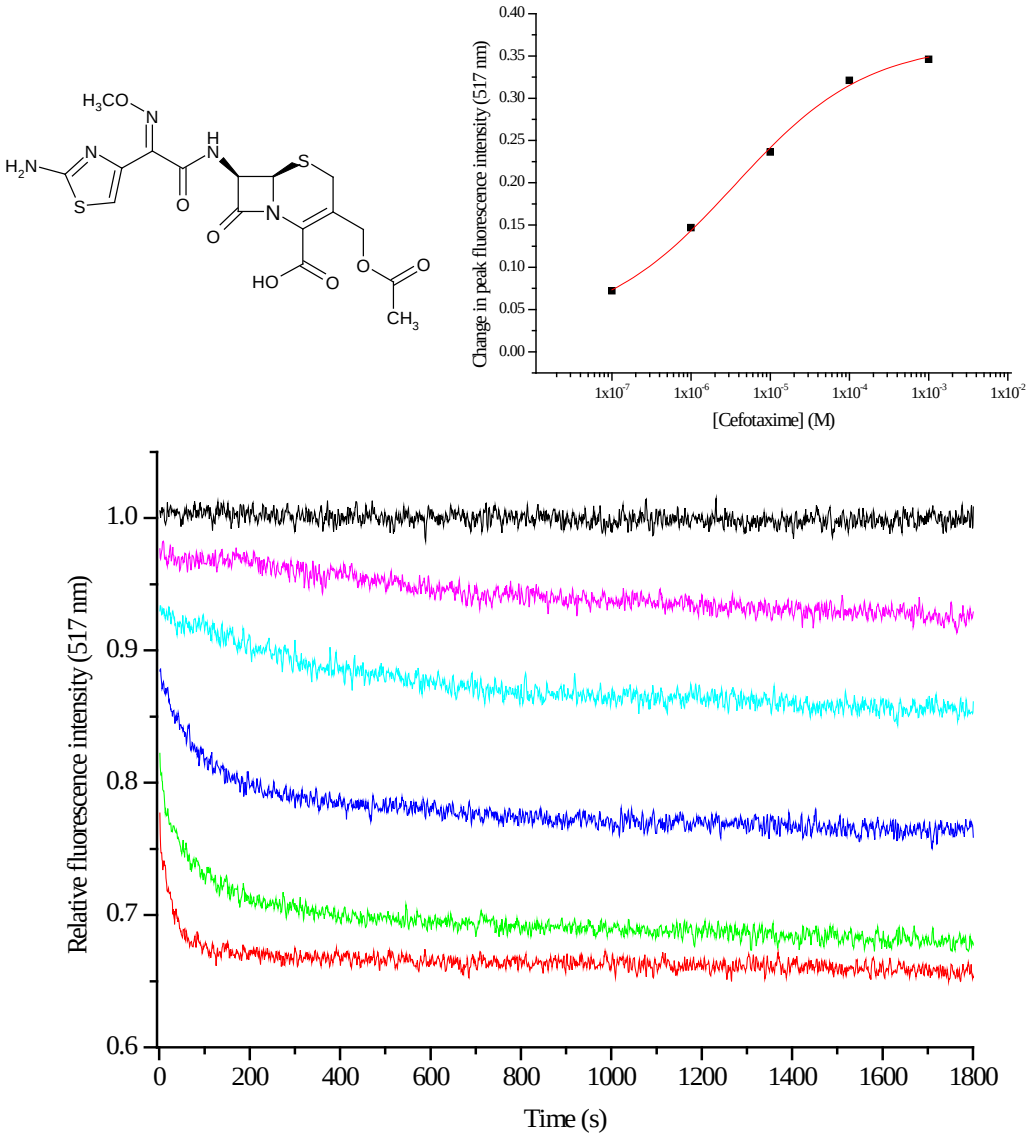

Figure III.4.4. Time-resolved fluorescence spectra of 1.0×10^{-7} M Y150S/V211Cf in 50 mM potassium phosphate (pH 7.0) with cefotaxime at the concentrations of 0 M (black), 1.0×10^{-7} M (magenta), 1.0×10^{-6} M (cyan), 1.0×10^{-5} M (blue), 1.0×10^{-4} M (green), and 1.0×10^{-3} M (red). Excitation wavelength: 496 nm. The inset shows the plot of change in peak fluorescence intensity as a function of concentration of cefotaxime.

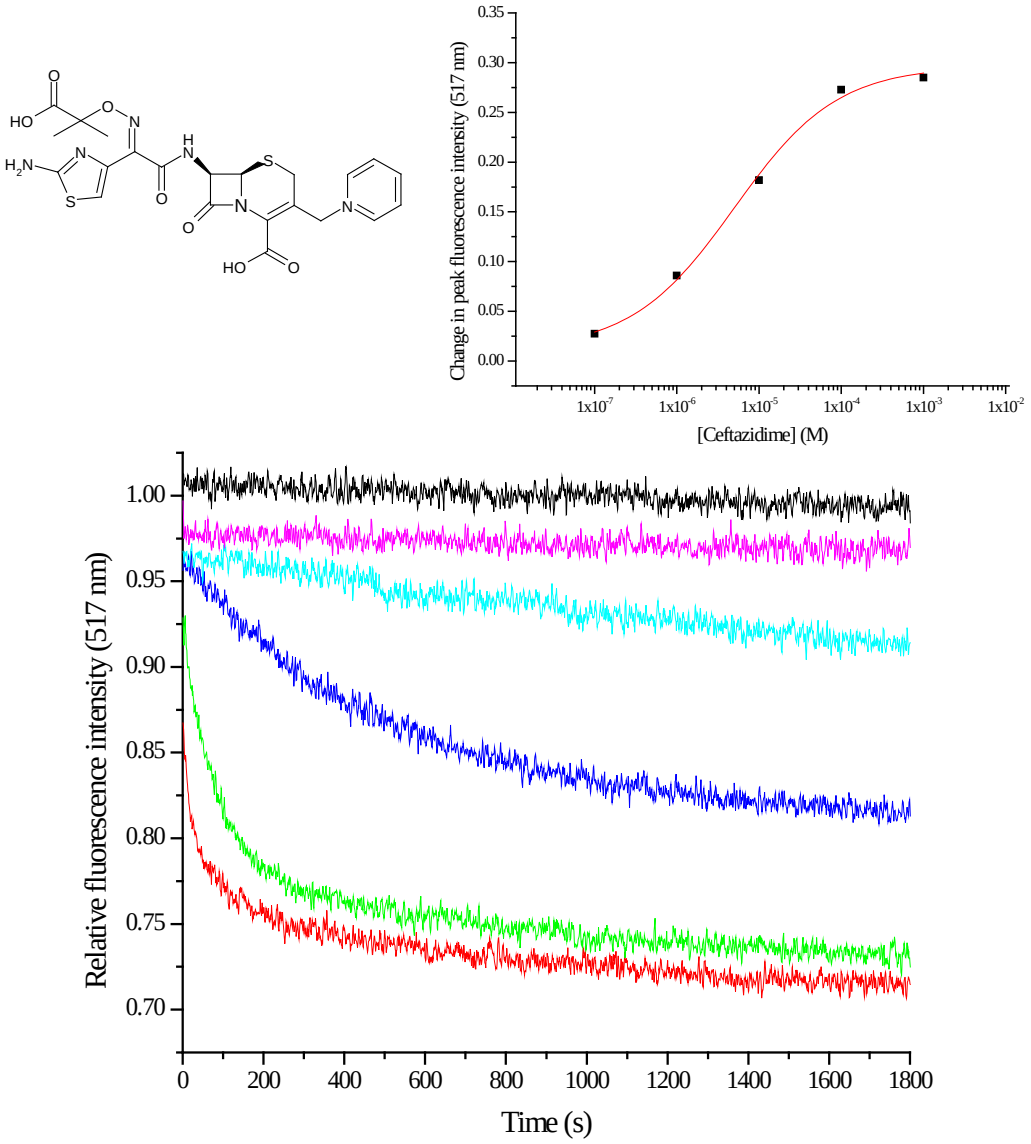

Figure III.4.5. Time-resolved fluorescence spectra of 1.0×10^{-7} M Y150S/V211Cf in 50 mM potassium phosphate (pH 7.0) with ceftazidime at the concentrations of 0 M (black), 1.0×10^{-7} M (magenta), 1.0×10^{-6} M (cyan), 1.0×10^{-5} M (blue), 1.0×10^{-4} M (green), and 1.0×10^{-3} M (red). Excitation wavelength: 496 nm. The inset shows the plot of change in peak fluorescence intensity as a function of concentration of ceftazidime.

III.4.4. Concluding remarks

In conclusion, Y150S/V211Cf, which was a hydrolytic-defective derivative of V211Cf, was specific for detecting cephalsoporins as it only displayed fluorescence signals in the presence of cephalosporins rather than penicillins. It had a detection limit of 1.0×10^{-6} M for our tested cephalosporins. Moreover, it possessed the characteristic of improved signal stability over V211Cf. These findings not only revealed the potential of Y150S/V211Cf in the application for sensing cephalosporins but also validated the versatility of the elegant approach of obtaining a fluorescent-modified hydrolase with impaired activity for detecting its substrates in the previously mentioned E166Cf.

Chapter IV

Comparison of fluorescein-labeled class A and class C *β*-lactamases in detecting cephalosporins

IV.1. Introduction

Cephalosporins, one of the most popular classes of *β*-lactam antibiotics (Gustaferro and Stecjelberg, 1999; Page, 2004), are commonly found-type of antibiotic residues in the food, thus detection of these antibiotics are particularly important for reducing the antibiotic contamination incidences. As described in Section I.4, an elegantly designed class A *β*-lactamase-based biosensor, E166Cf has previously illustrated its potential for being a sensitive efficient screening system for *β*-lactams. However, as class A *β*-lactamase is a poor cephalosporinase having poor affinities with cephalosporins, E166Cf exhibited relatively slow response towards the cephalosporins than penicillins, resulting in exceedingly long detection duration for these antibiotics (Chan, 2000). With the aim of developing a rapid sensing tool for the cephalosporin antibiotics, our present study rationally protein-engineered a class C *β*-lactamase, which is a good cephalosporinase, into two fluorescent biosensing molecules designated as V211Cf and Y150S/V211Cf because we postulated that the fluorescent sensors

derived from a cephalosporin-preferred β-lactamase would have a better binding with these substrates, thus possessing improved performance in cephalosporin detection. The two fluorescein-labeled class C β-lactamases has previously demonstrated their capabilities of detecting the presence of the cephalosporins in Chapter III.2 and Chapter III.4 respectively. With emphasis on the perspective application of these fluorescent class C β-lactamases for rapid cephalosporin detection, this chapter aimed at assessing the performance of the class A β-lactamase-based E166Cf and our two fluorescein-labeled class C β-lactamases in detecting cephalosporin through the comparison of their fluorescence behaviors in the presence of the first generation cephalosporin, cephalothin.

IV.2. Methods

IV.2.1. Preparation of fluorescein-labeled class A β-lactamase

To prepare the fluorescein-labeled class A β-lactamase, E166C mutant was first expressed and purified as described in Section II.4 and Section.II.5.1 respectively. Afterwards, the mutant was unfolded for the labeling with fluorescein-5-maleimide and allowed to refold by the removal of the denaturant by extensive buffer exchange after the labeling reaction as listed in Section II.6.2.

IV.2.2. Preparation of fluorescein-labeled class C *β*-lactamases

The procedures for the preparation of V211Cf and Y150S/V211Cf were described in Section III.1.2.1.

IV.2.3. Fluorometric studies

The procedure was described in Section II.10. For fluorescence measurement, E166Cf, excitation and emission wavelengths were 494 nm and emission at 515 nm whereas for V211Cf and Y150S/V211Cf, excitation and emission wavelengths were set at 498 nm and 517 nm respectively. For experiments with the stopped-flow instrumentation, the emitted light was observed through a 515 nm cut-off filter with the excitation on 494 nm for E166Cf and 498 nm for V211Cf.

IV.3. Results and discussions

IV.3.1. Performance of the fluorescein-labeled class A and class C *β*-lactamases in detecting cephalothin

The performances of the fluorescent class A and class C *β*-lactamases in detecting cephalosporin will herein be evaluated by their fluorescence behaviors in the presence of a rapidly-hydrolyzed cephalosporin, cephalothin. Figure IV.1 and Figure IV.2 show the fluorescence traces of E166Cf, V211Cf and

Y150S/V211Cf recorded over 1800 s (30 min) after adding various concentrations of cephalothin; and their dose response curves for cephalothin respectively. In addition, Table IV.1 summarizes the biosensor characteristics of the three fluorescent proteins in cephalothin detection.

As revealed from the fluorescence traces, the fluorescent enzymes typically exhibited signals with an increase and leveling-off of fluorescence intensity in response to cephalothin addition. As V211Cf retained most of the wild-type's hydrolytic activity, it exhibited the shortest response time among the three fluorescein-modified β-lactamases by showing a plateau signal 1000-fold faster than E166Cf and Y150S/V211Cf. Of the two catalytically impaired β-lactamases, the class C enzyme-based Y150S/V211Cf displayed a response shorter by two-times than the class A β-lactamase-derived E166Cf. These findings suggested that the fluorescein-labeled class C β-lactamases were superior to the class A β-lactamase-based sensor in the detection time, validating our speculation that a cephalosporinase-based sensor would provide a rapid response in cephalosporin detection than the fluorescent class A penicillinase.

Despite the fast response time, the class C-based biosensors generally

showed signals with smaller magnitude (a smaller change in the fluorescence intensity) than the E166Cf did. Regarding the saturated cephalothin concentration (1.0×10^{-7} M), the percentage changes in the fluorescence intensity of V211Cf and Y150S/V211Cf were 37% and 28% respectively, approximately 2-fold lower than that of E166Cf. Thus, the class A E166Cf offered higher sensitivity in sensing cephalothin than the two fluorescein-modified class C β-lactamases.

In terms of signal stability, with suppressed hydrolytic activity, the class A E166Cf and class C Y150S/V211Cf demonstrated stable signal over the 30 min-time-course of fluorescence monitoring whereas V211Cf with full hydrolytic activity rapidly hydrolyzed cephalothin, resulting in unstable transient signals towards this good cephalosporin substrate. In addition, V211Cf had a detection limit of 10^{-5} M for cephalothin, which was 10-fold higher than the hydrolytic defective E166Cf and Y150S/V211Cf as it rapidly hydrolyzed the substrate, thereby failing to give detectable fluorescence signal towards trace amounts of cephalothin.

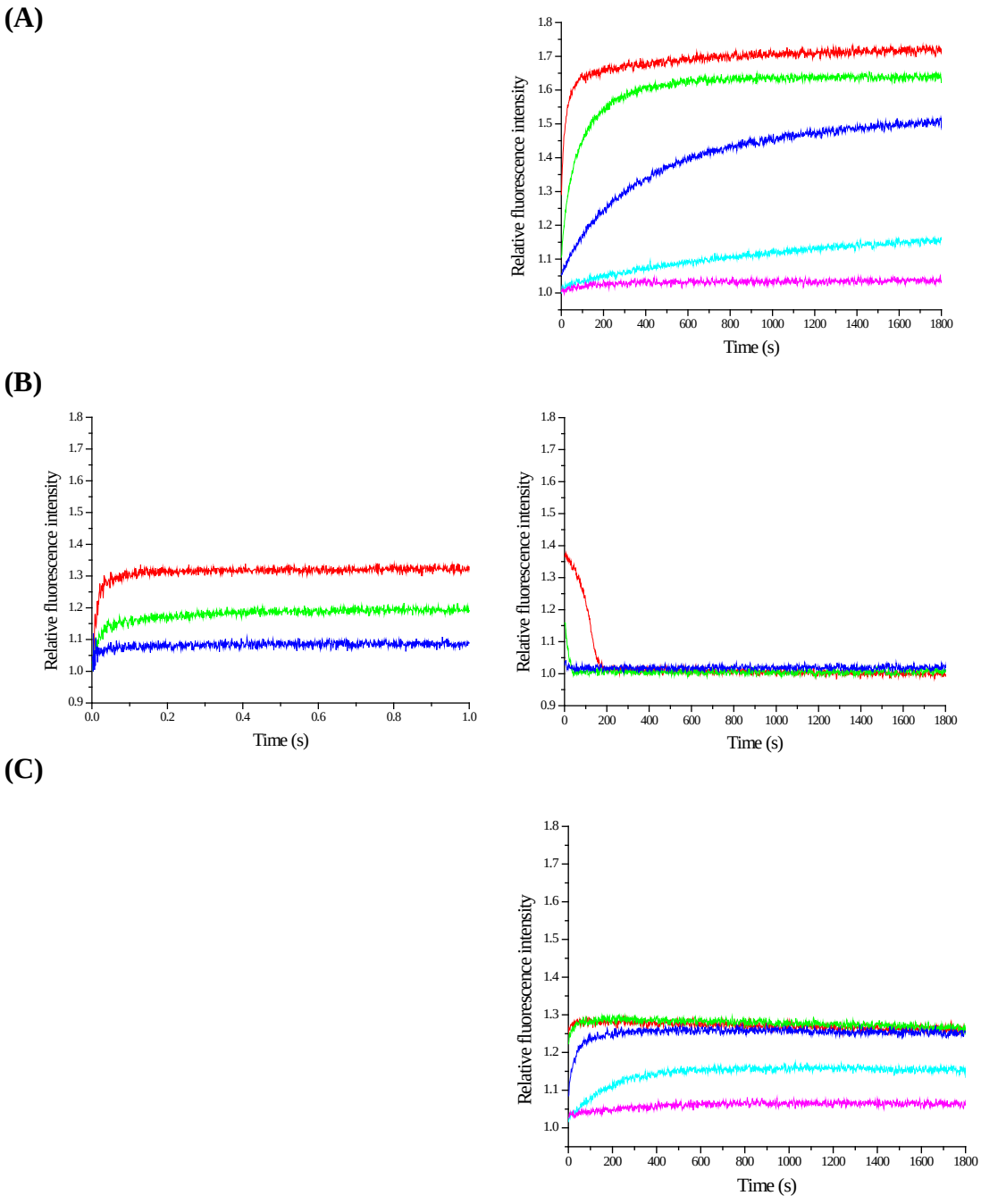

Figure IV.1. Time-resolved fluorescence spectra for 1.0×10^{-7} M of E166Cf (A), V211Cf (B) and Y150S/V211Cf (C) in 50 mM potassium phosphate with various concentrations of cephalothin: 1.0×10^{-7} M (magenta), 1.0×10^{-6} M (cyan), 1.0×10^{-5} M (blue), 1.0×10^{-4} M (green) and 1.0×10^{-3} M (red).

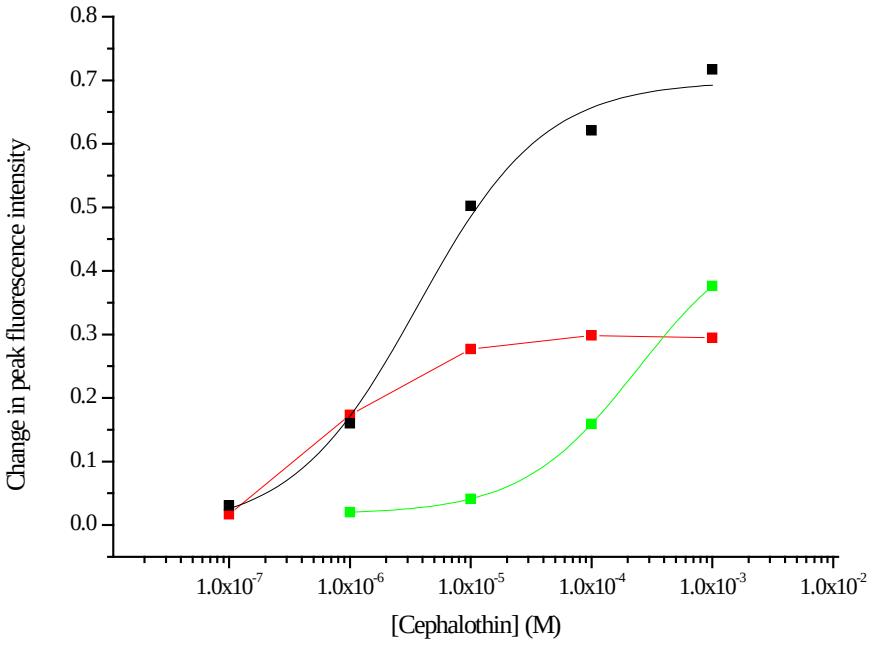

Figure IV.2. Plots of change in peak fluorescence intensity as a function of concentration of cephalothin for E166Cf (in black line), V211Cf (in green line) and Y150S/V211Cf (in red line).

Table IV.1. Biosensor characteristics in detecting cephalothin.

	Response time[a] (s)	Recovery time[b] (s)	Maximum percentage change in fuorescence intensity[c] (%)	Linear response range (M)
E166Cf	100	---[d]	70	10^{-6} – 10^{-3}
V211Cf	0.05	210	37	10^{-5} –10^{-3}
Y150S/V211Cf	50	---[d]	28	10^{-6} –10^{-3}

Remarks:

a. Response time is defined as the time required by the biosensor to give a signal reaching a level-off plateau level after adding 1.0×10^{-3} M of cephalothin.

b. Recovery time is defined as the time required by the biosensor to return the fluorescence signal to its original basal level after adding 1.0×10^{-3} M of cephalothin.

c. Maximum percentage change in fluorescence intensity is assessed at the concentration of 1.0×10^{-3} M cephalothin.

d. ---, not applicable

IV.4. Concluding remarks

In short, although E166Cf could give a larger change in the fluorescence intensity than the fluorescent class C β-lactamases, showing higher signal sensitivity, the detection limit for E166Cf and catalytically-impaired Y150S/V211Cf were comparable. In addition, the fluorescent class C β-lactamases, V211Cf and Y150S/V211Cf displayed a faster response to cephalothin than the class A E166Cf. Furthermore, as demonstrated in Chapter III.4, Y150S/V211Cf was found to be specific for detecting cephalosporins. Taken together, these results illustrated that there is good potential for the class C β-lactamases to be developed into a rapid system for detecting cephalosporins.

Chapter V

Conclusions

To conclude, our present study reported for the first time the protein engineering of a class C β-lactamase into fluorescent sensing molecules for the detection of β-lactam antibiotics and inhibitors. With a fluorescent probe attached to a strategic site on the periphery of the active site entrance, the fluorescein-labeled enzyme was able to track the dynamic reactions occurred at the active site, thereby allowing the detection of its β-lactam substrates and inhibitors.

Of the two prepared fluorescein-labeled β-lactamases, V211Cf mimicked the wild-type enzyme with conserved hydrolytic activity. The fluorescence trace of V211Cf attributed to the enzyme-substrate/inhibitor complexes could thus provide a sensible estimation of the intermediate formation in the hydrolytic reaction or inactivation in the wild-type β-lactamase. This demonstrated the potential of V211Cf for the biosensor profiling of molecular interactions between β-lactamase and the substrate/inhibitor which could help better understand the β-lactamase mechanistic action and provide valuable information for drug design and lead

optimization. Furthermore, the fluorescence responses of V211Cf towards the *β*-lactam based inhibitors and transition state analogs demonstrated its feasibility in inhibitor screening. The distinct fluorescence signals of V211Cf towards various classes of *β*-lactamase inhibitors offered the opportunity for inhibitor fingerprinting and inactivation mechanistic study.

In contrast, Y150S/V211Cf was a derivative of V211Cf with suppressed enzymatic activity. With severe impairment in the catalytic capability, Y150S/V211Cf possessed characteristic of improved fluorescence signal stability towards the *β*-lactam substrates, making it a suitable candidate for the direct, reagentless detection of *β*-lactam antibiotics. Interestingly, Y150S/V211Cf demonstrated specificity towards cephalsoporins and gave no signals in the presence of penicillins, thus having a good prospect in cephalosporin detection.

When comparing the performance of these two fluorescent class C enzymes with the fluorescein-labeled class A enzyme, the class C *β*-lactamase-based biosensors exhibited poorer sensitivity (with a detection limit 10- to 100- fold higher than E166Cf) in detecting the *β*-lactam antibiotics than E166Cf. Conversely, class C proteins demonstrated a faster response towards

cephalosporin than E166Cf. Therefore, this indicated the attractiveness of developing the fluorescent class C β-lactamases for the rapid detection of cephalsoporins but efforts should be made to improve their sensitivities towards the β-lactam antibiotics.

The present study preliminarily opened up interesting perspectives of the fluorescent class C β-lactamases as useful tools for mechanistic study, β-lactam detection and drug screening. The fluorescein-modified enzymes, V211Cf and Y150S/V211Cf presented here probably provided good starting templates for the further development of class C β-lactamase-based fluorescent biosensors. Derivatives of fluorescent class C β-lactamases for optimized biosensing properties may be given rise by labeling the cysteine mutant with other environment-sensitive fluorophore or incorporating other mutations to the enzyme for fluorophore attachment and catalytic impairment. Furthermore, the rational design concept and technology of using a non-allosteric hydrolase with a fluorophore conjugated close to its active site for direct substrate and inhibitor detection illustrated here could be extended to other non-allosteric hydrolytic enzymes, paving the way for developing a variety of reagentless biosensors for drug screening and ligand detection.

References

1. Adachi, H., Ohta, T., and Matsuzawa, H. Site-directed mutants, at position 166, of RTEM-1 β-lactamase that form a stable acyl-enzyme intermediate with penicillin. *The Journal of Biological Chemistry*, 1991, 266, 3186 – 3191.

2. Ahlestedt, S. Penicillin allergy – can the incidence be reduced? *Allergy*, 1984, 39, 151 – 164.

3. Alba, J., Bauvois, C., Ishii, Y., Galleni, M., Masuda, K., Ishiguro, M., Ito, M., Frère, J.-M., Yamaguchi, K. A detailed kinetic study of Mox-1, a plasmid-encoded class C β-lactamase. *FEMS Microbiology Letters*, 2003, 225, 183 – 188.

4. Ambler, R.P. The structure of β-lactamases. *Philosophical Transactions of the Royal Society of London. Series B, Biological sciences*, 1980, 289, 321 – 331.

5. Anderson, E.G., and Pratt, R.F. Pre-steady state β-lactamase kinetics: Observation of a covalent intermediate during turnover of a fluorescent cephalosporin by the β-lactamase of *Staphylococcus aureus* PC1. *The*

Journal of Biological Chemistry, 1981, 256, 11401 – 11404.

6. Anderson, E.G., and Pratt, R.F. Pre-steady state of β-lactamase kinetics: The trapping of a covalent intermediate and the interpretation of pH rate profiles. *The Journal of Biological Chemistry*, 1983, 258, 13120 – 13126.

7. Anderson, K.L., Moats, W.A., Rushing, J.E., Wesen, D.P., and Papich, M.G. Ampicillin and amoxicillin residue detection in milk, using microbial receptor assay (Charm II) and liquid chromatography methods after extra-label administration of the drugs to lactating cows. *American Journal of Veterinary Research*, 1996, 57, 73 – 78.

8. Banerjee, S., Pieper, U., Kapadia, G., Pannell, L.K., and Herzberg, O. Role of the Ω-loop in the activity, substrate specificity, and the structure of class A β-lactamase. *Biochemistry*, 1998, 37, 3286 – 3296.

9. Banic, S. Detection of bacterial strains producing sulbactam- or tazobactam-sensitive β-lactamases by use of disks containing the inhibitors alone instead of combining them with antibiotics. *Acta Pathologica, Microbiologica, et Immunologica Scandinavica*, 2006, 114, 3 – 9.

10. Barker, K.F. Antibiotic resistance: a current perspective. *British Journal of Clinical Pharmacology*, 1999, 48, 109 – 124.

11. Bauernfeind, A., Chong, Y., and Lee, K. Plasmid-encoded AmpC β-lactamases: How far have we gone 10 years after the discovery? *Yonsei Medical Journal*, 39, 520 – 525.

12. Beadle, B.M., Trehan, I., Focia, P.J., and Shoichet, B.K. Structural milestones in the reaction pathway of an amide hydrolase: substrate, acyl, and product complexes of cephalothin with AmpC β-lactamase. *Structure*, 2002, 10, 413 – 424.

13. Bell, J.H., and Pratt, R.F. Mechanism of inhibition of the β-lactamase of *Enterobacter cloacae* P99 by 1:1 complexes of vanadate with hydroxamic acids. *Biochemistry*, 2002, 41, 4329 – 4338.

14. Benito-Peña, E., Moreno-Bondi, M.C., Orellana, G., Maquieira, Á., and Amerongen, A.V. Development of a novel and automated fluorescent immunoassay for the analysis of β-lactam antibiotics. *Journal of Agricultural and Food Chemistry*, 2005, 53, 6635 – 6642.

15. Bethel. C.R., Hujer, A.M., Helfand, M.S., and Bonomo, R.A. Exploring the effectiveness of tazobactam against ceftazidime resistant *Escherichia coli*: insights from the comparison between susceptibility and β-lactamase inhibition. *FEBS Microbiology Letters*, 2004, 234, 99 – 103.

16. Bicknell, R., and Waley, S.G. Single-turnover and steady-state kinetics of hydrolysis of cephalosporins by β-lactamase I from *Bacillus cereus*. *The Biochemical Journal*, 1985, 231, 83 – 88.

17. Bitha, P., Li, Z., Fracisco, G.D., Rasmussen, B.A., and Lin Y.-I. 6-(1-hydroxyalkyl)penam sulfone derivatives as inhibitors of class A and class C β-lactamase I. *Bioorganic & Medicinal Chemistry Letters*, 1999a, 9, 999 – 996.

18. Bitha, P., Li, Z., Francisco, G.D., Yang, Y., Peterson, P.J., Lenoy, E., and Lin, Y.-I. 6-(1-hydroxylalkyl)penam sulfone derivatives as inhibitors of class A and class C β-lactamases II. *Bioorganic & Medicinal Chemistry Letters*, 1999b, 9, 997 – 1002.

19. Bonnefoy, A., Dupuis-Hamelin, C., Steier, V., Delachaume, C., Seys, C., Stachyra, T., Fairley, M., Guitton, M., and Lampilas, M. *In vitro* activity of AVE1330A, an innovative broad-spectrum non-β-lactam β-lactamase inhibitor. *Journal of Antimicrobial Chemotherapy*, 2004, 54, 410 – 417.

20. Bonomo, R.A., Liu, J., Chen, Y., Ng, L., Hujer, A.M., and Anderson, V.E. Inactivation of CMY-2 β-lactamase by tazobactam: initial mass spectroscopic characterization. *Biochimica et Biophysica Acta*, 2001, 1547, 196 – 205.

21. Bradford, M.M. A rapid and sensitive method for the quantitation of microgram quantities of protein utilizing the principle of protein-dye binding. *Analytical Biochemistry*, 1976, 72, 248 – 254.

22. Bradford, P.A. Extended-spectrum β-lactamases in the 21st century: Characterization, epidemiology, and detection of this important resistance threat. *Clinical Microbiology Reviews*, 2001, 14, 933 – 951.

23. Breaker, R.R. Engineered allosteric ribozymes as biosensor components. *Current Opinion in Biotecchnology*, 2002, 13, 31 – 39.

24. Brook, I. β-lactamase-producing bacteria in mixed infections. *Clinical Microbiology and Infection*, 2004, 10, 777 – 784.

25. Brown, A.G. Clavulanic acid, a novel β-lactamase inhibitor – a case study in drug discovery and development. *Drug Design and Delivery*, 1986, 1, 1 – 21.

26. Bulychev, A., and Mobashery, S. Class C β-lactamases operate at the diffusion limit for turnover of their preferred cephalosporin substrates. *Antimicrobial Agents and Chemotherapy*, 1999, 43, 1743 – 1746.

27. Bush, K. β-lactamase inhibitors from laboratory to clinic. *Clinical Microbiology Reviews*, 1988, 1, 109 – 123.

28. Bush, K. Antibacterial drug discovery in the 21st century. *Clinical Microbiology and Infection*, 2004, 10, Supplement 4, 10 – 17.

29. Bush, K. New β-lactamases in gram-negative bacteria: Diversity and impact on the selection of antimicrobial therapy. *Clinical Infectious Diseases*, 2001, 32, 1085 – 1089.

30. Bush, K., Macalintal, C., Rasmussen, B.A., Lee, V.J., and Yang, Y. Kinetic interactions of tazobactam with β-lactamases from all major structural classes. *Antimicrobial Agents and Chemotherapy*, 1993, 37, 851 – 858.

31. Buynak, J.D., Vogeti, L., Doppalapudi, V.R., Solomon, G.M., and Chen, H. Cephalosporin-derived inhibitors of β-lactamase. Part 4: The C3 substituent. *Bioorganic & Medicinal Chemistry Letters*, 2002, 12, 1663 – 1666.

32. Buzzoni, V., Blazquez, J., Ferrari, S., Calò, S., Venturelli, A., and Costi, M.P. Aza-boronic acids as non-β-lactam inhibitors of AmpC-β-lactamase. *Bioorganic and Medicinal Chemistry Letters*, 2004, 14, 3979 – 3983.

33. Caselli, E., Powers, R.A., Blasczcak, L.C., Wu, C.Y.E., Prati, F., and Shoichet, B.K. Energetic, structural, and antimicrobial analyses of β-lactam side chain recognition by β-lactamases. *Chemistry & Biology*, 2001, 8, 17 – 31.

34. Chambers, S.J., Wyatt, G.M., and Morgan, M.R.A. Investigation of the interactions between β-lactams and a metallo-β-lactamase from *Bacillus cereus* using a monoclonal antibody. *Analytical biochemistry*, 2001, 288, 149 – 155.

35. Chan, P.H. A fluorescein-modified β-lactamase as biosensor for β-lactam antibiotics, *MPhil thesis*, The Hong Kong Polytechnic University, 2002.

36. Chan, P.H., Chan, K.C., Liu, H.B., Chung, W.H., Leung, Y.C., and Wong, K.Y. Fluorescein-labeled β-lactamase mutant for high-throughput screening of bacterial β-lactamases against β-lactam antibiotics. *Analytical Chemistry*, 2005, 77, 5268 – 5276.

37. Chan, P.H., Liu, H.B., Chen, Y.W., Chan, K.C., Tsang, C.W., Leung, Y.C., and Wong, K.Y. Rational design of novel fluorescent biosensor for β-lactam antibiotics from a class A β-lactamase. *Journal of the American Chemical Society*, 2004, 126, 4074 – 4075.

38. Charm, S.E., and Chi, R.K. Rapid screening assay for β-lactam antibiotics in milk: Collaborative study. *Journal – Association of Official Analytical Chemists*, 1982, 65, 1186 – 1192.

39. Charnas, R.L., Fisher, J., and Knowles, J.R. Chemical studies on the

inactivation of *Escherichia coli* RTEM *β*-lactamase by clavulanic acid. *Biochemistry*, 1978, 17, 2185 – 2189.

40. Chen, C.C.H., and Herzberg, O. Inhibition of *β*-lactamase by clavulanate trapped intermediates in cryostallographic studies. *Journal of Molecular Biology*, 1992, 224, 1103 – 1113.

41. Christensen, H., Martin, M.T., and Waley, S.G. *β*-lactamases as fully efficient enzymes. *The Biochemical Journal*, 1990, 266, 853 – 861.

42. Chudakov, D.M., Lukyanov, S., and Lukyanov, K.A. Fluorescent proteins as a toolkit for *in vivo* imaging. *Trends in Biotechnology*, 2005, 23, 605 – 613.

43. Crichlow, G.V., Nukaga, M., Doppalapudi, V.R., Buynak, J.D., and Knox, J.R. Inhibition of class C *β*-lactamases: Structure of a reaction intermediate with cephem sulfone. *Biochemistry*, 2001, 40, 6233 – 6239.

44. Crompton, I.E., Cuthbert, B.K., Lowe, G., and Waley, S.G. *β*-lactamase inhibitors. *The Biochemical Journal*, 1988, 251, 453 – 459.

45. Cutting, J.H., Kiessling, W.M., Bond, F.L., McCarron, J.E., Kreuzer, K.S., Hurlbut, J.A., and Sofos, J.N. Agarose gel electrophoretic detection of six *β*-lactam antibiotic residues in milk. *Journal of Association of Official Analytical Chemists International*, 1995, 78, 663 – 667.

46. D'Auria, S., and Lakowicz, J.R. Enzyme fluorescence as a sensing tool: new perspectives in biotechnology. *Current Opinion in Biotechnology*, 2001, 12, 99 – 104.

47. De Lorimier, R.M., Smith, J.J., Dwyer, M.A., Looger, L.L., Sali, K.M., Paavola, C.D., Rizk, S.S., Sadigov, S., Conrad, D.W., Loew, L., and Hellinga, H.W. Construction of a fluorescent biosensor family. *Protein Science*, 2002, 11, 2655 – 2675.

48. DiPiro, J.T., and May, J.R. Use of cephalosporins with enhanced anti-anaeroboic activity for treatment and prevention of anaerobic and mixed infections. *Clinical Pharmacy*, 1988, 7, 285 – 302.

49. Doi, N., and Yanagawa, H. Design of generic biosensors based on green fluorescent proteins with allosteric sites by directed evolution. *FEBS Letters*, 1999, 453, 305 – 307.

50. Dubus, A., Ledent, P., Lamotte-Brasseur, J., and Frère, J.-M. The roles of residues Tyr150, Glu272, and His314 in class C β-lactamase. *Proteins: Structure, Function, and Genetics*, 1996, 25, 473 – 485.

51. Dubus, A., Normark, S., Kania, M., and Page, M.G..P. The role of tyrosine 150 in catalysis of β-lactam hydrolysis by AmpC β-lactamase from

Escherichia coli investigated by site-directed mutagenesis. *Biochemistry*, 1994, 33, 8577 – 8586.

52. Elander, R.P. Industrial production of β-lactam antibiotics. *Applied Microbiology and Biotechnology*, 2003, 61, 385 – 392.

53. Escobar, W.A., Tan, A.K., and Fink, A.L. Site-directed mutagenesis of β-lactamase leading to accumulation of a catalytic intermediate. *Biochemistry*, 1991, 30, 10783 – 10787.

54. Essack, S.Y. The development of β-lactam antibiotics in response to the evolution of β-lactamases. *Pharmaceutical Research*, 2001, 18, 1391 – 1399.

55. Fenollar-Ferrer, C., Frau, J., Donoso, J., and Muñoz, F. Role of β-lactam carboxyl group on binding of penicillins and cephalosporins to class C β-lactamases. *Proteins: Structure, Function, and Genetics*, 2003, 51, 442 – 452.

56. Finch, R. Bacterial resistance – the clinical challenge. C*linical Microbiology and Infection*, 2002, 8, Supplement 3, 21 – 32.

57. Fisher, J., Belasco, J.G., Khosla, S., and Knowles, J.R. β-lactamase proceeds via an acyl-enzyme intermediate. Interaction of the *Escherichia coli* RTEM enzyme with cefoxitin. *Biochemistry*, 1980, 19, 2895 – 2901.

58. Fisher, J., Charnas, R.L., and Knowles, J.R. Kinetic studies on the inactivation of *Escherichia coli* RTEM *β*-lactamase by clavulanic acid. *Biochemistry*, 1978, 17, 2180 – 2184.

59. Fisher, J.F., Meroueh, S.O., and Mobashery, S. Bacterial resistance to *β*-lactam antibiotics: compelling opportunism, compelling opportunity. *Chemical Reviews*, 2005, 105, 395 – 424.

60. Fonacier, L., Hirscherg, R., and Gerson, S. Adverse drug reactions to cephalosporins in hospitalized patients with a history of penicillin allergy. *Allergy and Asthma Proceedings*, 2005, 26, 135 – 141.

61. Food Safety Authority of Ireland, Rapid test kits for the detection of antibiotics and sulphonamides in milk, 2002, available at: http://www.fsai.ie/publications/index.asp

62. Frère, J.-M. Beta-lactamases and bacterial resistance to antibiotics. *Molecular Microbiology*, 1995, 16, 385 – 395.

63. Frère, J.-M., Dubus, A., Galleni, M., Matagne, A., and Amicosante, G. Mechanistic diversity of *β*-lactamases. *Biochemistry Society Transactions*, 1999, 27, 58 – 63.

64. Frère, J.-M., Nguyen-Distèche, M., Coyette, J., and Joris, B. Mode of action:

Interaction with the penicillin binding proteins. In: Page, M.I. ed. *The Chemistry of β-lactams*. Glasgow: Blackie Academic & Professional, an imprint of Chapman & Hall, 1992.

65. Galleni, M., and Frère, J.-M. A survey of the kinetic parameters of class C β-lactamases: Penicillins. *The Biochemical Journal*, 1988a, 255, 119 – 122.

66. Galleni, M., Amicosante, G., and Frère, J.-M. A survey of the kinetic parameters of class C β-lactamases: Cephalosporins and other β-lactam compounds. *The Biochemical Journal*, 1988b, 255, 123 – 129.

67. Galleni, M., Lamotte-Brasseur, J., Raquet, X., Dubus, A., Monnaie, D., Knox, J.R., and Frère, J.-M. The enigmatic catalytic mechanism of active-site serine β-lactamases. *Biochemical Pharmacology*, 1995, 49, 1171 – 1178.

68. Galleni, M., Lindberg, F., Normark, S., Cole, S., Honore, N., Joris, B., and Frère, J.-M. Sequence and comparative analysis of three *Enterobacter cloacae amp* C β-lactamase genes and their products. *The Biochemical Journal*, 1988, 250, 753 – 760.

69. García, J.L., Nuñez, C.J., González, E.G., Osuna, J., Soberón, X., and Galindo, E. Microbial sensor for new-generation cephalosporins based in a protein-engineered β-lactamase. *Applied Biochemistry and Biochemistry*,

1998, 73, 243 – 256.

70. Ghidini, S., Zanardi, E., Varisco, G., and Chizzolini, R. Residues of β-lactam antibiotics in bovine milk: confirmatory analysis by liquid chromatography tandem mass spectrometry after microbial assay screening. *Food Additives and Contaminants*, 2003, 20, 528 – 534.

71. Gilardi, G., Zhou, L.Q., Hibbert, L., and Cass, A.E.G. Engineering the maltose binding protein for reagentless fluorescence sensing. *Analytical Chemistry*, 1994, 66, 3840 – 3847.

72. Giuliano, K.A., and Taylor, D.L. Fluorescent-protein biosensors: new tools for drug discovery. *Trends in Biotechnology*, 1998, 16, 135 – 140.

73. Goldberg, S.D., Iannuccilli, W., Nguyen, T., Ju, J., and Cornish, V.W. Identification of residues critical for catalysis in a class C β-lactamase by combinatorial scanning mutagenesis. *Protein Science*, 2003, 12, 1633 – 1645.

74. Guex, N., and Peitsch, M.C. SWISS-MODEL and the Swiss-Pdb Viewer: An environment for comparative protein modeling. *Electrophoresis*, 1997, 18, 2714 – 2723.

75. Guillaume, G., Vanhove, M., Lamotte-Brasseur, J., Ledent, P., Jamin, M., Joris, B., and Frère, J.-M. Site-directed mutagenesis of glutamate 166 in two

β-lactamases: Kinetic and molecular modeling studies. *The Journal of Biology Chemistry*, 1997, 272, 5438 – 5444.

76. Gustaferro, C.A., and Stecjelberg, J.M. Cephalosporin antimicrobial agents and related compounds. *Mayo Clinic Proceedings*, 1991, 66, 1064 – 1073.

77. Gustavsson, E., Degelaen, J., Bjurling, P., and Sternesjö, Å. Determination of *β*-lactams in milk using a surface plasmon resonance-based biosensor. *Journal of Agricultural and Food Chemistry*, 2004, 52, 2791 – 2796.

78. Hahn, K., and Toutchkine, A. Live-cell fluorescent biosensors for activated signaling proteins. *Current Opinion in Cell Biology*, 2002, 14, 167 – 172.

79. Hall, B.G., and Barlow, M. Evolution of the serine *β*-lactamases: past, present and future. *Drug Resistance Updates*, 2004, 7, 111 – 123.

80. Hall, B.G., and Barlow, M. Structure-based phylogenies of the serine *β*-lactamases. *Journal of Molecular Evolution*, 2003, 57, 255 – 260.

81. Healey, B.G., and Walt, D.R. Development of a penicillin biosensor using a single optical imaging fiber. In: Lakowicz, J.R. ed. *Advances in fluorescence sensing technology II*. Bellingham, Wash: SPIE – the International Society for Optical Engineering, 1995.

82. Hechler, U., Van den Weghe, M., Martin, H.H., Frère, J.-M. Overproduced *β*-lactamase and the outer-membrane barrier as resistance factors in *Serratia marcescens* highly resistance to *β*-lactamase-stable *β*-lactam antibiotics. *Journal of General Microbiology*, 1989, 135, 1275 – 1290.

83. Hellinga, H.W., and Marvin, J.S. Protein engineering and the development of generic biosensors. T*rends in biotechnology*, 1998, 16, 183 – 189.

84. Ho, S.N., Hunt, H.D., Horton, R.M., Pullen, J.K., and Pease, L.R. Site-directed mutagenesis by overlap extension using the polymerase chain reaction. *Gene*, 1989, 77, 51 – 59.

85. Holstege, D.M., Puschner, B., Whitehead, G., and Galey, F.D. Screening and mass spectral confirmation of *β*-lactam antibiotic residues in milk using LC-MS/MS. *Journal of Agricultural and Food Chemistry*, 2002, 50, 406 – 411.

86. Huth, S.P., Warholic, P.S., Devou, J.M., Chaney, L.K., and Clark, G.H. Parallux™ *β*-lactam: A capillary-based fluorescent immunoassay for the determination of penicillin-G, ampicillin, amoxicillin, cloxacillin, cepapiriin, and ceftiofur in bovine milk. *Journal of AOAC International*, 2002, 85, 355 – 364.

87. Joshi, N., and Milfred, D. The use and misuse of new antibiotics: a perspective. *Archives of Internal Medicine*, 1995, 155, 569 – 577.

88. Kai, M., Kinoshita, H., Ohta, K., Hara, S., Lee, M.K., Lu, J. Sensitive determination of a β-lactam antibiotic, cefaclor by liquid chromatography with chemiluminescence detection. *Journal of Pharmaceutical and Biomedical Analysis*, 2003, 30, 1765 – 1771.

89. Kato-Toma, K., and Ishiguro, M. Reaction of Lys-Tyr-Lys Triad mimics with benzylpenicillin: Insight into the role of Tyr150 in class C β-lactamase. *Bioorganic & Medicinal Chemistry Letters*, 2001, 11, 1161 – 1164.

90. Kaur, K., Adedirian, S.A., Lan, M.J.K., and Pratt, R.F. Inhibition of β-lactamases by monocyclic acyl phosph(on)ates. *Biochemistry*, 2003, 42, 1529 – 1536.

91. Kim, S., Song, K.S., Kim, H.O., and Lee, H.M. Ceftriaxone induced immune hemolytic anemia: Detection of drug-dependent antibody by ex-vivo antigen in urine. *Yonsei Medical Journal*, 2002, 43, 391 – 394.

92. Knott-Hunziker, V., Orlek, B.S., Sammes, P.G., and Waley, S.G. Kinetics of inactivation of β-lactamase I by 6β-bromopenicillanic acid. *The Biochemical Journal*, 1980, 187, 797 – 802.

93. Knott-Hunziker, V., Petursson, S., Waley, S.G., Jaurin, B., and Grundström, T. The acyl-enzyme mechanism of β-lactamase action: The evidence for class C β-lactamases. *The Biochemical Journal*, 1982, 207, 315 – 322.

94. Knox, J.R., Moews, P.C., and Frère, J.-M. Molecular evolution of bacterial β-lactam resistance. *Chemistry & Biochemistry*, 1996, 3, 937 – 947.

95. Kotra, L.P., Samama, J.-P., and Mobashery, S. β-lactamases and resistance to β-lactam antibiotics. In: Lewis, K., Salyers, A.A., Taber, H.W., and Wax, R.G ed. *Bacterial resistance to antimicrobials*. New York: Marcel Dekker, Inc., 2002.

96. Lamotte-Brasseur, J., Dubus, A., and Wade, R.C. pK_a calculations for class C β-lactamases: The role of Tyr-150. *Proteins: Structure, Function, and Genetics*, 2000, 40, 23 – 28.

97. Lee, B. Conformation of penicillin as a transition-state analog of the substrate of peptidoglycan transpeptidase. *Journal of Molecular Biology*, 1971, 61, 463 – 469.

98. Lee, M.D., and Maurer, J.J. The genetic basis for emerging antibiotic resistance in veterinary pathogens. *Annals of the New York Academy of Sciences*, 2000, 916, 643 – 645.

99. Lee, N., Yuen, K.-Y., and Kumana, C.R. Clinical role of *β*-lactam/*β*-lactamase inhibitor combinations. *Drugs*, 2003, 63, 1511 – 1524.

100. Lee, W., McDonough, M.A., Kotra, L.P., Li, Z., Silvagg, N.R., Takeda, Y., Kelly, J.A., and Mobashery, S. A 1.2-Å snapshot of the final step of bacterial cell wall biosynthesis. *Proceedings of the National Academy of Sciences of the United States of America*, 2001, 98, 1427 – 1431.

101. Leung, Y.C. and Errington, J. Characterization of an insertion in the phage ϕ105 genome that blocks host *Bacillus subtilis* lysis and provides strong expression of heterologous genes. *Gene*, 1995, 154, 1 – 6.

102. Leung, Y.C., Robinson, C.V., Aplin, R.T. and Waley, S.G. Site-directed mutagenesis of *β*-lactamase I: role of Glu-166. *The Biochemical Journal*, 1994, 299, 671 – 678.

103. Liang, P., Sanchez, R.I., and Martin, M.T. Electrochemiluminescence-based detection of *β*-lactam antibiotics and *β*-lactamases. *Analytical Chemistry*, 1996, 68, 2426 – 2431.

104. Liu, H.B., Chui, K.S., Chan, C.L., Tsang, C.W., and Leung, Y.C. An efficient heat-inducible *Bacillus subtilis* bacteriophage ϕ105 expression and secretion for the production of the *Streptomyces clavuligerus β*-lactamase inhibitory

protein (BLIP). *Journal of Biotechnology*, 2004, 108, 207 – 217.

105. Livermore, D.M. β-lactamase-mediated resistance and opportunities for its control. *Journal of Antimicrobial Chemotherapy*, 1998, 41, Supplement D, 25 – 41.

106. Lobkovsky, E., Billings, E.M., Moews, P.C., Rahil, J., Pratt, R.F., and Knox, J.R. Crystallographic structure of a phosphonate derivative of the *Enterobacter cloacae* P99 cephalosporinase: Mechanistic interpretation of a β--lactamase transition-state analog. *Biochemistry*, 1994, 33, 6762 – 6772.

107. Lobkovsky, E., Moews, P.C., Liu, H., Zhao, H., and Frère, J.-M. Evolution of an enzyme activity: Crystallographic structure at 2-Å resolution of cephalopsorinase from the *amp*C gene of *Enterobacter cloacae* P99 and comparison with a class A penicillinase. *Proceedings of the National Academy of Sciences of the United States of America*, 1993, 90, 11257 – 11261.

108. Maiti, S.N., Philips, O.A., Micetich, R.G., and Livermore, D.M. β-lactamase inhibitors: Agents to overcome bacterial resistance. *Current Medicinal Chemistry*, 1998, 5, 441 – 456.

109. Majiduddin, F.K., Materon, I.C., and Palzkill, T.G. Molecular analysis of

beta-lactamase structure and function. *International Journal of Medical Microbiology*, 2002, 292, 127 – 137.

110. Marvin, J.S., and Hellinga, H.W. Engineering biosensors by introducing fluorescent allosteric signal transducers: Construction of a novel glucose sensor. *Journal of the American Chemical Society*, 1998, 120, 7 – 11.

111. Marvin, J.S., Corcoran, E.E., Hattangadi, N.A., Zhang, J.V., Gere, S.A., and Hellinga, H.W. The rational design of allosteric interactions in a monomeric protein and its applications to the construction of biosensors. *Proceedings of the National Academy of Sciences of the United States of America*, 1997, 84, 4366 – 4371.

112. Massova, I., and Mobashery, S. Kinship and diversification of bacterial penicillin-binding proteins and β-lactamases. *Antimicrobial Agents and chemotherapy*, 1998, 42, 1 – 17.

113. Massova, I., and Mobashery, S. Structural and mechanistic aspects of evolution of β-lactamases and penicillin-binding proteins. *Current Pharmaceutical Design*, 1999, 5, 929 – 937.

114. Matagne, A., Dubus, A., Galleni, M., and Frère, J.-M. The β-lactamase cycle: a tale of selective pressure and bacterial ingenuity. *Natural Product Reports*,

1999, 16, 1 – 19.

115. Matagne, A., Lamotte-Brasseur, J., and Frère, J.-M. Catalytic properties of class A β-lactamases: efficiency and diversity. *The Biochemical Journal*, 1998, 330, 581 – 598.

116. Matagne, A., Misselyn-Bauduin, A.-M., Joris, B., Erpicum, T., Granier, B., and Frère, J.-M. The diversity of the catalytic properties of class A β-lactamases. *The Biochemical Journal*, 1990, 265, 131 – 146.

117. Medeiros, A.A. Evolution and dissemination of β-lactamases accelerated by generations of β-lactam antibiotics. *Clinical Infectious Diseases*, 1997, 24, Supplement 1, S19 – 45.

118. Miyawaki, A. Fluorescent proteins in a new light. *Nature Biotechnology*, 2004, 22, 1374 – 1376.

119. Miyawaki, A., Nagai, T., and Mizuno, H. Mechanisms of protein fluorophores formation and engineering. *Current Opinion in Chemical Biology*, 2003, 7, 557 – 562.

120. Monnaie, D., Virden, R., and Frère, J.-M. A rapid-kinetic study of the class C β-lactamase of *Enterobacter cloacae* 908R. *European Journal of Biochemistry*, 1992, 306, 108 – 112.

121. Morandi, F., Caselli, E., Morandi, S., Focia, P.J., Blázquez, J., Shoichet, B.K., and Prati, F. Nanomolar inhibitors of Amp C β-lactamase. *Journal of the American Chemical Society*, 2003, 125, 685 – 695.

122. Morii, T., Sugimoto, K., Makino, K., Otsuka, M., Imoto, K., and Mori, Y. A new fluorescent biosensor for inositol triphosphate. *Journal of the American Chemical Society*, 2002, 124, 1138 – 1139.

123. Murphy, B.P., and Pratt, R.F. Evidence for an oxyanion hole in serine beta-lactamases and DD-peptidases. *The Biochemical Journal*, 1988, 256, 669 – 672.

124. Musser, J.M.B., Anderson, K.L., Rushing, J.E., and Moats, W.A. Potential for milk containing penicillin G or amoxicillin to cause residues in calves. *Journal of Dairy Science*, 2001, 84, 126 – 133.

125. Mustafi, D., Hofer, J.E., Huang, W., Palzkill, T., and Makinen, M.W. Chromophoric spin-labeled β-lactam antibiotics for ENDOR structural characterization of reaction intermediates of class A and class C β-lactamases. *Spectrochimica Acta Part A*, 2004, 60, 1279 – 1289.

126. Nagase, T., Nakata, E., Shinkai, S., and Hamachi, I. Construction of artifical signal transducers on a lectin surface by post-photoaffinity-labeling

modification for fluorescent saccharide biosensors. *Chemistry – A European Journal*, 2003, 9, 3660 – 3669.

127. Nakata, E., Koshi, Y., Koga, E., Katayama, Y., and Hamachi, I. Double-modification of lectin using two distinct chemistries for fluorescent ratiometric sensing and imaging saccharides in test tube or in cell. *Journal of the American Chemical Society*, 2005, 127, 13253 – 13261.

128. Nakata, E., Nagase, T., Shinkai, S., and Hamachi, I. Coupling a natural receptor protein with an artificial receptor to afford a semisynthetic fluorescent biosensor. *Journal of the American Chemical Society*, 2004, 126, 490 – 495.

129. Neu, H.C. The crisis in antibiotic resistance. *Science*, 1992, 257, 1064 – 1072.

130. Normark, S., Lindquist, S., and Lindberg, F. Chromosomal beta-lactam resistance in *Enterobacteria*. *Scandinavian Journal of Infectious Diseases. Supplementum*, 1986, 49, 38 – 45.

131. Nouws, J.F.M., Van Egmond, H., Loeffen, G., Schouten, J., Keukens, H., Smulders, I., and Stegeman, H. Suitability of the Charm HVS and a microbiological multiplate system for detection of residues in raw milk at EU

maximum residue levels. *The Veterinary Quarterly*, 1999, 21, 21 – 27.

132. Nukaga, M., Abe, T., Venkatesan, A.M., Mansour, T.S., Bonomo, R.A., and Knox, J.R. Inhibition of class A and class C β-lactamases by penems: crystallographic structures of a novel 1,4-thiazepine intermediate. *Biochemistry*, 2003, 42, 13152 – 13159.

133. Nukaga, M., Kumar, S., Nukaga, K., Pratt, R.F., and Knox, J.R. Hydrolysis of third-generation cephalosporins by class C β-lactamases. *The Journal of Biological Chemistry*, 2004, 279, 9344 – 9352.

134. Nukaga, M., Taniguchi, K., Washio, Y., and Sawai, T. Effect of an amino acid insertion into the omega loop region of a class C β-lactamase on its substrate specificity. *Biochemistry*, 1998, 37, 10461 – 10468.

135. Nukaga, M., Tanimoto, K., Tsukamoto, K., Imajo, S., Ishiguro, M., and Sawai, T. A survey of a functional amino acid of class C β-lactamase corresponding to Glu^{166} of class A β-lactamases. *Federation of European Biochemical Societies,* 1993, 332, 93 – 98.

136. Odeh, R., Kelkar, S., Hujer, A.M., Bonomo, R.A., Schreckenberger, P.C., and Quinn, J.P. Broad resistance due to plasmid-mediated AmpC β-lactamases in clinical isolates of *Escherichia coli*. *Clinical Infectious Diseases*, 2002, 35,

140 – 145.

137. Oefner, C., D'Arcy, A., Daly, J.J., Gubernator, K., Charnas, R.L., Heinze, I., Hubschwerlen, C., and Winkler, F.K. Refined crystal structure of β-lactamase from *Citrobacter freundii* indicates a mechanism for β-lactam hydrolysis. *Nature*, 1990, 343, 284 – 288.

138. Ogawara, H. Antibiotic resistance in pathogen and producing bacteria, with special reference to β-lactam antibiotics. *Microbiological Reviews*, 1981, 45, 591 – 619.

139. Okerman, L., Croubels, S., De Baere, S., Van Hoof, J., De Backer, P., and De Brabander, H. Inhibition tests for detection and presumptive identification of tetracyclines, beta-lactam antibiotics and quinolones in poultry meat. *Food Additives and Contaminants*, 2001, 18, 385 – 393.

140. Okumoto, S., Looger, L.L., Micheva, K.D., Reimer, R.J. Smith, S.J. and Frommer, W.B. Detection of glutamate release from neurons by genetically encoded surface-displayed FRET nanosensors. *Proceedings of the National Academy of Sciences of the United States of America*, 2005, 102, 8740 – 8745.

141. Padayatto, P.S., Helfand, M.S., Totir, M.A., Carey, M.P., Carey, P.R.,

Bonomo, R.A., and Van den Akker, F. High resolution crystal structures of the *trans*-enamine intermediates formed by sulbactam and clavulanic acid and E166A SHV-1 β-lactamase. *The Journal of Biological Chemistry*, 2005, 280, 34900 – 34907.

142. Page, M.G. Cephalosporins in clinical development. *Expert Opinion on Investigational Drugs*, 2004, 13, 973 – 985.

143. Page, M.G.P. β-lactamase inhibitors. *Drug Resistance Updates*, 2000, 3, 109 – 125.

144. Page, M.I. The reactivity of β-lactams, the mechanism of catalysis and the inhibition of β-lactamases. *Current Pharmaceutical Design*, 1999, 5, 895 – 913.

145. Page, M.I., and Laws, A.P. The mechanism of catalysis and the inhibition of β-lactamases. *Chemical Communications*, 1998, 16, 1609 – 1617.

146. Payne, D., and Tomasz, A. The challenge of antibiotic resistant bacterial pathogens: the medical need, the market and prospects for new antimicrobial agents. *Current Opinion in Microbiology*, 2004, 7, 435 – 438.

147. Payne, D.J., Du, W., and Bateson, J.H. β-lactamase epidemiology and the utility of established and novel β-lactamase inhibitors. *Expert Opinion on*

Investigational Drugs, 2000, 9, 247 – 261.

148. Peláez, F. The historical delivery of antibiotics from microbial natural products – can history repeat? *Biochemical Pharmacology*, 2006, 71, 981 – 990.

149. Perilli, M., Franceschini, N., Bonfiglio, G., Segatore, B., Stefani, S., Nicoletti, G., Tavio Perez, Md, Bianchi, C., Zollo, A., and Amicosante, G. A kinetic study on the interaction between tazobactam (a penicillanic acid sulphone derivative) and active-site serine β-lactamases. *Journal of Enzyme Inhibition*, 1999, 15, 1 – 10.

150. Petrosino, J., Cantu III, C., and Palzkill, T. β-lactamases: protein evolution in real time. *Trends in Microbiology*, 1998, 6, 323 – 327.

151. Phillips, O.A., Reddy, A.V.N., Setti, E.L., Spevak, P., Czajkowski, D.P., Atwal, H., Salama, S., Micetich, R.G., and Maiti, S.N. Synthesis and biological evaluation of penem sulfones as inhibitors of β-lactamases. *Bioorganic & Medicinal Chemistry*, 2005, 13, 2847 – 2858.

152. Pires de Abreu, L.R., Ortiz, R.A.M., de Castro, S.C., and Pedrazzoli, J. Jr. HPLC determination of amoxicillin comparative bioavailability in healthy volunteers after a single dose administration. *Journal of Pharmacy &*

Pharmaceutical Sciences, 2003, 6, 223 – 230.

153. Pollok, B.A., and Heim, R. Using GFP in FRET-based applications. *Trends in Cell Biology*, 1999, 9, 57 – 60.

154. Powers, R.A., and Shoichet, B.K. Structure-based approach for binding site identification on AmpC β-lactamase. *Journal of Medicinal Chemistry*, 2002, 45, 3222 – 3234.

155. Powers, R.A., Blázquez, J., Weston, G.S., Morosini, M.-I., Baquero, F., and Shoichet, B.K. The complexed structure and antimicrobial activity of a non-β-lactam inhibitor of AmpC β-lactamase. *Protein Science*, 1999, 8, 2330 – 2337.

156. Pratt, R.F., McConnell, T.S., and Murphy, S.J. Accumulation of acyl-enzyme intermediates during turnover of penicillins by class A β-lactamase of *Staphylococcus aureus* PC1. *The Biochemical Journal*, 1988, 254, 919 – 922.

157. Projan, S.J. New (and not so new) antibacterial targets – from where and when will the novel drugs come? *Current Opinion in Pharmacology*, 2002, 2, 513 – 522.

158. Quesada, A.R., Cañedo, A., Moreno, M.A., and Fernández-Puentes, J.L. A microtitre plate-based assay for the screening of β-lactams. *Letters in Applied*

Microbiology, 1996, 22, 303 – 306.

159. Rahal, J.J. Extended-spectrum β-lactamases: how big is the problem? *Clinical Microbiology and Infection*, 2000, 6, Supplement 2, 2 – 6.

160. Rice, L.B., and Bonomo, R.A. β-lactamases: which ones are clinically important? *Drug Resistance Updates*, 2000, 3, 178 – 189.

161. Richter, H.G.F., Angehrn, P., Hubschwerlen, C., Kania, M., Page, M.G.P., Specklin, J.-L., and Winkler, F.K. Design, synthesis, and evaluation of 2β-alkenyl penam suflone acids as inhibitors of β-lactamases. *Journal of Medicinal Chemistry*, 1996, 39, 3712 – 3722.

162. Riediker, S., and Stadler, R.H. Simultaneous determination of five β-lactam antibiotics in bovine milk using liquid chromatography coupled with electrospray ionization tandem mass spectrometry. *Analytical chemistry*, 2001, 73, 1614 – 1621.

163. Rizwi, I., Tan, A.K., Fink, A.L., and Virden, R. Clavulanate inactivation of *Staphylococcus aureus* β-lactamase. *The Biochemical Journal*, 1989, 258, 205 – 209.

164. Rizzo, R.A., Springer, G.H., Granada, B., and Piston, D.W. An improved cyan fluorescent protein useful for FRET. *Nature Biotechnology*, 2004, 22,

445 – 499.

165. Salins, L.L.E., Ware, R.A., Ensor, C.M., and Daunert, S. A novel reagentless sensing system for measuring glucose based on the galactose/glucose-binding protein. *Analytical Biochemistry*, 2001, 294, 19 – 26.

166. Samaha-Kfoury, J.N., and Araj, G.F. Recent developments in β-lactamases and extended spectrum β-lactamases. *British Medical Journal*, 2003, 327, 1209 – 1213.

167. Sandanayaka, V.P, Prashad, A.S., Yang, Y., Williamson, R.T., Lin, Y.I., and Mansour, T.S. Spirocyclopropyl β-lactams as mechanism-based inhibitors of serine β-lactamases. Synthesis by rhodium-catalyzed cyclopropanation of 6-diazopenicillanate sulfone. *Journal of Medicinal Chemistry*, 2003, 46, 2569 – 2571.

168. Sandanayaka, V.P., and Yang, Y. Dipolar cycloaddition of novel 6-(nitrileoxidomethyl) penam sulfone: an efficient route to a new class of β-lactamase inhibitors. *Organic Letters*, 2000, 2, 3087 – 309.

169. Saxon, A., Beall, G.N., Rohr, A.S., and Adelman, D.C. Immediate hypersensitivity reactions to β-lactam antibiotics. *Annales Medicinae*

Internae Fenniae, 1987, 107, 204 – 215.

170. Schmid, M.B. Crystallizing new approaches for antimicrobial drug discovery, *Biochemical Pharmacology*, 2006, 71, 1048 – 1056.

171. Shea, K.M. Antibiotic resistance: What is the impact of agricultural uses of antibiotics on children's health? *Pediatrics*, 2003, 112, 253 – 258.

172. Shi, J., Boyd, A.E., Radic, Z., and Taylor, P. Reversibly bound and covalently attached ligands induce conformational changes in the omega loop, Cys^{69} – Cys^{96}, of mouse acetylcholinesterase. *The Journal of Biological Chemistry*, 2001, 276, 42196 – 42204.

173. Shi, J., Radić, Z., and Taylor, P. Inhibitors of different structure induce distinguishing conformations in the omega loop, Cys^{69} – Cys^{96}, of mouse acetylcholinesterase. *The Journal of Biological Chemistry*, 2002, 277, 43301 – 43308.

174. Shrestha, S., Salins, L.L.E., Ensor, M., and Daunert, S. Rationally designed fluorescently labeled sulfate-binding protein mutants: evaluation in the development of a sensing system for sulfate. *Biotechnology and Engineering*, 2002, 78, 517 – 526.

175. Siu, L.K. Antibiotics: action and resistance in gram-negative bacteria.

Journal of Microbiology, Immunology, and Infection, 2002, 35, 1 – 11.

176. Sloan, D.J., and Hellinga, H.W. Structure-based engineering of environmentally sensitive fluorophores for monitoring protein-protein interactions. *Protein Engineering*, 1998, 11, 819 – 823.

177. Smith, D.M. Decreased antimicrobial resistance following changes in antibiotic use. *Surgical Infections*, 2000, 1, 73 – 78.

178. Sternesjö, Å., and Johnsson, G. A novel rapid enzyme immunoassay (Fluorophos BetaScreen) for detection of β-lactam residues in ex-farm raw milk. *Journal of Food Protection*, 1998, 61, 808 – 811.

179. Sulton, D., Pagan-Rodriguez, D., Zhou, X., Liu, Y., Hujer, A.M., Bethel, C.R., Helfand, M.S., Thomson, J.M., Anderson, V.E., Buynak, J.D., and Ng, L.M. Clavulanic acid inactivation of SHV-1 and the inhibitor-resistant S130G SHV-1 β-lactamase: Insights into the mechanism of inhibition. *The Journal of Biological Chemistry*, 2005, 280, 35528 – 35536.

180. Tabei, K., Feng, X., Venkatesan, A.M., Abe, T., Hideki, U., Mansour, T.S., and Siegel, M.M. Mechanism of inactivation of β-lactamases by novel 6-methylidene penems elucidated using electrospray ionization mass spectrometry. *Journal of Medicinal Chemistry*, 2004, 47, 3674 – 3688.

181. Takaoka, Y., Tsutsumi, H., Kasagi, N., Nakata, E., and Hamachi, I. One-pot and sequential organic chemistry on an enzyme surface to tether a fluorescent probe at the proximity at the active site with restoring enzyme activity. *Journal of the American Chemical Society*, 2006, 128, 3273 – 3280.

182. Tejedor-Junco, M.T., González-Martín, M., Lupiola, P., and Gonález-Lama, Z. Type I *β*-lactamases of *Enterobacter cloacae* and resistance of *β*-lactam antibiotics. *Folia Mcrobiologica*, 1998, 43 (6), 683 – 686.

183. Tenover, F.C. Mechanisms of antimicrobial resistance in bacteria. *The American Journal of Medicine*, 2006, 119 (6A), S3 –S10.

184. Therrien, C., and Levesque, R.C. Molecular basis of antibiotic resistance and *β*-lactamase inhibition by mechanism-based inactivators: perspectives and future directions. *FEMS Microbiology Reviews*, 2000, 24, 251 – 262.

185. Thomson, C.J., Power, E., Ruebsamen-Waigmann, H., and Labischinski, H. Antibacterial research and development in the 21st century – an industry perspective of the challenges. *Current Opinion in Microbiology*, 2004, 7, 445 – 450.

186. Tipper, D.J. and Strominger, J.L., Mechanism of action of penicillins: A proposal based on their structural similarity to acyl-D-alanyl-D-alanine.

Proceedings of the National Academy of Sciences of the United States of America, 1965, 54, 1133 – 1141.

187. Tollefson, L., and Karp, B.E. Human health impact from antimicrobial use in food animals. *Médecine et Maladies Infectieuses*, 2004, 43, 514 – 521.

188. Tondi, D., Powers, R.A., Caselli, E., Negri, M-C., Blázquez, J., Costi, M.P., and Shoichet, B.K. Structure-based design and in-parallel synthesis of inhibitors of Amp C β-lactamase. *Chemistry & Biology*, 2001, 8, 593 – 610.

189. Tsang, W.Y., Ahmed, N., Hinchliffe, P.S., Wood, J.M., Harding, L.P., Laws, A.P., and Page, M.I. Different transition-state structures for the reactions of β-lactams and analogous β-sultams with serine β-lactamases. *Journal of the American Chemical Society*, 2005, 127, 17556 – 17564.

190. Tsukamoto, K., Kikura, R., Ohno, R., and Sawai, T. Substitution of aspartic acid-217 of *Citrobacter freudii* cephalosporinase and properties of the mutant enzymes. *European Journal of Biochemistry*, 1990, 264, 211 – 214.

191. Tsutui, H., Karasawa, S., Shimizu, H., Nukina, N., and Miyawaki, A. Semi-rational engineering of a coral fluorescent protein into an efficient highlighter. *EMBO reports*, 2005, 6, 233 – 238.

192. Usher, K.C., Blaszczka, L.C., Weston, G.S., Shoichet, B.K., and Remington,

S.J. Three-dimensional structure of AmpC *β*-lactamase from *Escherichia coli* bound to a transition-state analogue: Possible implications for oxyanion hypothesis and for inhibitor design. *Biochemistry*, 1988, 37, 16082 – 16092.

193. Vilar, M., Galleni, M., Solmajer, T., Turk, B., Frère, J.-M., and Matagne, M. Kinetic study of two novel enantiomeric tricyclic *β*-lactams which efficiently inactivate class C *β*-lactamases. *Antimicrobial Agents and Chemotherapy*, 2001, 45, 2215 – 2223.

194. Waley, S.G. *β*-lactamase: mechanism of action. In: Page, M.I. ed. *The Chemistry of β-lactams*. Glasgow: Blackie Academic & Professional, an imprint of Chapman & Hall, 1992.

195. Walsh, C. Molecular mechanisms that confer antibacterial drug resistance. *Nature*, 2000, 406, 775 – 781.

196. Walsh, C. Where will new antibiotics come from? *Nature Reviews Microbiology*, 2003, 1, 65 – 70.

197. Walsh, T.R. The emergence and implications of metallo-*β*-lactamases in Gram-negative bacteria. *Clinical Microbiology and Infection*, 2005, 11, Supplement 6, 2 – 9.

198. Weston, G.S., Blázquez, J., Baquero, F., and Shoichet, B.K., Structure-based

enhancement of boronic acid-based inhibitors of AmpC β-lactamase. *Journal of Medicinal Chemistry*, 1998, 41, 4577 – 4586.

199. Wilke, M.S., Andrew, L.L., and Strynadka, N.C.J. β-lactam antibiotic resistance: a current structural perspective. *Current Opinion in Microbiology*, 2005, 8, 525 – 533.

200. Williams, J.D. β-lactamases and β-lactamase inhibitors. *International Journal of Antimicrobial Agents*, 1999, 12, Supplement 1, S3 – S7.

201. Wouters, J., Fonzè, E., Vermeire, M., Frère, J.-M., and Charlier, P. Crystal structure of *Enterobacter cloacae* 908R class C β-lactamase bound to iodo-acetamido-phenyl boronic acid, a transition-state analogue. *Cellular and Molecular Life Sciences*, 2003, 60, 1764 – 1773.

202. Yamaguchi, A., Hirata, T., and Sawai, T. Kinetic studies on inactivation of *Citrobacter freundii* cephalosporinase by sulbactam. *Antimicrobial Agents and Chemotherapy*, 1983, 24, 23 – 30.

203. Yang, Y., Janota, K., Tabei, K., Huang, N., Siegel, M.M., Lin, Y-I., Rasmussen, B.A., and Shlaes, D.M. Mechanism of inhibition of the class A β-lactamases PC1 and TEM-1 by tazobactam. *The Journal of Biological Chemistry*, 2000, 275, 26674 – 26682.

204. Yang, Y., Rasmussen, B.A., and Shlaes, D.M. Class A β-lactamases – enzyme-inhibitor interactions and resistance. *Pharmacology & Therapeutics*, 1999, 83, 141 – 151.

205. Zhang, Z., Yu, Y., Musser, J.M., and Palzkill, T. Amino acid sequence determinants of extended spectrum cephalosporin hydrolysis by the class C P99 β-lactamase. *The Journal of Biological Chemistry*, 2001, 276, 46568 – 46574.

Appendix

Media composition

Composition of 2×YT medium	
Distilled water (ml)	100
Tryptone (g)	1.6
Yeast extract (g)	1
Sodium chloride (g)	0.5

Composition of spizizen minimal medium

Ammonium sulphate (mM)	15
Potassium hydrogen phosphate (mM)	80
Potassium dihydrogen phosphate (mM)	44
Sodium citrate dihydrate (mM)	4
Magnesium sulphate (mM)	1

Composition of pre-transformation medium

	Spizizen minimal medium
Calcium chloride (mM)	0.05
Magnesium sulphate (mM)	2.5
Manganese sulphate (μM)	0.5
Glucose (%)	1
Isoleucine (mg/ml)	0.2
Leucine (mg/ml)	0.2
Methionine (mg/ml)	0.05
Tryptophan (mg/ml)	0.02
Valine (mg/ml)	0.2
Casamino acid (% w/v)	0.4

Composition of transformation medium

	Spizizen minimal medium
Magnesium sulphate (mM)	5
Glucose (%)	0.6
Isoleucine (mg/ml)	0.2
Leucine (mg/ml)	0.2
Methionine (mg/ml)	0.05
Tryptophan (mg/ml)	0.02
Valine (mg/ml)	0.2
Casamino acid (% w/v)	1×10^{-4}